Metal complex catalysis in Biological conditions

Literature Seminar
2013.12.2 (Mon.)
Takushi Araya

Contents

Biological condition
- buffer (pH7.4)
- protein (many functional groups)
- cell (surface or inside)

Good points

- Modification in Living cell

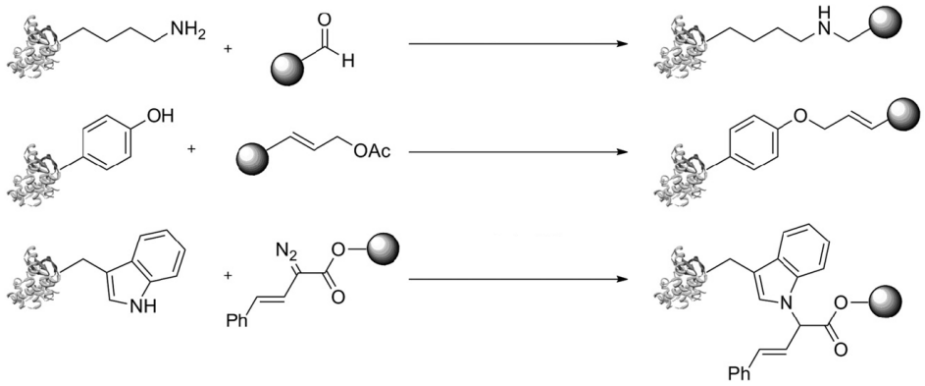

- Site specific prodrug activation

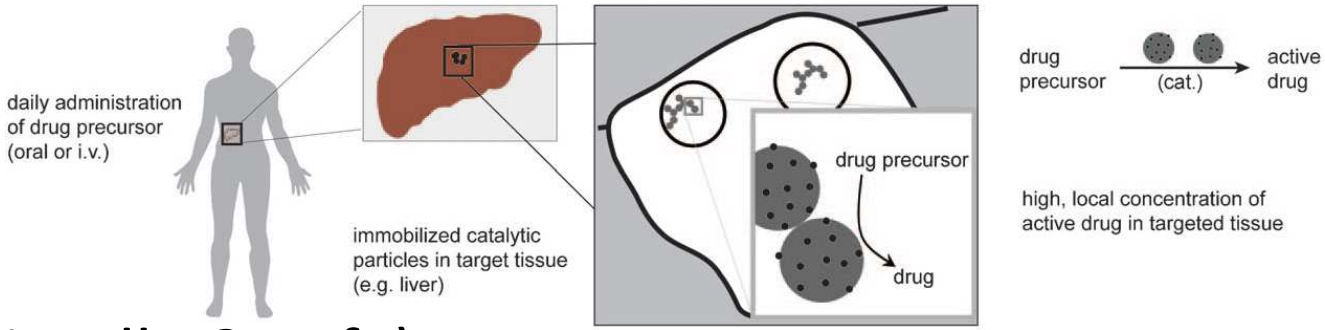

(- Eco-friendly & safe)

Low H_2O & O_2 tolerence
Temperature, *hv* sensitive

Just mixing

Problematic points

- Low functional group tolerance

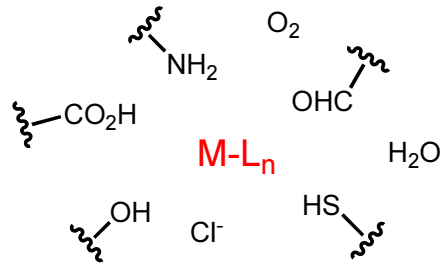

- Toxicity

e.g.) Fenton reaction

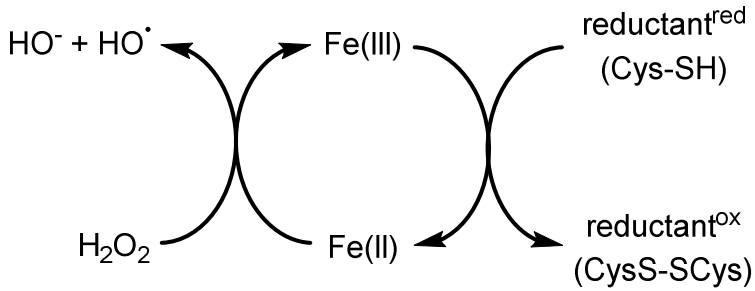

- Low water solubility

J. A. Imalay *et al., J. Bacteriol.* **2003**, 185, 1942-1950

$Pd(PPh_3)_4$, Hoveyda-Grubbs 2nd cat. etc…

Ligand must be
- protect active site
- water soluble

Contents

2-1. R-SH oxidation (1)-1

Cytotoxic [Ru] complex oxidize GSH to GSSG

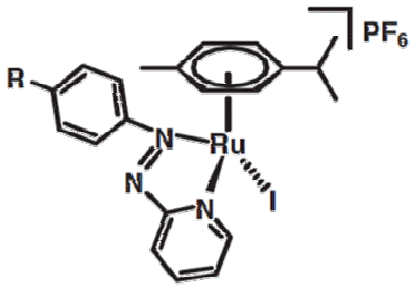

1: R = NMe_2
2: R = OH
3: R = H

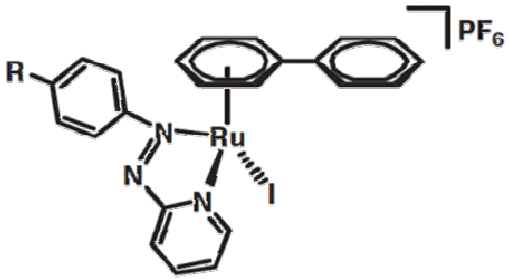

4: R = NMe_2
5: R = OH
6: R = H

	IC_{50}, μM		
Complex*	A2780	A549	E_{red}, V
1 (1-Cl)	4 (>100)	3 (>100)	−0.40, −1.00
4 (4-Cl)	3 (44)	2 (49)	−0.36
Azpy-NMe_2	>100	14	−1.28
2 (2-Cl)	4 (58)	4 (>100)	−0.33, −0.77
5 (5-Cl)	5 (18)	6 (56)	−0.26, −0.72
Azpy-OH	>100	>100	nd†
3 (3-Cl)	>100 (>100)	>100 (>100)	−0.22, −0.74
6 (6-Cl)	39 (>100)	51 (>100)	−0.18, −0.67
Azpy	>100	>100	−1.31 (vs.SCE)‡

(A2780 ovarian and A549 lung cancer cell lines)

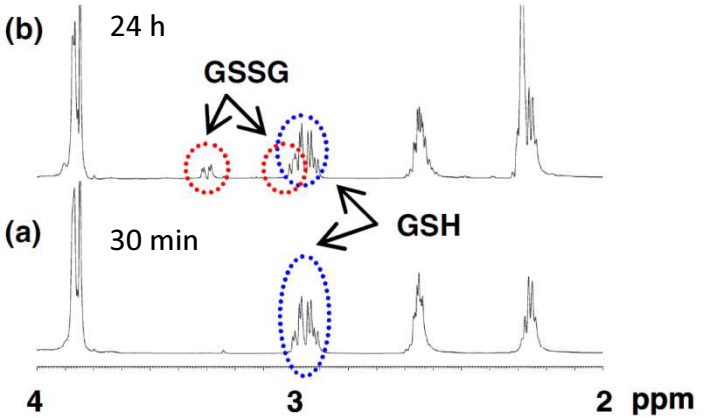

^{1}H NMR spectra of GSH after incubation (37°C) with **4** for (*a*) 30 min and (*b*) 24 h

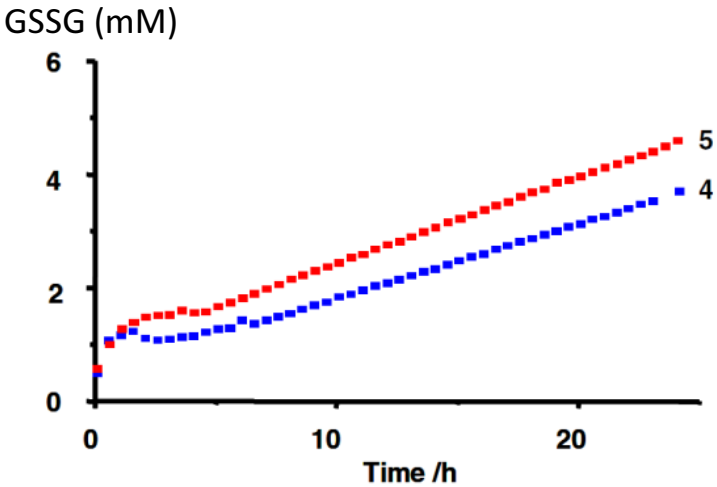

Catalytic oxidation of GSH (10 mM) to GSSG by **4** (100 μM; blue) or **5** (100 μM; red) for 24 h, 37°C

P. J. Sadler *et al. Proc. Natl. Acad. Sci. USA* **2008**, *105*, 11628-11633

2-1. R-SH oxidation (1)-2

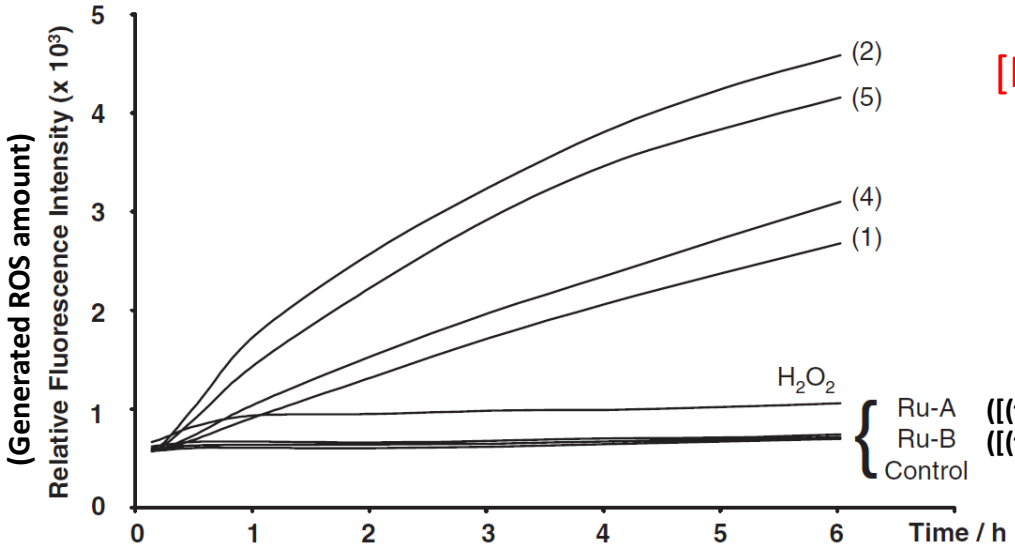

[Ru] increases cell ROS level

Incubation of A549 cancer cells with Ru complex (25 μM)

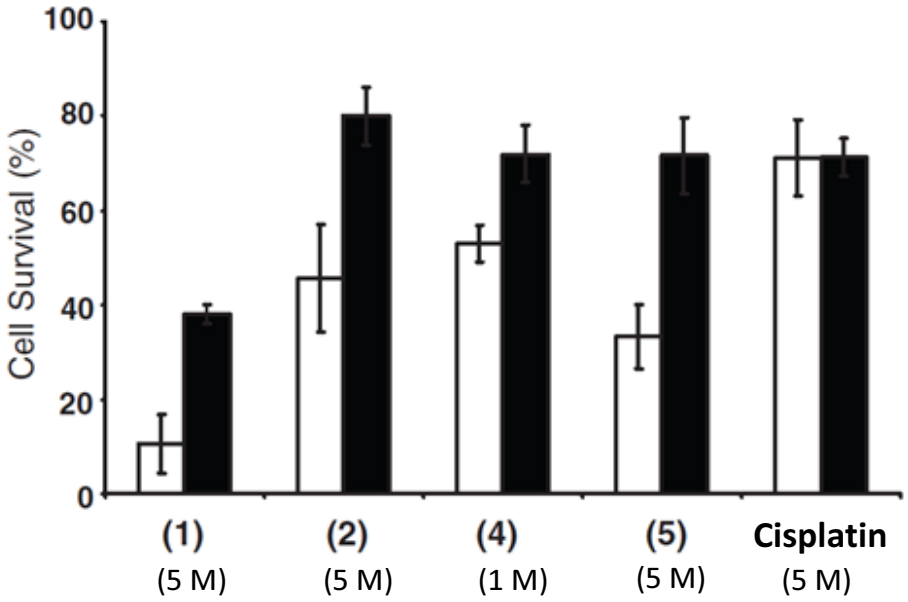

Thiol cancels [Ru] cytotoxicity

After 24 h exposure to ruthenium compounds,
Lighter : 96 h recovery for A549 lung cancer cells
Darker : same but pretreated to increase intracellular thiol level
(retreated 5 mM *N*-Ac-Cys for 2 h)

P. J. Sadler *et al. Proc. Natl. Acad. Sci. USA* **2008**, *105*, 11628-11633

2-1. R-SH oxidation (1)-3

Ru-X is replaced to Ru-SG

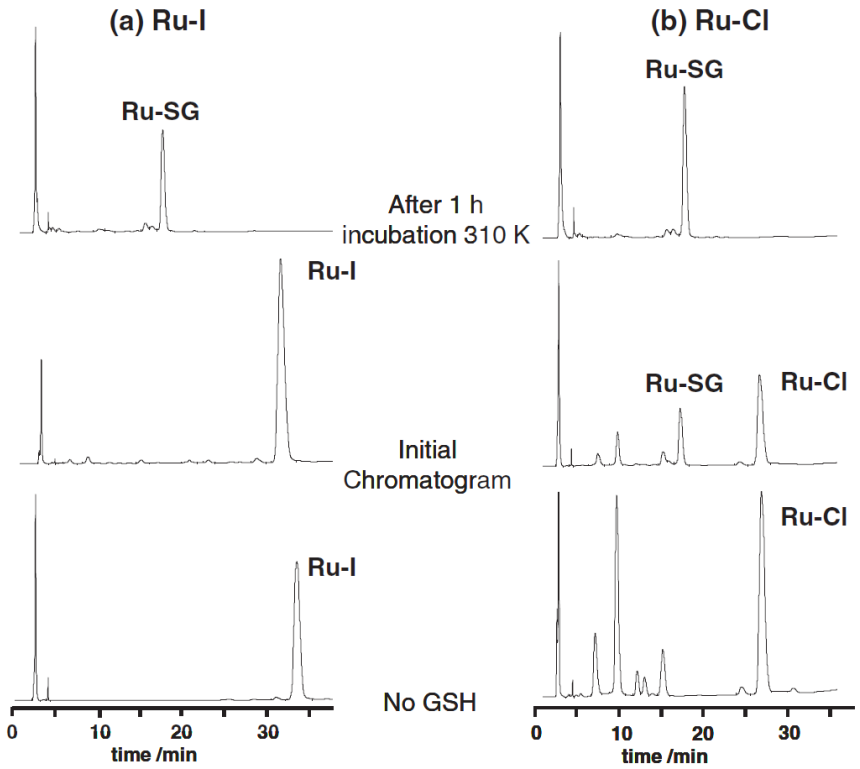

HPLC-analysis

Reaction of GSH (5 mM) with **4** (Ru-I) (*a*)
and corresponding chlorido complex (50 M) (Ru-Cl) (*b*)
(10 mM phosphate buffer (pH 7.9), 95% H_2O, 5% MeOH)

After 1 h incubation at 37°C, GS^- adduct is major peak
and peaks of starting material have disappeared.

Proposed catalytic cycle

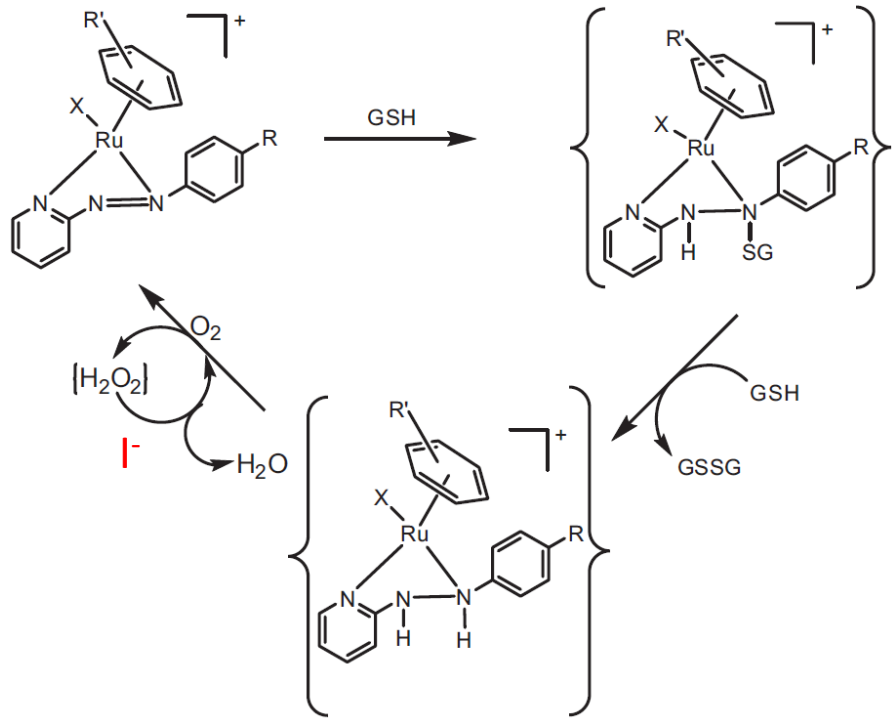

*X is initially I^-, which is displaced GS^- during the early stage

**I^--Catalyzed Decomposition of H_2O_2

J. C. Hansen, *J. Chem. Educ.*, 1996, *73*, 728-732

P. J. Sadler *et al. Proc. Natl. Acad. Sci. USA* **2008**, *105*, 11628-11633

2-1. R-SH oxidation (2)-1

Allylcarbamate cleavage by Ru(cod) complex

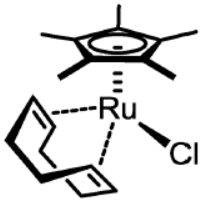

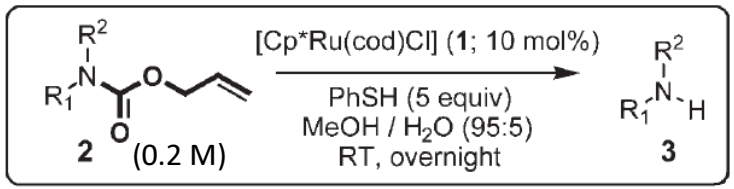

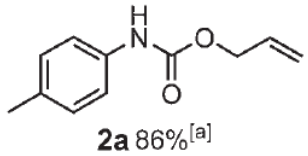

2a 86%[a]

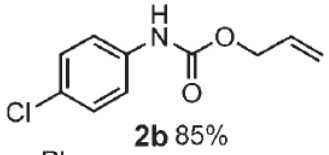

2b 85%

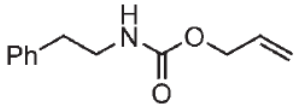

2c 94%[a]

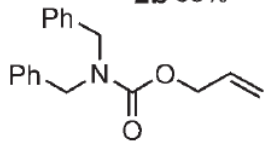

2d 87%

yield determined by GC-MS

Table 1: Catalytic cleavage of allylcarbamate **2a** to *p*-methylaniline with [Cp*Ru(cod)Cl].[a]

Entry	Thiol	Solvent	Atm.	*T*	Yield
1	PhSH	$MeOH/H_2O$ (95:5)	air	RT	89%
2	PhSH	MeOH	air	RT	93%
3	PhSH	$MeOH/H_2O$ (95:5)	argon	RT	96%
4	no thiols	$MeOH/H_2O$ (95:5)	air	RT	0%
5	PhSH and $PhCH_2CH_2SH$	$MeOH/H_2O$ (95:5)	air	RT	93%
6	$PhCH_2CH_2SH$	$MeOH/H_2O$ (95:5)	air	RT	34%
7	$PhCH_2CH_2SH$	$MeOH/H_2O$ (95:5)	air	37°C	67%

*Presence of excess thiol, no negative influence observed
yield determined by GC-MS
Obtain as byproduct PhS-SPh

E. Meggers *et al. Angew. Chem., Int. Ed*. **2006**, *45*, 5645-5648

2-1. R-SH oxidation (2)-2

Reaction occurred in cell extract, HeLa cell and *E. coli*

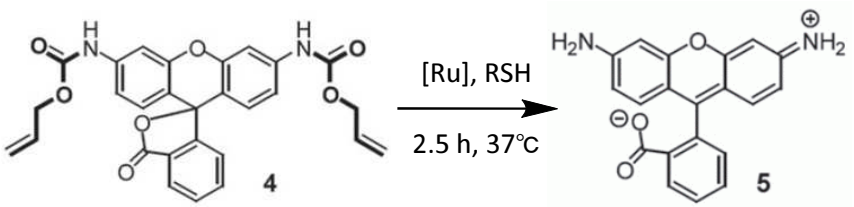

Entry	1	2	3	4
Carbamate **4**	+	+	+	+
Cell Extract + GSH	–	+	+	+
[Cp*Ru(cod)Cl]	–	–	+	+
PhSH	–	–	–	+
Yields of **5**	0%	0%	6%	80%

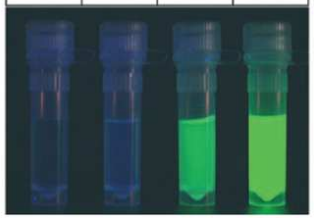

Entry 1: **4** (0.5 mM) in DMSO/H2O (1:1)
Entry 2: **4** (0.5 mM) in DMSO/cell extract (1:1), and GSH (3.5 mM), pH 7.0
Entry 3: Same as entry 2, but with [Cp*Ru(cod)Cl] (100 ~~m~~μM)
Entry 4: Same as entry 2, but with [Cp*Ru(cod)Cl] (100 ~~m~~μM) and PhSH (3.5 mM)
*Yields determined by fluorescence intensity

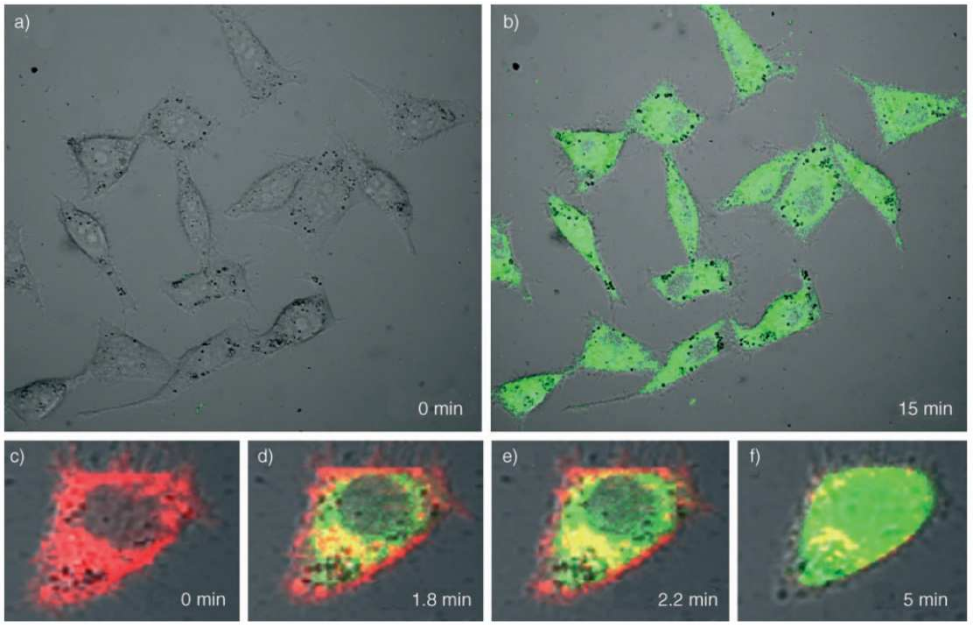

Fluorescence imaging of HeLa cells
a) and b): preincubated with **4** (100 ~~m~~μM) for 30 min, washed with PBS buffer, then treated with [Cp*Ru(cod)Cl] (20 ~~m~~μM) and PhSH (500 ~~m~~μM)
a) right after this addition
b) after 15 min

c)–f): preincubated with **4** (100 ~~m~~μM) for 30 min and at same time with membrane carbocyanine dye DiIC18(5). After washing with PBS buffer, cells were treated with [Cp*Ru(cod)Cl] (40 ~~m~~μM) and PhSH (100 ~~m~~μM)
c) right after this addition
d)–f) after the indicated times.

No cytotoxicity observed (no figure)

E. Meggers *et al. Angew. Chem., Int. Ed*. **2006**, *45*, 5645-5648

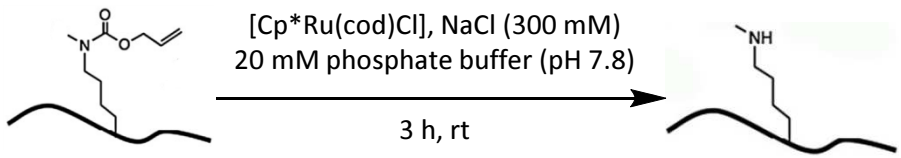

Histone H2B-Lys27(*N*-alloc)Lys in *E. coli*
P. G. Schultz *et al, Chem. Commun.*, **2010**, *46*, 5506-5508

2-1. R-SH oxidation (3)-1

Photoactivatable catalyst

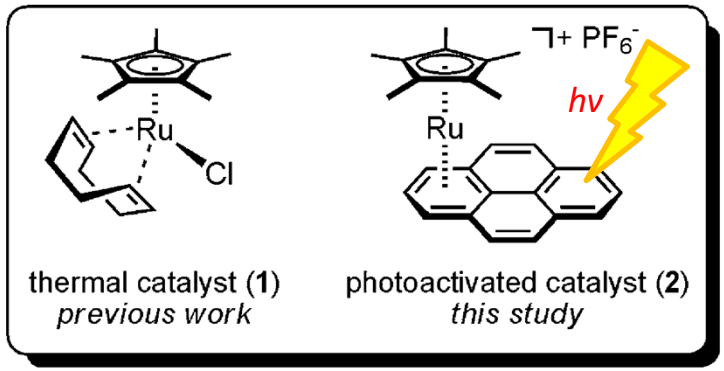

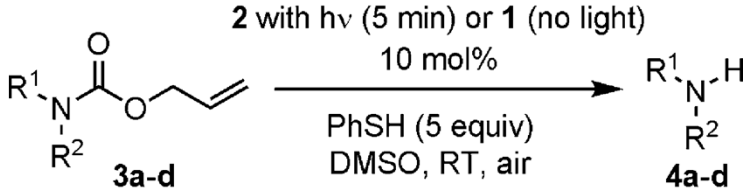

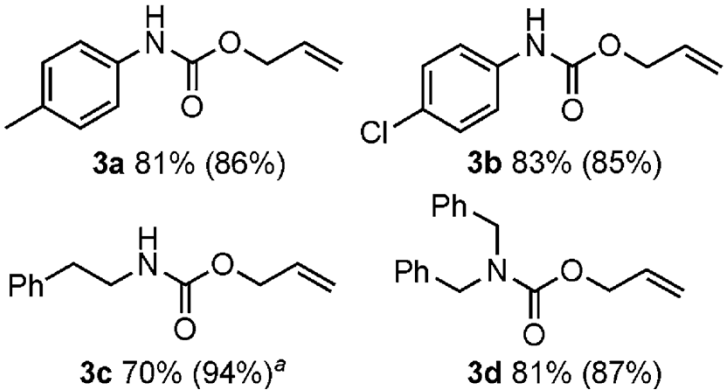

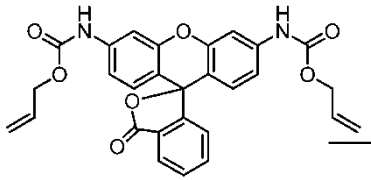

5 (0.5 mM)
(non-fluorescent)

2 (0.1 mM)
DMSO:1 mM phosphate buffer (pH 7.25) = 1:1

37℃, 10 min, *hv* (λ ≥330 nm)

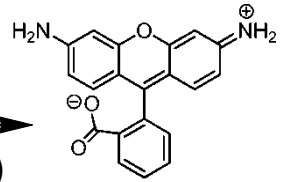

6 (fluorescent)

entry	amt of cat. (mol %)	thiol	yield (%)[b]
1	none	ME	0.5 ± 0.1
2	20	none	1.2 ± 0.3
3	20	ME	13 ± 2
4	20	Cys	14 ± 2
5	20	PhSH	93 ± 4
6	20	ME + PhSH	90 ± 3

β-mercaptoethanol (ME), PhSH, and cysteine (Cys) were all 5 mM
Yields determined by fluorescence intensity
(rhodamine 110: λex 488 nm, λem 520 nm)

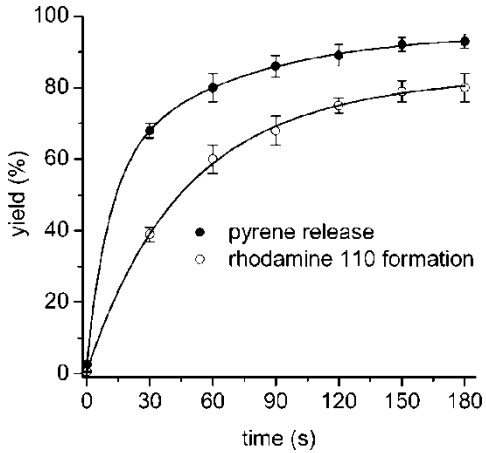

Reaction dynamics

2 (0.1 mM), **5** (0.5 mM), β-ME (5 mM), PhSH (5 mM), DMSO/H2O (1/1), hν (λ ≥330 nm)
Yields determined by fluorescence intensity
(pyrene, λex 319 nm, λem 390 nm;
rhodamine 110, λex 488 nm, λem 520 nm)

E. Meggers *et al. Organometallics,* **2012**, *31*, 5968−5970

2-1. R-SH oxidation (3)-2

Inside HeLa cells

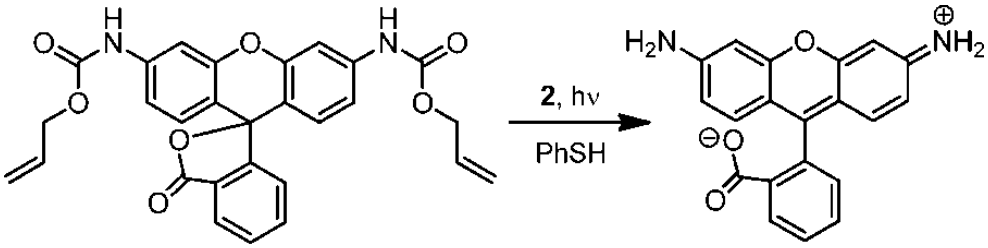

5 *(non-fluorescent)* **6** *(fluorescent)*

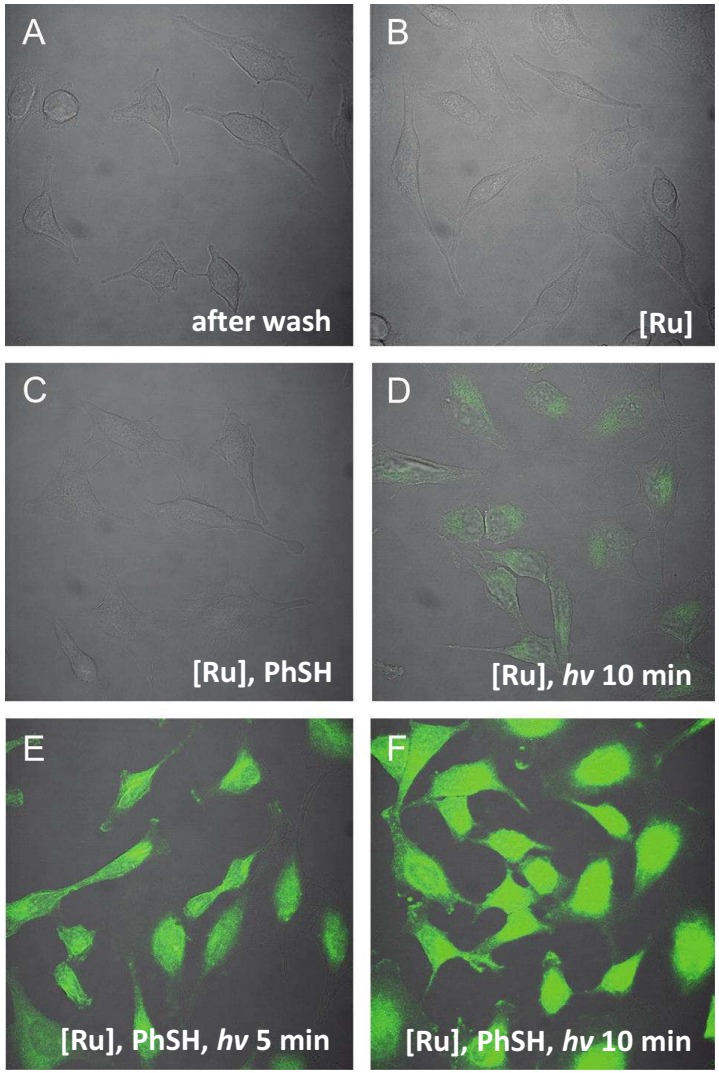

Figure 2. Confocal fluorescence imaging of [Cp*Ru(pyrene)]PF_6-induced uncaging of the bisallylcarbamate-protected rhodamine 110 (**5**) inside HeLa cells. HeLa cells were incubated with caged rhodamine **5** (100 μM) for 25 min and then washed with PBS buffer. (A) after the washing step; (B) after the addition of ruthenium complex **2** (20 μM) and a 10 min incubation time; (C) after the addition of ruthenium complex **2** (20 μM) and thiophenol (1 mM) and a 10 min incubation time without photolysis; (D) ruthenium complex **2** (20 μM) added and photolyzed for 10 min with $\lambda \geq 330$ nm; (E) ruthenium complex **2** (20 μM) and thiophenol (1 mM) added and photolyzed for 5 min with $\lambda \geq 330$ nm; (F) ruthenium complex **2** (20 μM) and thiophenol (1 mM) added and photolyzed for 10 min with $\lambda \geq 330$ nm.

E. Meggers *et al. Organometallics,* **2012**, *31*, 5968−5970

2-1. R-SH oxidation (4)

Ar-N_3 reduction by FeTPP and R-SH

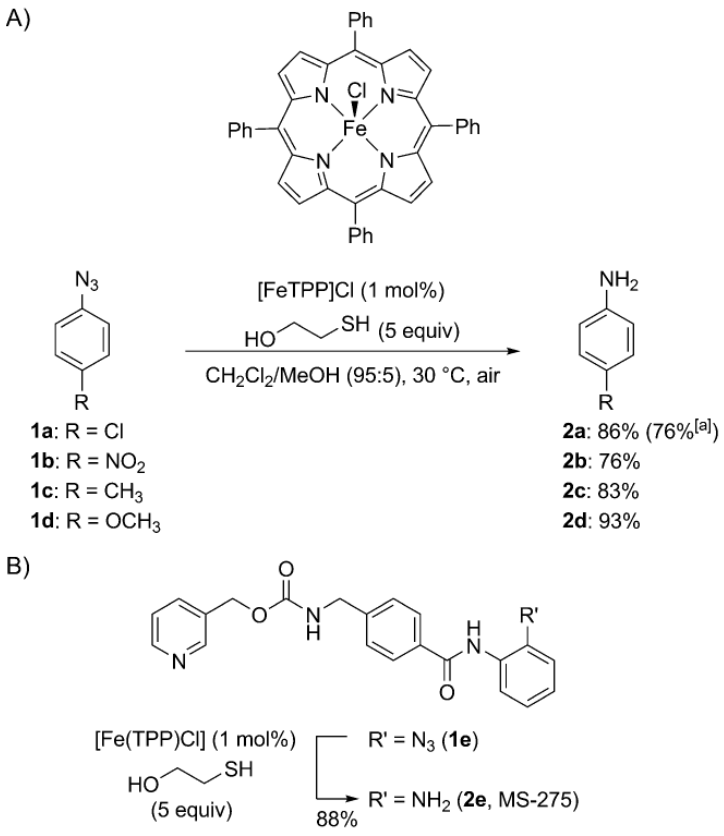

Scheme 1. [Fe(TPP)]Cl-catalyzed reduction of aromatic azides to amines with thiols. A) Reduction of simple aromatic azides. B) [Fe(TPP)]Cl-catalyzed formation of the anticancer drug candidate MS-275. [a] Only 0.05 mol% [Fe(TPP)]Cl used in the reaction.

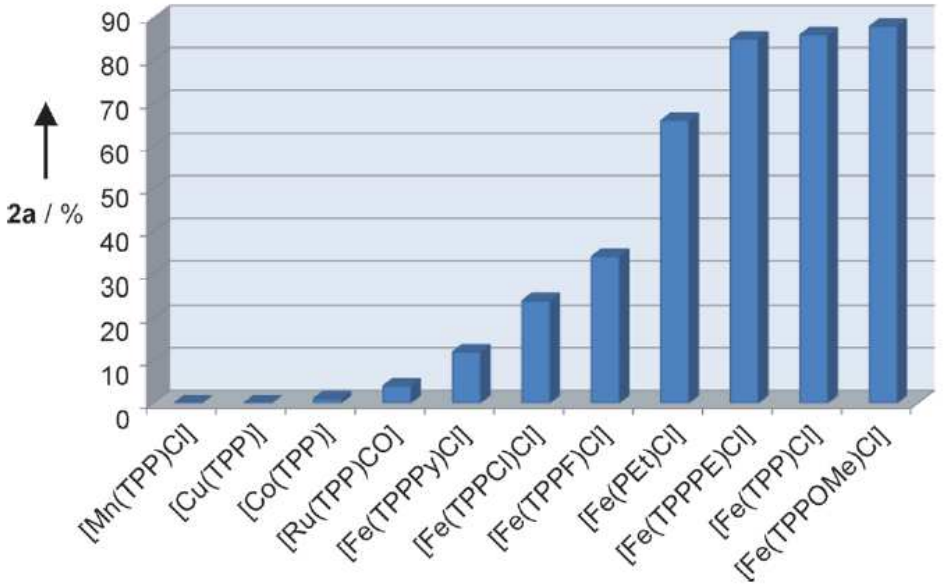

Figure 1. Comparison of different metalloporphyrins for the catalytic reduction of aromatic azides with thiols. Shown are isolated yields of **2a**. TPPPy: 5,10,15,20-tetra(*N*-methyl-4-pyridyl)porphine, TPPCl: 5,10,15,20-tetra(*o*-dichlorophenyl)-21*H*,23*H*-porphine, TPPE: 5,10,15,20-tetraphenyl-21*H*,23*H*-porphine modified with ethylene glycol chains, TPPF: 5,10,15,20-tetra(pentafluorophenyl)-21*H*,23*H*-porphine, PEt: 2,3,7,8,12,13,17,18-octaethyl-21*H*,23*H*-porphine, TPPOMe: 5,10,15,20-tetra(4-methoxyphenyl)-21*H*,23*H*-porphine. Reaction conditions: azide **1a** (1 M), β-mercaptoethanol (5 equiv), and metalloporphyrin (1 mol%) were reacted in CH_2Cl_2/MeOH (95:5) for 30 min at 30 °C. See the Supporting Information for more details.

E. Meggers *et al. ChemBioChem* **2012**, *13*, 1116-1120

2-1. R-SH oxidation (4)

Reductant scope

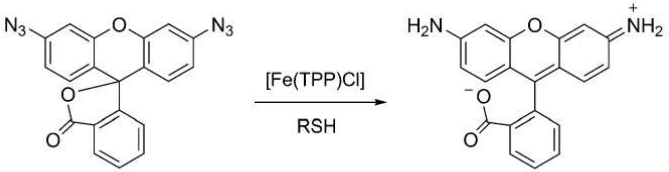

3
nonfluorescent

4
fluorescent

Table 1. Influence of biorelevant reaction conditions on the catalytic reduction of rhodamine bisazide **3** by [Fe(TPP)Cl].[a]

	[Fe(TPP)Cl] [mol%]	Thiol	Ascorbate [mM]	Yield [%][b]
1	5	–	–	0.2±0.1
2	5	Cys (5 mM)	–	13±2
3	5	Cys (5 mM)	10	40±3
4	5	Cys (15 mM)	10	77±5
5	5	PhSH (5 mM)	10	85±5[d]
6	5	Cys (5 mM)	10[c]	41±2
7	–	Cys (5 mM)	10	2.3±0.5

[a] Bisazide **3** (0.5 mM) was treated with the indicated amounts of [Fe(TPP)Cl] in DMSO/phosphate buffer (1:1, 20 mM, pH 7.25) at 37 °C for 1 h. [b] Standard deviations from three independent experiments. [c] Reaction performed in DMEM instead of phosphate buffer. [d] In the absence of [Fe(TPP)Cl] the yield is only 1%.

Ar-N3 were reduced in cell

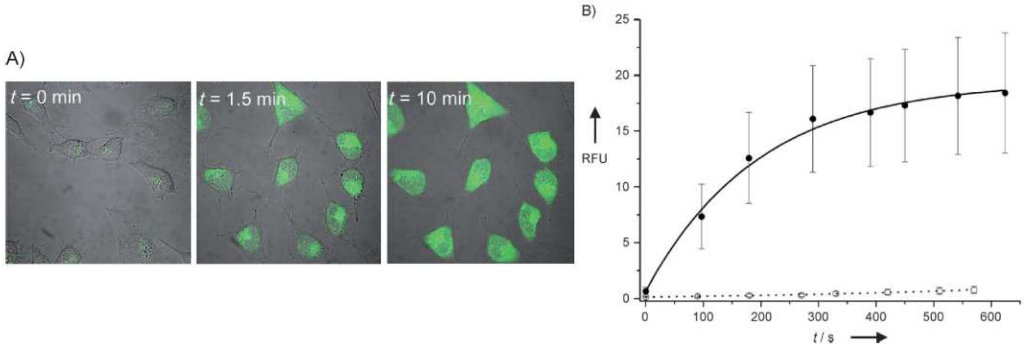

Figure 2. [Fe(TPP)Cl]-induced reduction of bisazide **3** to fluorescent rhodamine 110 inside HeLa cells. A) Superimposed phase contrast and confocal fluorescence images. HeLa cells were pre-incubated with bisazide **3** (100 μM) for 25 min, washed with PBS, and subsequently treated with [Fe(TPP)Cl] (10 μM). See the Supporting Information for more details. B) Quantified time-dependent increase of fluorescence emission within the cellular cytosol of HeLa cells upon [Fe(TPP)Cl] addition (●) and the corresponding time-dependent fluorescence in the absence of catalyst (○). The image analysis was performed on regions of interest (ROIs) for eight individual HeLa cells with the software ImageJ. The fluorescence evolution was analyzed for eight different HeLa cells. The data for the catalytic reaction were fitted to an exponential equation with the exponent being the rate constant [s^{-1}] of the intensity increase.

Fluorescence were observed *in vivo*, due to reductive metabolism of Ar-N3

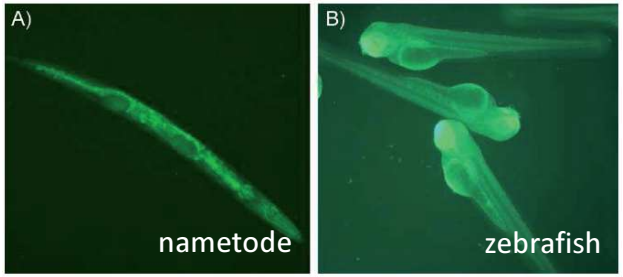

Figure 3. Activation of bisazide **3** in vivo. A) Adult *C. elegans* nematode incubated with bisazide **3** (25 μM) in M9 buffer with 1% DMSO for 20 min, before being pelleted, washed with M9 buffer (1 mL), concentrated to 100 μL by decanting, placed on a slide, and treated with one drop of 10% azide, followed by fluorescence imaging. B) 2.5-day-old transparent zebrafish embryos incubated with bisazide **3** (100 μM) for 30 min followed by fluorescence imaging.

E. Meggers *et al. ChemBioChem* **2012**, *13*, 1116-1120

2-2. Reduction by HCO_2H (1)

Reductive alkylation by [Ir-H] and HCO_2^-

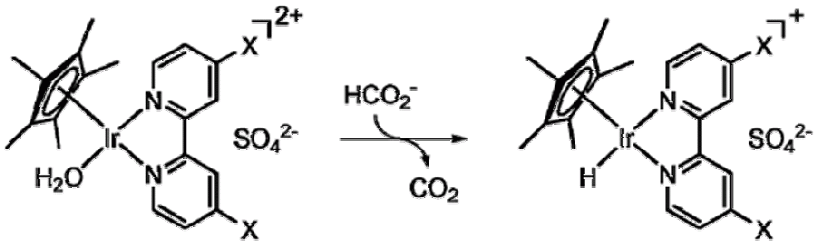

1a: X = H
1b: X = OMe
1c: X = CO_2Et

2a: X = H
2b: X = OMe
2c: X = CO_2Et

1b was best
(**1a** afford small amount of **2a**,
1c gave no product(data not shown))

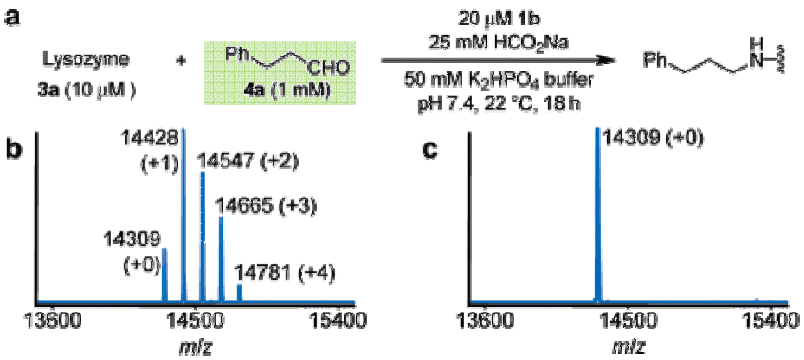

Figure 1. Modification of lysozyme using reductive alkylation. Under the reaction conditions summarized in (a), a distribution of alkylated products results (b). (c) Control experiments lacking catalyst yielded no reaction products. Spectra shown are reconstructed from charge ladders obtained using ESI-MS analysis.

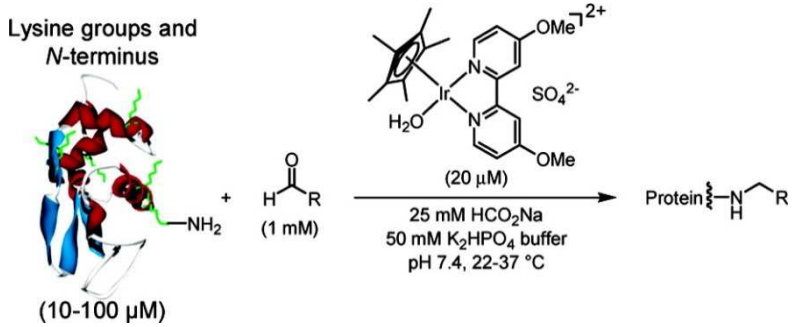

Table 1. Reductive Alkylation of Proteins Using **4a** and **1b**[a]

entry	protein	[1b] (μM)	*T* (°C)	Unmod (%)	+1 (%)	+2 (%)	+3 (%)	+4 (%)
1	**3a** (100 μM)	20	22	6	21	37	25	11
2	**3a** (100 μM)	10	37	20	33	29	16	2
3	**3a** (100 μM)	5	37	48	38	31	1	0
4	**3a** (100 μM)	2	37	84	16	0	0	0
5	**3a** (10 μM)	20	22	15	32	34	19	trace
6	**3b** (100 μM)	20	22	11	19	27	22	12[b]
7	**3c** (100 μM)	20	37	24	47	27	2	0
8	**3d** (100 μM)	20	37	85	15	0	0	0
9	**3e** (100 μM)	20	37	59	41	0	0	0
10	**3f** (100 μM)	20	37	70	30	trace	0	0

[a] Additional conditions: 1 mM **4a**, 25 mM HCO_2Na, 50 mM K_2HPO_4, pH 7.4, 18−22 h. Protein substrates: lysozyme (**3a**), cytochrome *c* (**3b**), α-chymotrypsinogen A (**3c**), h. h. myoglobin (**3d**), ribonuclease A (**3e**), and bacteriophage MS2 (**3f**). Product distributions were determined from ESI-MS analyses. [b] **3b** also gave small amounts of +5 (5%) and +6 (3%).

M. B. Francis *et al. J. Am. Chem. Soc*. **2005**, *127*, 13490-13491

2-2. Reduction by HCO_2H (1)

Aldehyde substrate scope

Table 2. Modification of Lysozyme (**3a**) By Reductive Alkylation[a]

Aldehyde/Ketone		Unmod (%)	+1 (%)	+2 (%)	+3 (%)	+4 (%)
4b	CH_3CH_2CHO	72	28	0	0	0
4c		41	43	16	0	0
4d	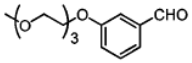	6	26	40	23	5
4e	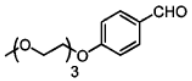	60	34	6	0	0
4f	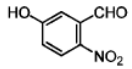	14	41	36	9	0
4g		100	0	0	0	0
4h	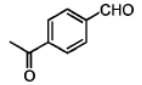	18	46	29	7	0
4i	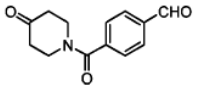	33	52	15	0	0

[a] Conditions: 100 μM lysozyme, 1 mM **4b**−**i**, 20 μM **1b**, 25 mM sodium formate, 50 mM K_2HPO_4, pH 7.4, 22 °C, 22 h. Product distributions were determined using ESI-MS analysis.

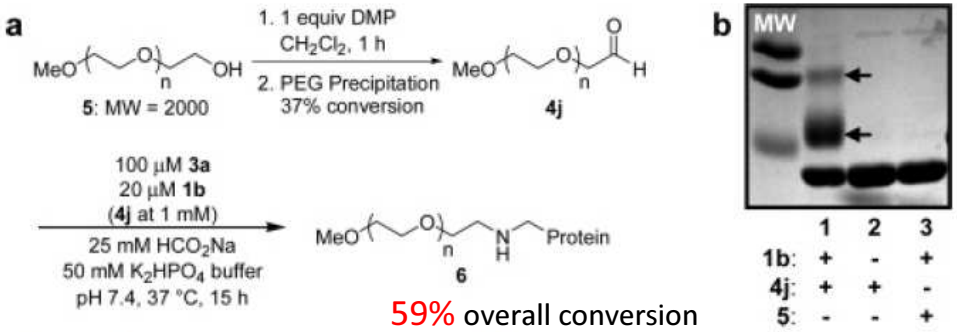

Figure 2. Conjugation of PEG to lysozyme using a simple two-step procedure. (a) Commercially available PEG alcohols can be oxidized to afford aldehydes before conjugation to proteins via reductive alkylation. (b) SDS−PAGE analysis of **6** shows the formation of singly and doubly alkylated conjugates. Control reactions run in the absence of catalyst (lane 2) or aldehyde (lane 3) afforded no conjugates. MW ladder: 25, 20, and 15 kD (from top). Lysozyme MW = 14.3 kD.

M. B. Francis *et al. J. Am. Chem. Soc*. **2005**, *127*, 13490-13491

2-2. Reduction by HCO_2H (2)-0

Precedents

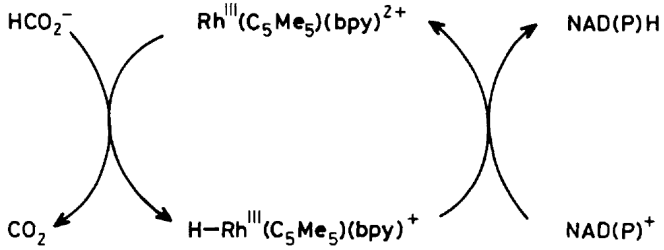

E. Steckhan *et al. J. Chem. Soc., Chem. Commun.* **1988**, 1150-1151

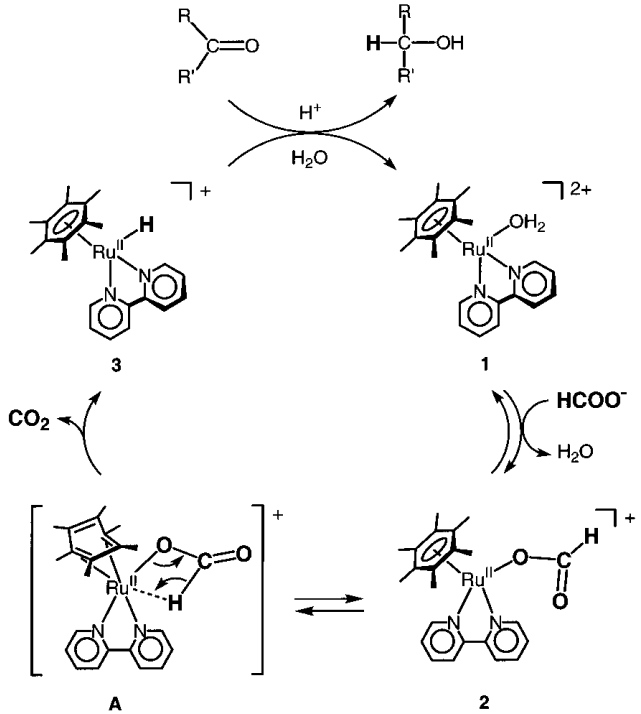

Y. Watanabe *et al. Organometallics,* **2002**, *21*, 2964-2969

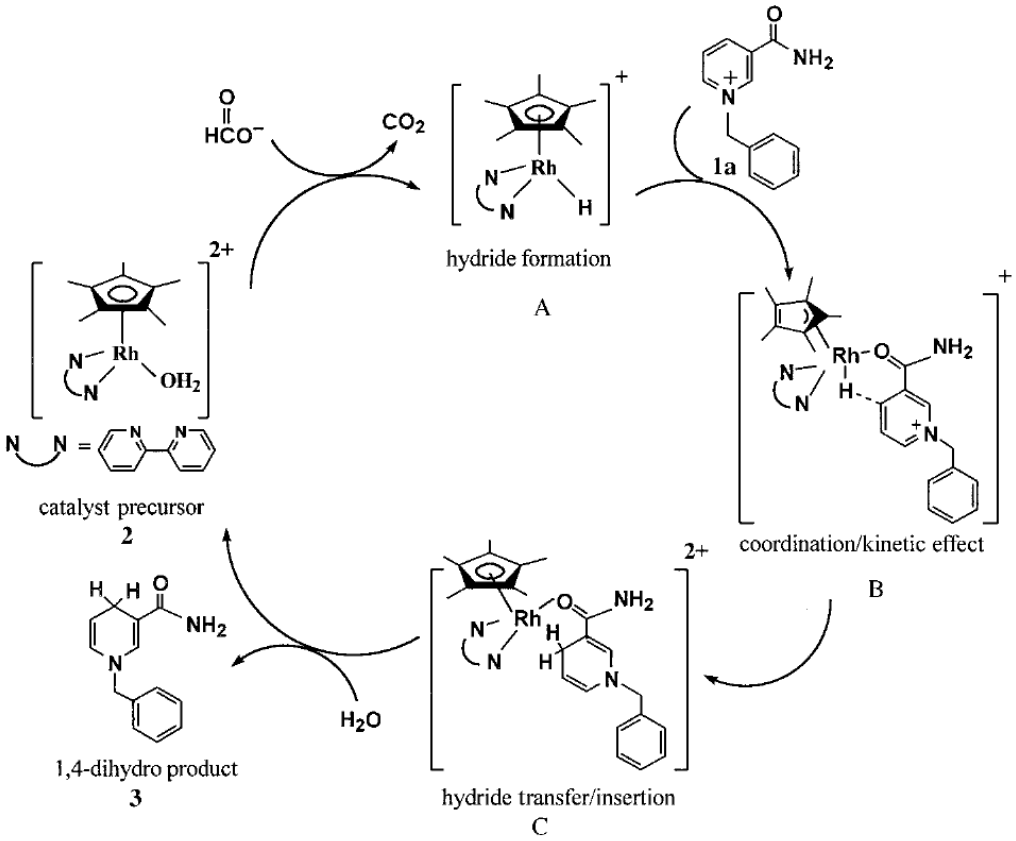

R. H. Fish *et al. Angew. Chem. Int. Ed.* **1990**, *38*, 1429-1432
R. H. Fish *et al. Inorg. Chem.* **2001,** *40,* 6705-6716

*Ir, Ru complex also reduce NAD^+ to NAD catalytically
P. Stepnicka *et al. Eur. J. Inorg. Chem.* **2007**, 4736-4742

2-2. Reduction by HCO_2H (2)-1

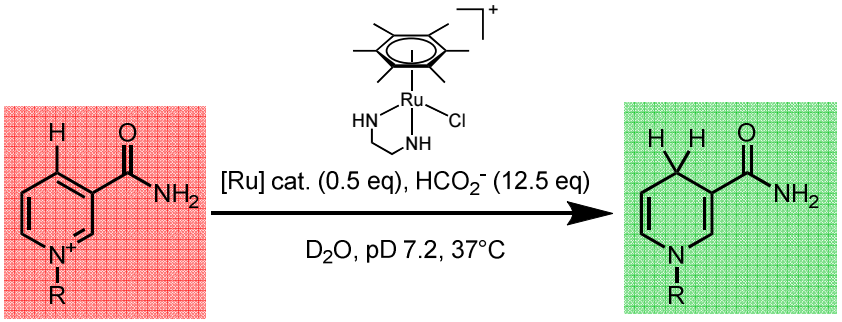

[Ru] complex reduces NAD^+

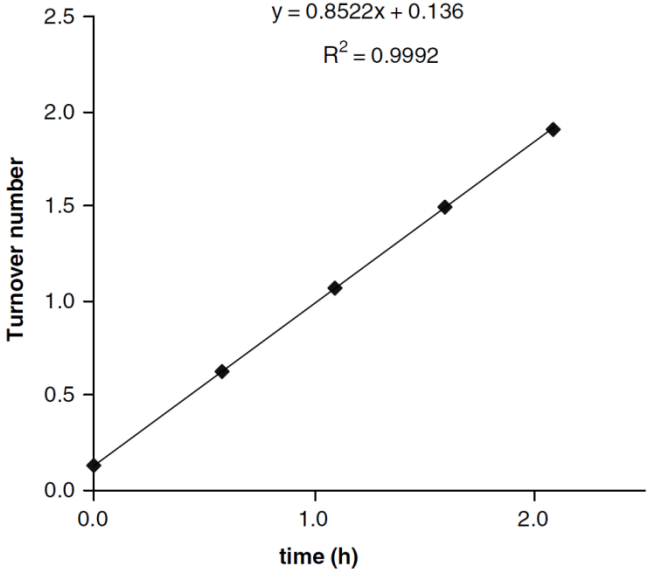

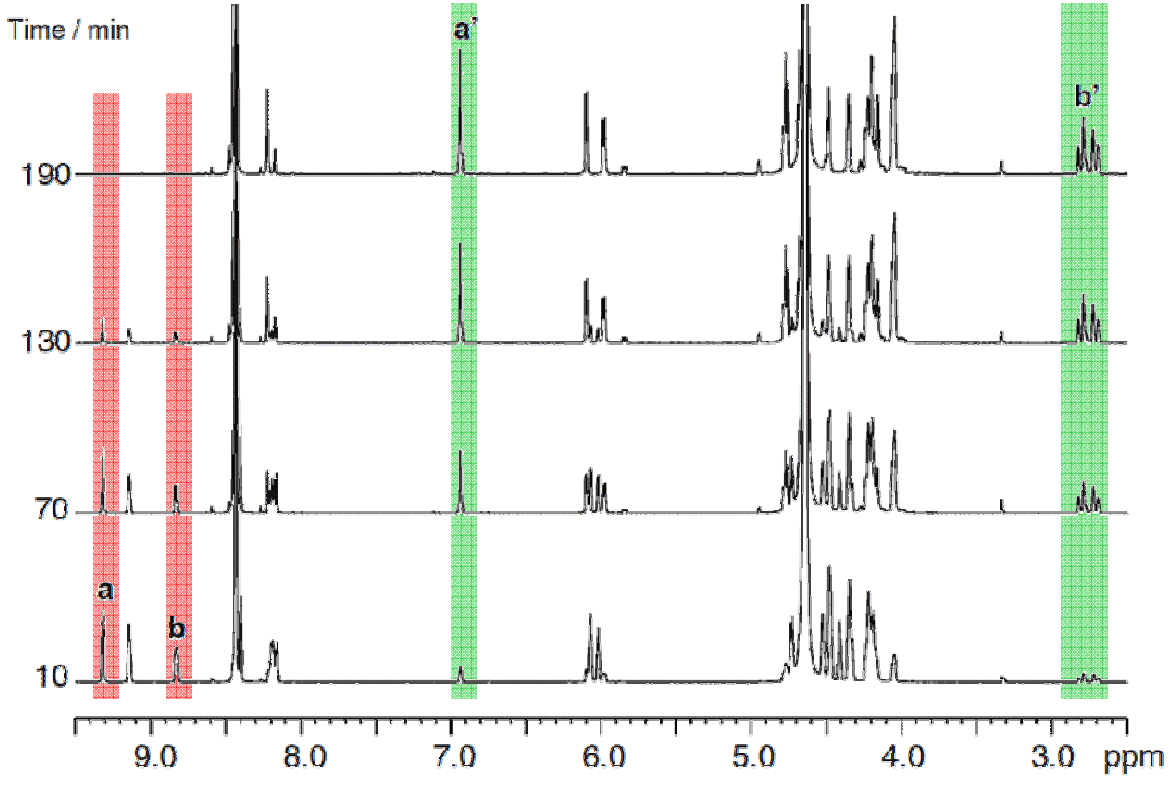

P. J. Sadler *et al. J. Biol. Inorg. Chem.* **2006**, *11*, 483-488

2-2. Reduction by HCO_2H (2)-2

Ligand effects

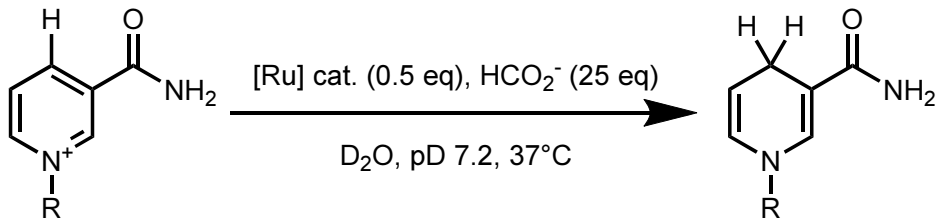

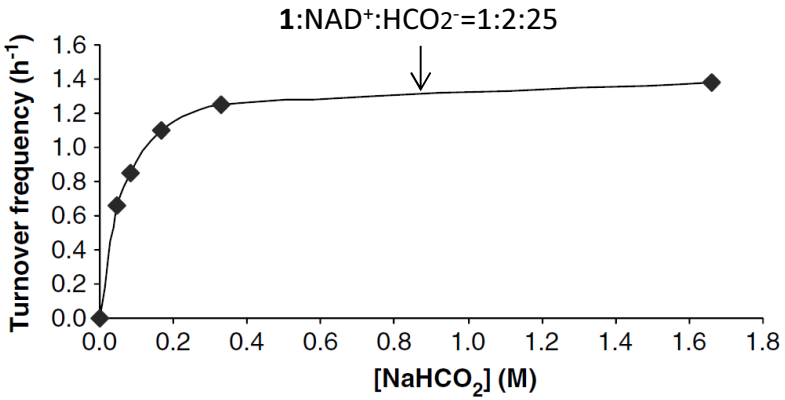

A549 (lung cancer cells)were tolerant to 2.5 mM HCO_2^- (highest concentration in this test, data not shown)

	Turnover frequency (h^{-1})
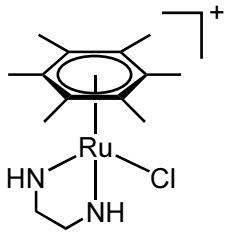	0.85
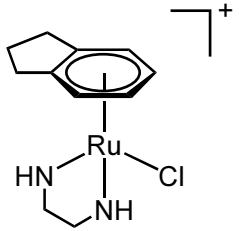	0.16
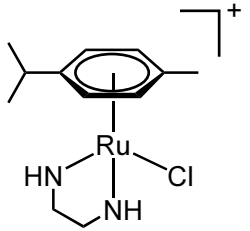	0.18
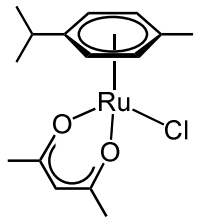	0.05

P. J. Sadler *et al. J. Biol. Inorg. Chem.* **2006**, *11*, 483-488

2-3. Reduction by NADH (1)-1

[Ru-H] (also [Ir-H]) reduces pyruvate

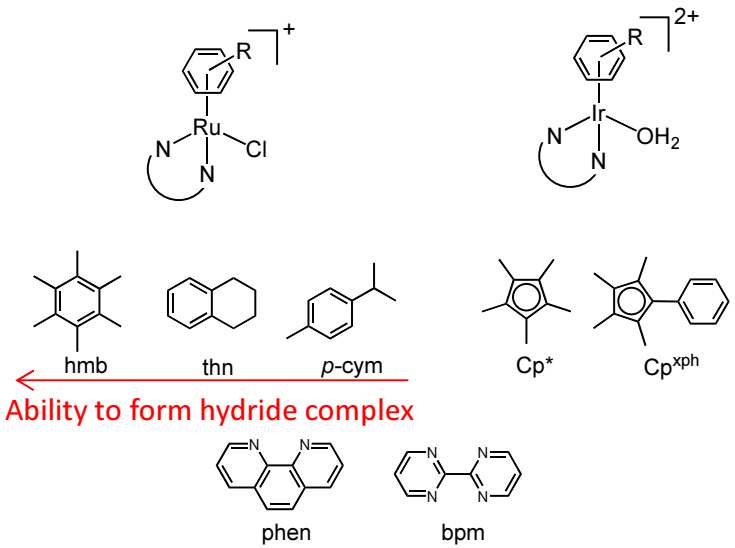

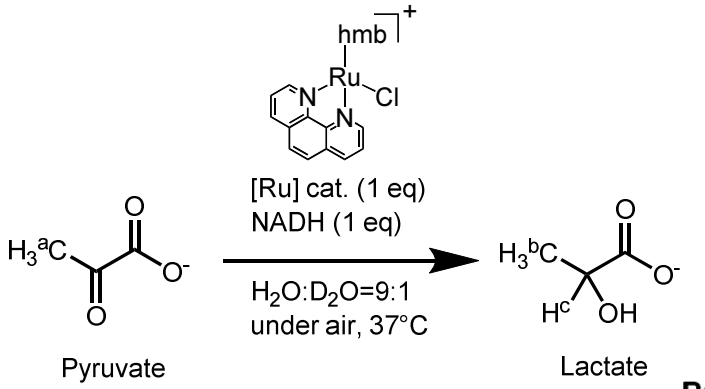

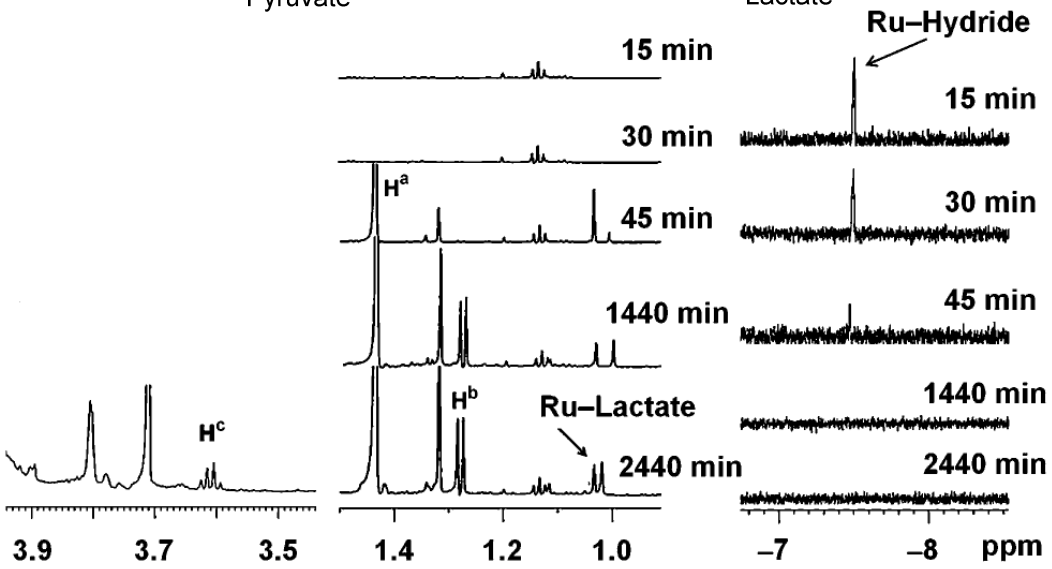

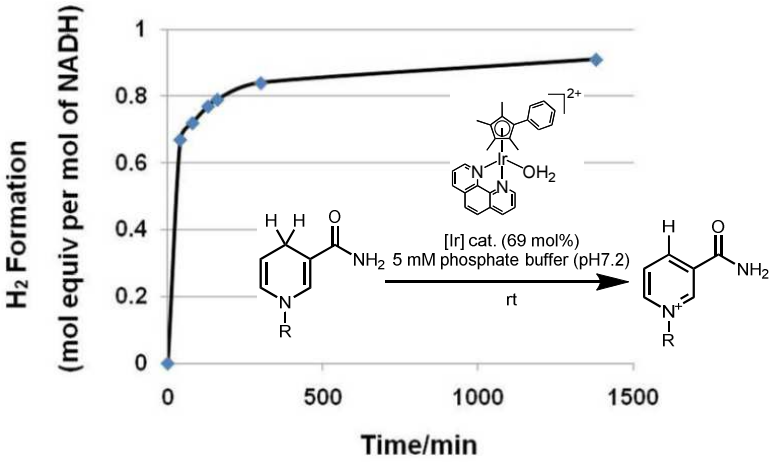

P. J. Sadler *et al.*, *Angew. Chem. Int. Ed*. **2012**, *51*, 3897 –3900

2-3. Reduction by NADH (1)-2

Proposed mechanism of hydride migration

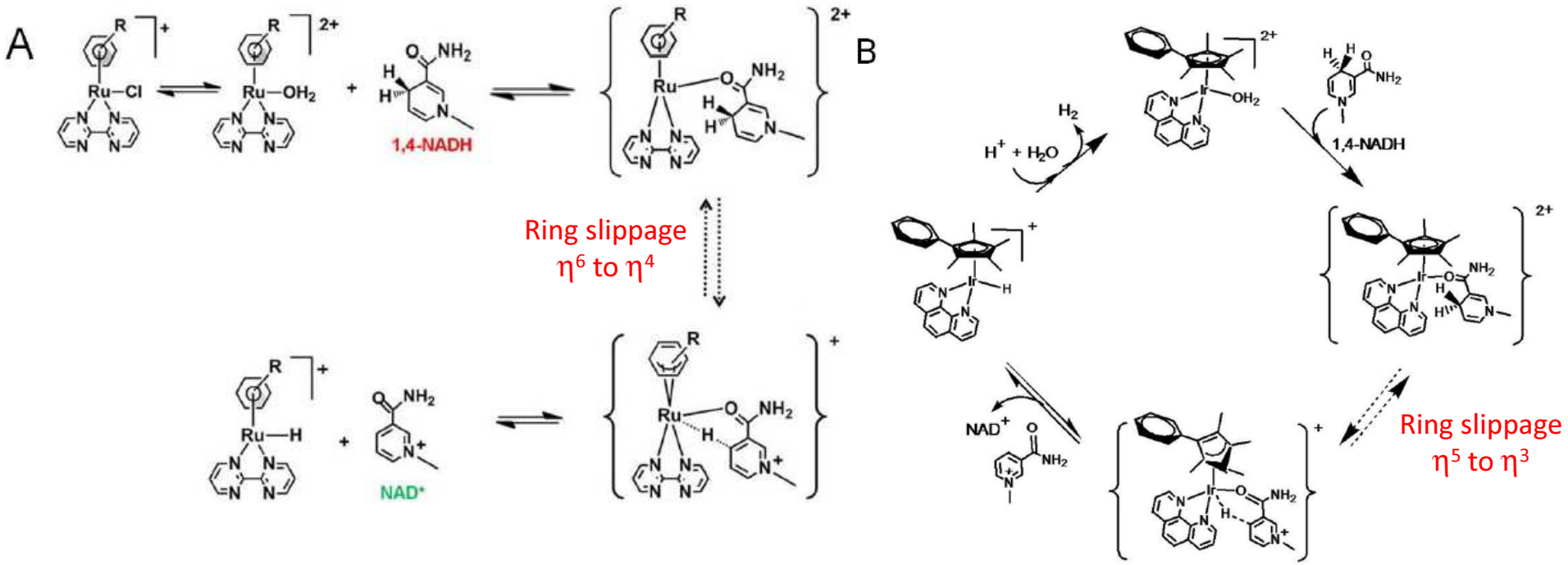

Figure S8. Proposed mechanism for transfer of hydride from 1,4-NADH to (*A*) Ru^{II} complexes **1**, **2**, and **4**, and (*B*) Ir^{III} complex (**7**).

Ring Slip Reaction of Cp*Rh complex

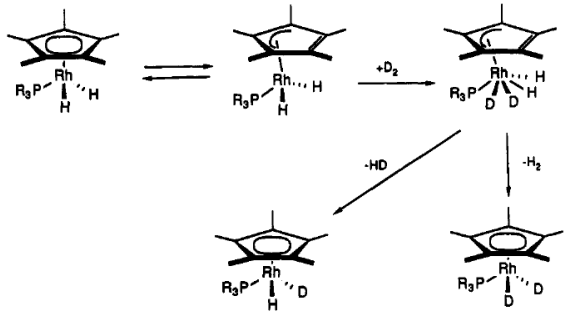

A. D. Selmeczy *et al. Organometallics* **1991**, *10*, 1577-1586.

P. J. Sadler *et al.*, *Angew. Chem. Int. Ed*. **2012**, *51*, 3897 –3900

2-3. Reduction by NADH (2)-1

[Ir-H] reduces quinones to…?

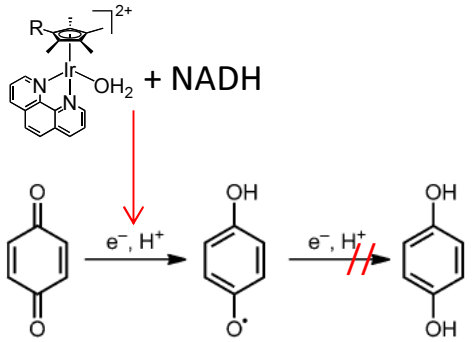

Scheme 1. One- and two-electron reduction of a quinone (e.g. benzoquinone) leading to semiquinone and hydroquinone, respectively.

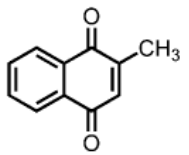

menadione
(Vitamin K_3)

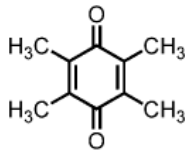

duroquinone

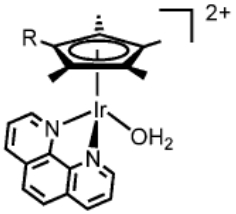

1 R = Me
3 R = Ph

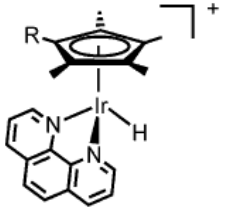

2 R = Me
4 R = Ph

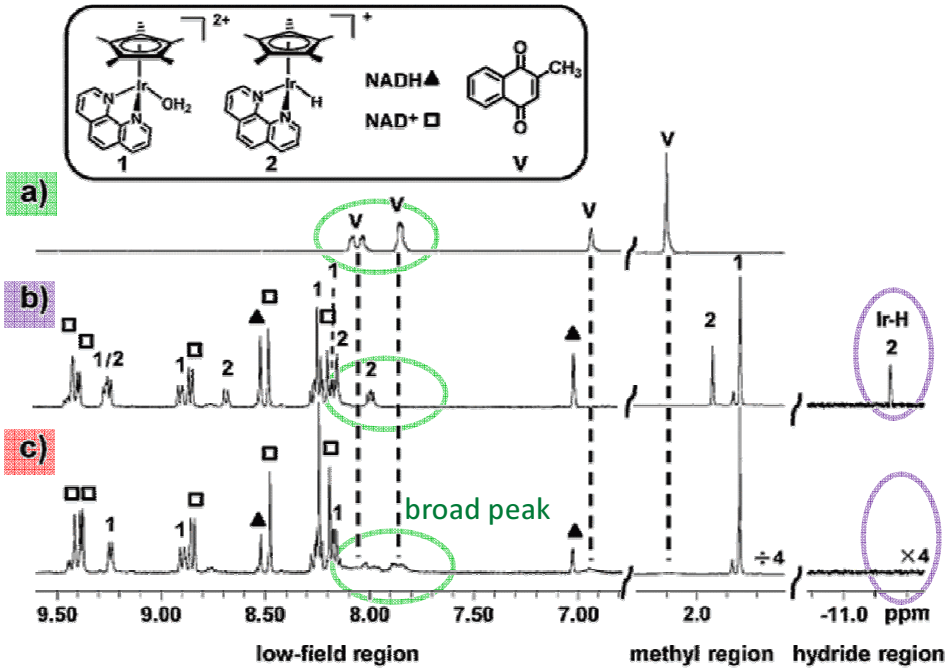

Figure 1. ^{1}H NMR spectra showing the formation of complex **2** [(η^5-C_5Me_5)Ir(phen)(H)]$^+$ and its reaction with menadione in [D_4]MeOD/H_2O (1:9) at 298 K. a) Menadione alone. b) Formation of hydrido complex **2** from reaction of [(η^5-C_5Me_5)Ir(phen)(H_2O)]$^{2+}$ (1; 1 mM) with NADH (2 mM). c) Disappearance of signals of hydride **2** and broadening of signals of menadione 10 min after addition of menadione (1 mM) to mixture in (b).

P. J. Sadler *et al.*, *Angew. Chem. Int. Ed*. **2013**, *52*, 4194-4197

2-3. Reduction by NADH (2)-2

[Ir-H] reduces quinones to semiquinone radical

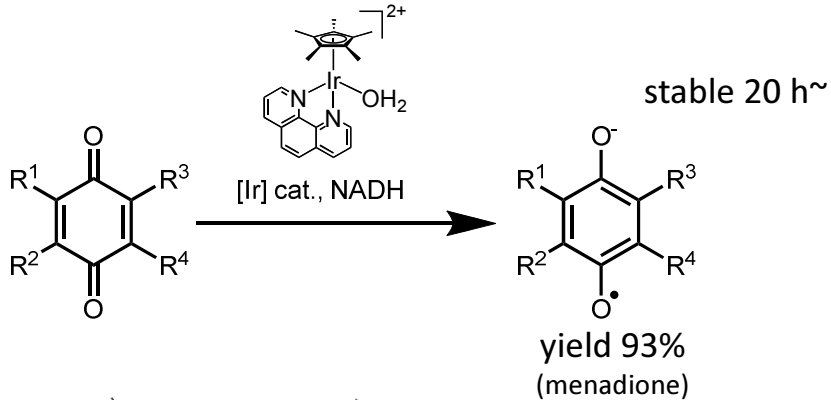

Figure 2. X-band EPR spectra at around 290 K. a) Menadione radical anion ($M^{\bullet-}$) generated by the reduction of menadione (1 mM) by NADH (0.5 mM) catalyzed by complex **1** or **3** (160 μM) in phosphate buffer (pH 7.2, 9 h). b) Simulated $M^{\bullet-}$ EPR spectrum with hyperfine coupling constants. c) Durosemiquinone radical anion ($D^{\bullet-}$) generated by reduction of duroquinone (2 mM) by NADH (1 mM) catalyzed by complex **1** or **3** (330 μM) in phosphate buffer (pH 7.2, 10 h). d) Simulated $D^{\bullet-}$ EPR spectrum with hyperfine coupling constants.

1 NADH reduces 2 quinone

menadione (VK_3)

Entry	Molar ratio 1: NADH: VK_3
1	1: 3: 25
2	1: 6: 25
3	1: 30: 80
4	1: 60: 120

duroquinone

Entry	Molar ratio 1: NADH: Duro
5	1: 30: 80
6	1: 15: 40

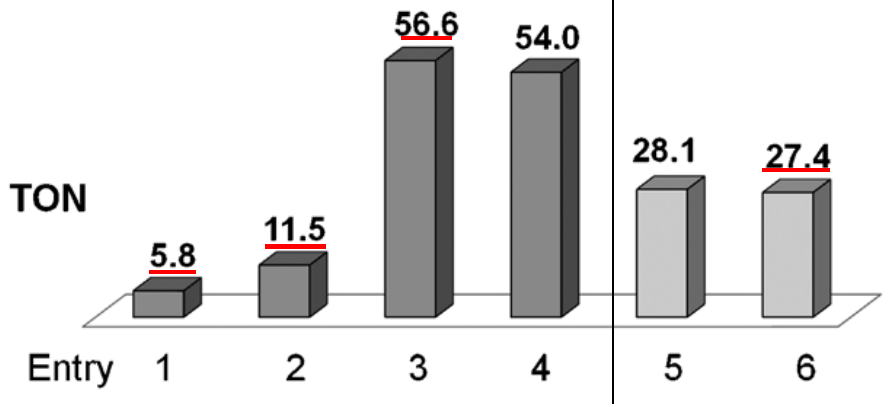

Figure 3. Reduction of menadione (VK_3, entries 1–4) and duroquinone (Duro, entries 5 and 6) by NADH catalyzed by complex **1** (80 μM).

P. J. Sadler *et al.*, *Angew. Chem. Int. Ed*. **2013**, *52*, 4194-4197

2-3. Reduction by NADH (2)-3

Proposed raction mechanism

a) One electron transfer × 2 (proposed)

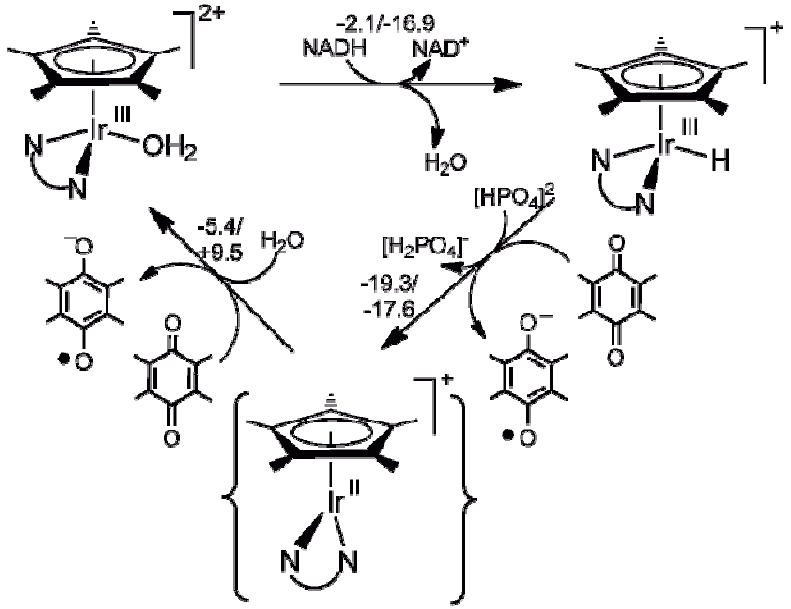

b) Two electron transfer

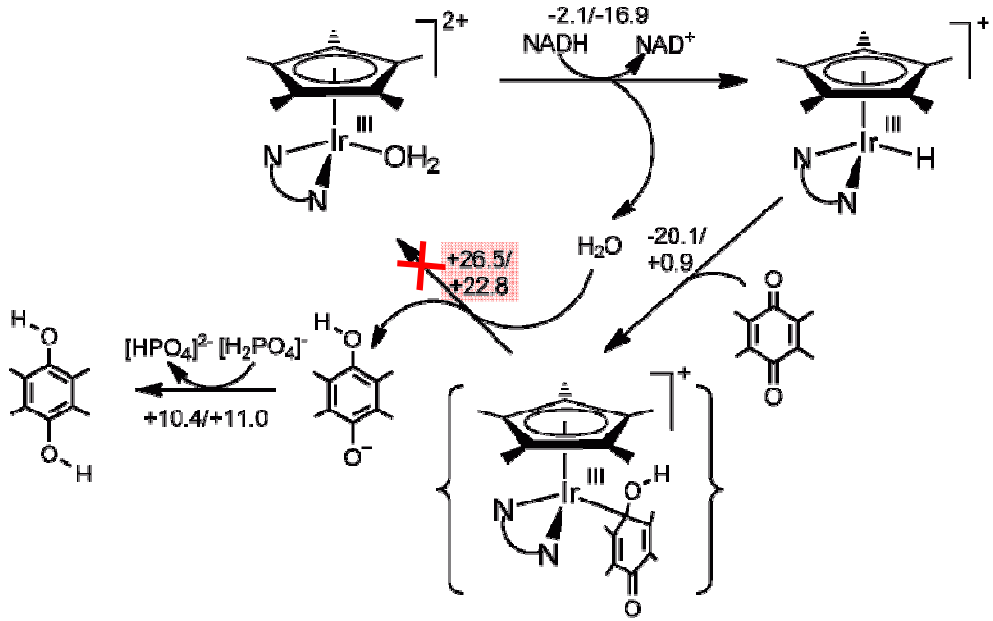

XX/YY is each potential-energy/free-energy difference (kcal・mol^{-1})
by DFT calculation

P. J. Sadler *et al.*, *Angew. Chem. Int. Ed*. **2013**, *52*, 4194-4197

Contents

3-0. History

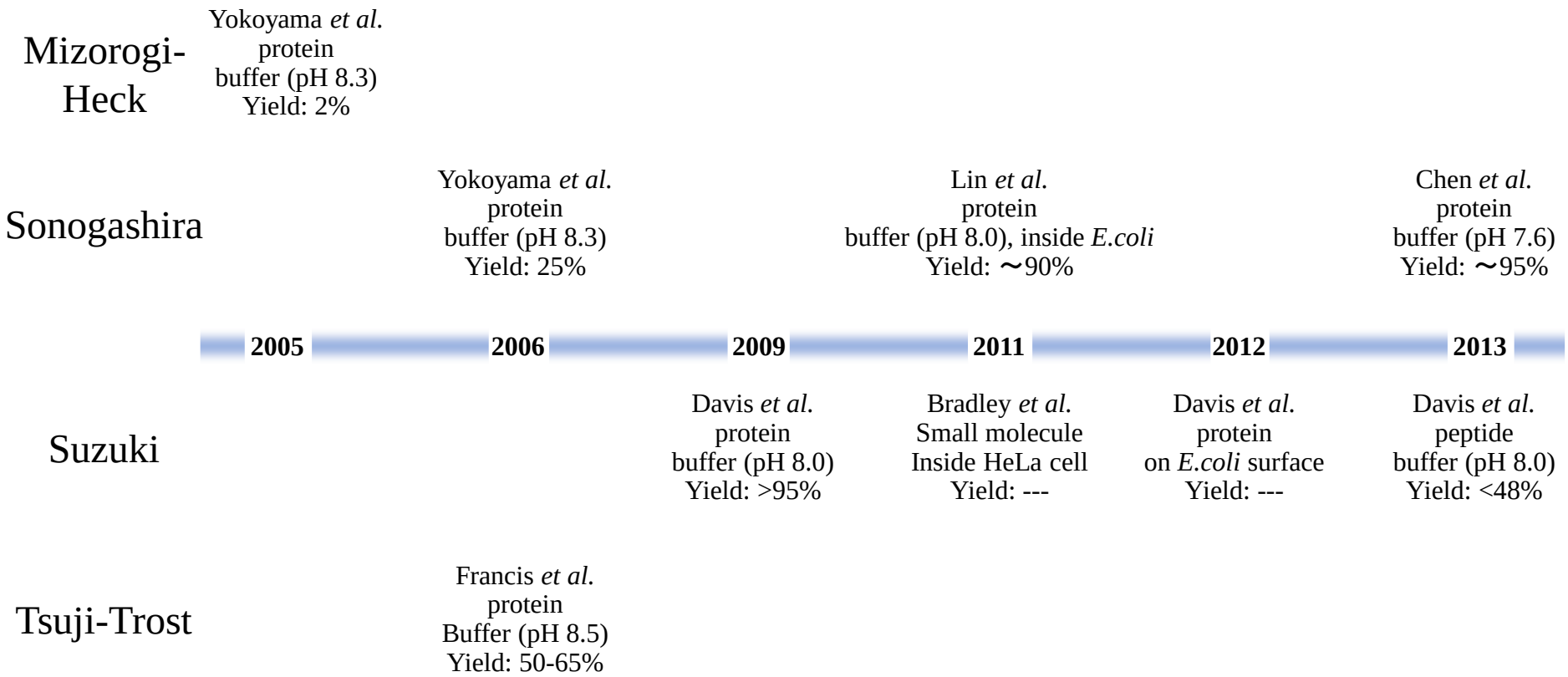
Mizorogi-Heck
Yokoyama *et al.*
protein
buffer (pH 8.3)
Yield: 2%
Sonogashira
Yokoyama *et al.*
protein
buffer (pH 8.3)
Yield: 25%
Lin *et al.*
protein
buffer (pH 8.0), inside *E.coli*
Yield: ～90%
Chen *et al.*
protein
buffer (pH 7.6)
Yield: ～95%
2005
2006
2009
2011
2012
2013
Suzuki
Davis *et al.*
protein
buffer (pH 8.0)
Yield: >95%
Bradley *et al.*
Small molecule
Inside HeLa cell
Yield: ---
Davis *et al.*
protein
on *E.coli* surface
Yield: ---
Davis *et al.*
peptide
buffer (pH 8.0)
Yield: <48%
Tsuji-Trost
Francis *et al.*
protein
Buffer (pH 8.5)
Yield: 50-65%

3-1. Mizorogi-Heck reaction

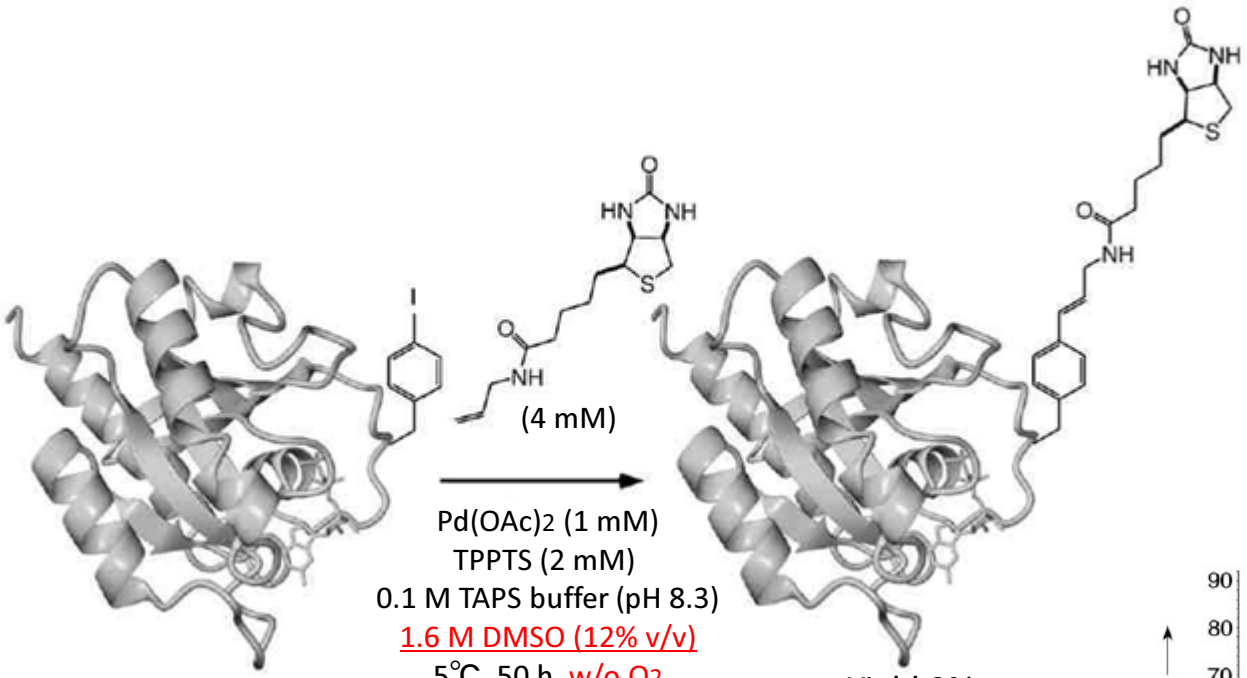

(*p*-I-Phe)32-Ras-His (13 μM)

Yield 2%
(28% : dehalogenated,
70% : starting material)
by protease→LC-MS/MS

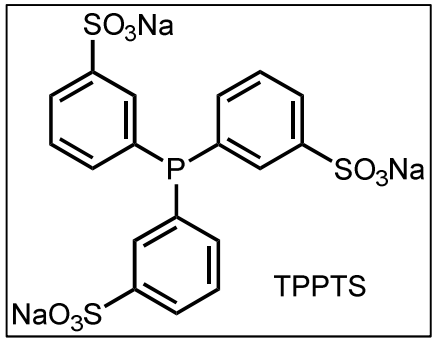

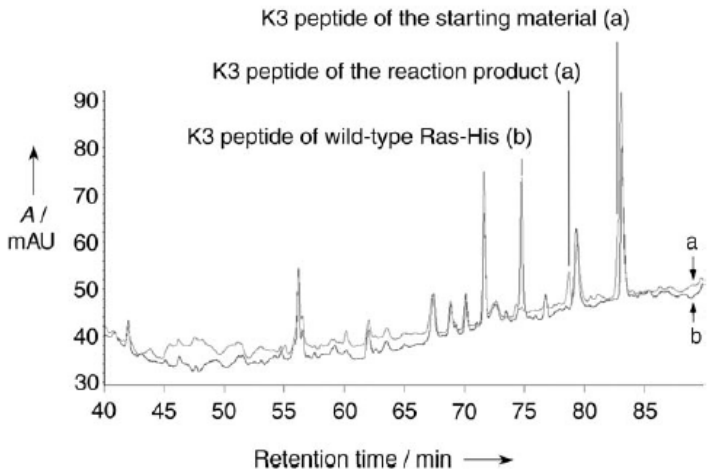

Figure 2. The HPLC chromatogram for Lys-C peptides of a) the crude reaction product and b) those of intact wild-type Ras-His, with ultraviolet (UV) detection at 215 nm. The K3 peptide (17–42) of the biotinylated product (bF32-Ras-His) and that of the dehalogenated product (iF32-Ras-His) were eluted as an overlapped peak at 77.9 min.

S. Yokoyama *et al. ChemBioChem* **2006**, *7*, 134-139

3-2. Sonogashira coupling (1)

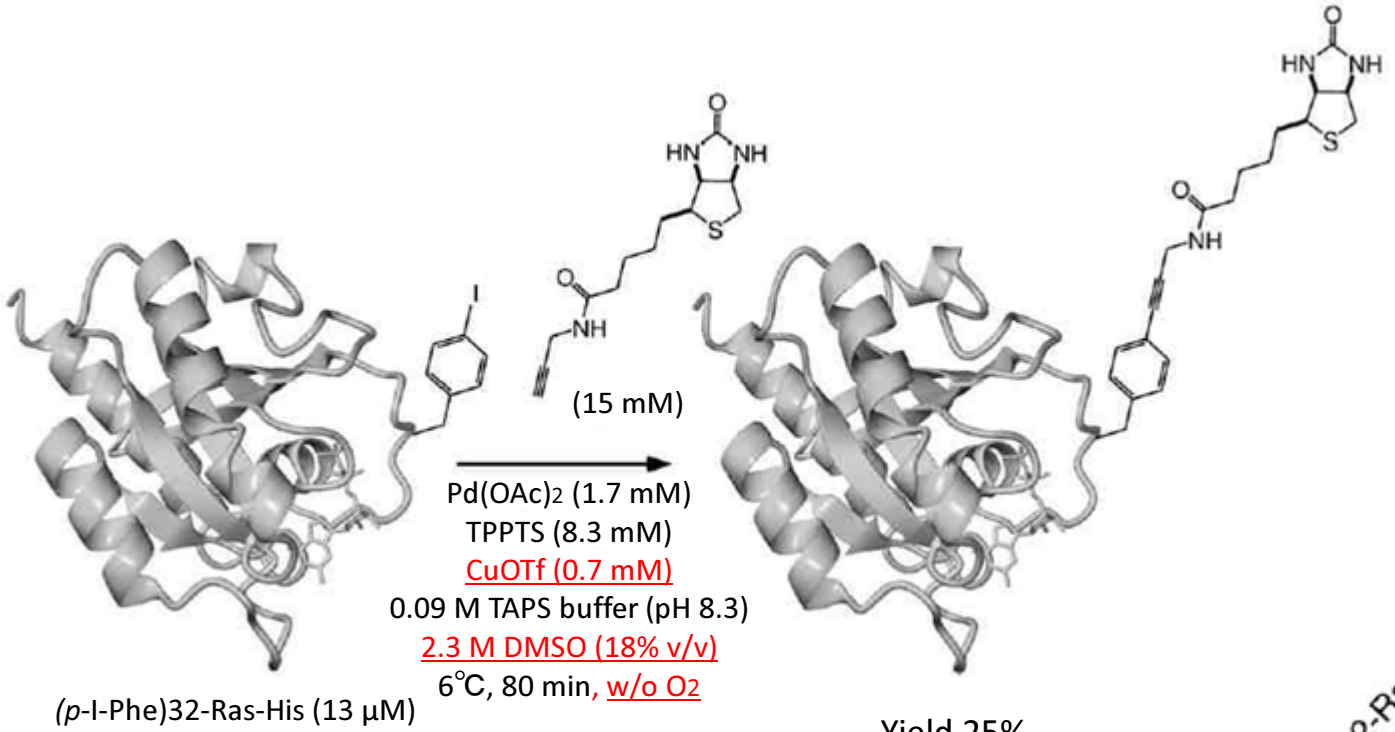

(*p*-I-Phe)32-Ras-His (13 μM)

Yield 25%
(13%:dehalogenated)

by SDS-PAGE,
protease→LC-MS/MS analysis

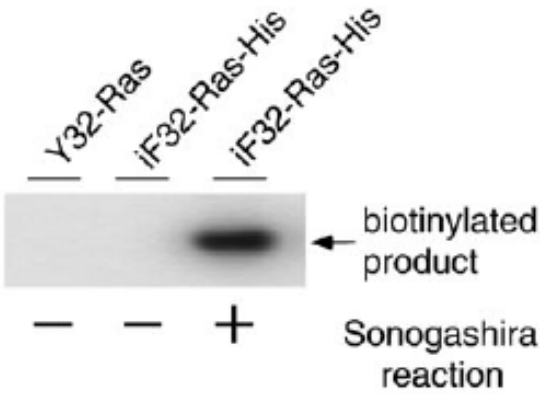

Detected by Streptoavidin-HRP

S. Yokoyama *et al. ChemBioChem* **2007**, *8*, 232-238

3-2. Sonogashira coupling (2)-1

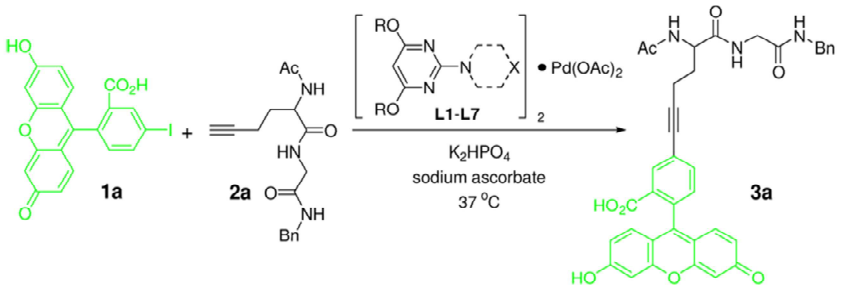

Good Suzuki-coupling Ligand in water*

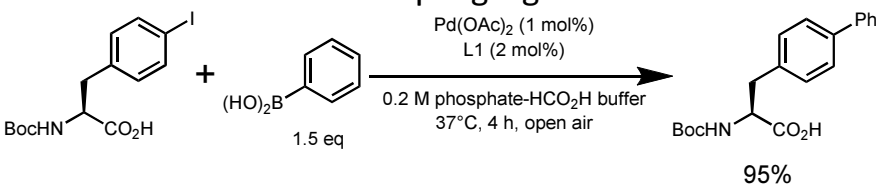

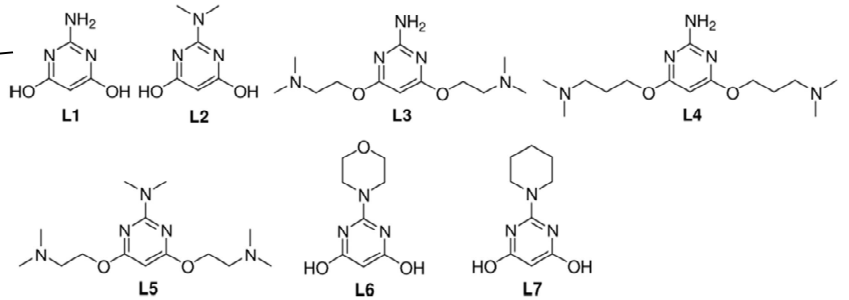

And Good Cu-free Sonogashira coupling Ligand in organic solvent**

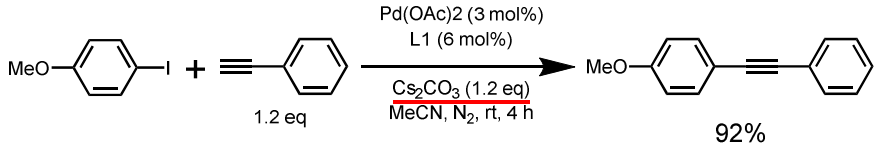

Entry	1a : 2a	Pd • ligand	Ligand	Time	Yield (%) *b*
1	1.05:1.00	20%	**L1**	30 min	NR
2	1.05:1.00	20%	**L2**	30 min	59
3	1.05:1.00	20%	**L3**	30 min	<5
4	1.05:1.00	20%	**L4**	30 min	<5
5	1.05:1.00	20%	**L5**	30 min	29
6	1.05:1.00	20%	**L6**	30 min	<5
7	1.05:1.00	20%	**L7**	30 min	13
8	1.00:2.40	30%	**L2**	40 min	91

[b]HPLC yield

Q. Lin *et al. J. Am. Chem. Soc*. **2011**, *133*, 15316-15319

*Described more detail in "3-3. Suzuki coupling (1)"
B. G. Davis *et al. J. Am. Chem. Soc*. **2009**, *131*, 16346-16347

Y. –X. Xie *et al*. *Eur. J. Org. Chem.* **2005, 4256–4259

3-2. Sonogashira coupling (2)-2

3. Pd

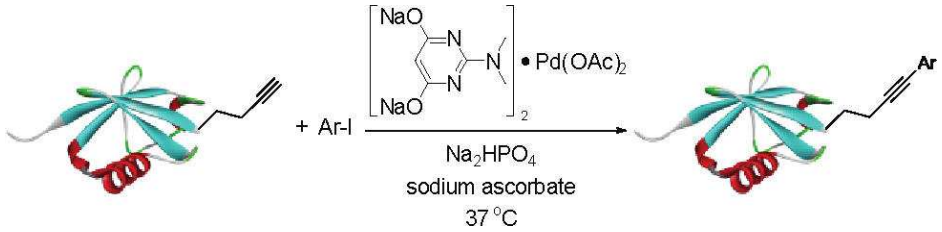

*Mixture of Ar-I, Pd complex, and sodium ascorbate was stirred at 37°C for 60 min to activate

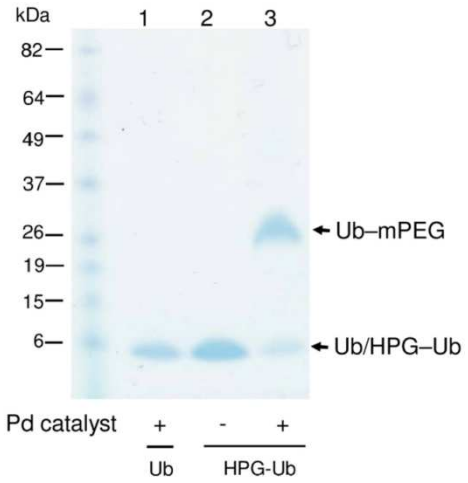

Ar-I =

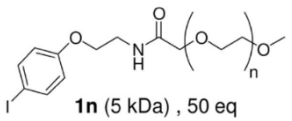

1n (5 kDa) , 50 eq

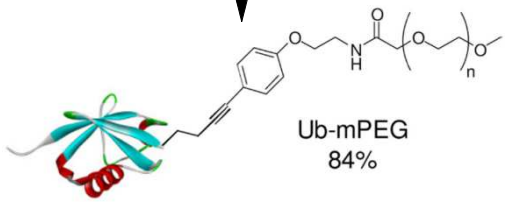

HPG:homopropargylglycine

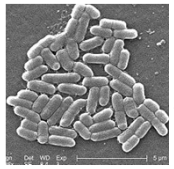

1a (100 μM)
$Pd(OAc)_2 \cdot L_2$ (1 mM)
5 mM sodium ascorbate

2 mM phosphate buffer (pH 8)
DMSO (0.1 mM), 37°C, 4 h

Centrifugation
(Figure a)

fluorescence
(Figure b, left)
+
Coomassie blue staining
(Figure b, right)

HPG-Ub overexpressing *E. coli*

1 : control (w/o Pd complex)
2 : add **1a** and Pd
3 : add preactivated 1a and Pd
(stirred at 37°C, 1 h before adding)

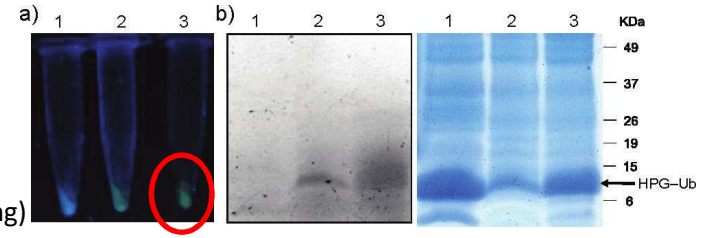

Entry	Ar-I	Time	Yield (%)[b]
1	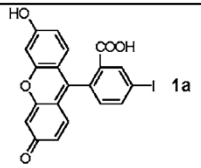 **1a**	30 min	93
2	 **1b**	30 min	83
3	 **1c**	30 min	55
4	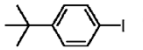 **1d**	30 min	86
5	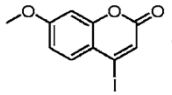 **1e**	240 min	73[c]
6	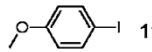 **1f**	30 min	83
7	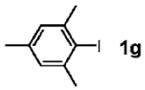 **1g**	180 min	73
8	 **1h**	30 min	82
9	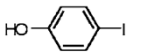 **1i**	30 min	85
10	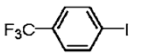 **1j**	30 min	78
11	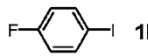 **1k**	30 min	79
12	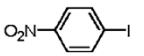 **1l**	180 min	66
13	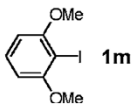 **1m**	180 min	60

[b]LC-MS yield

Q. Lin *et al. J. Am. Chem. Soc.* **2011**, *133*, 15316-15319

3-2. Sonogashira coupling (3)-1

Ligand-free, $Pd(NO_3)_2$ shows best conversion

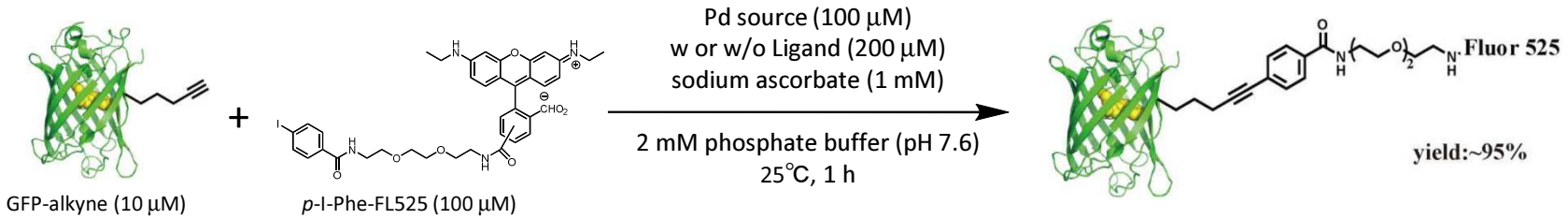

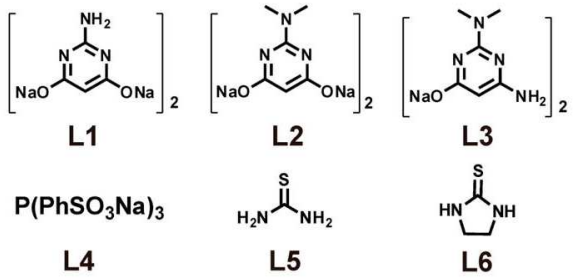

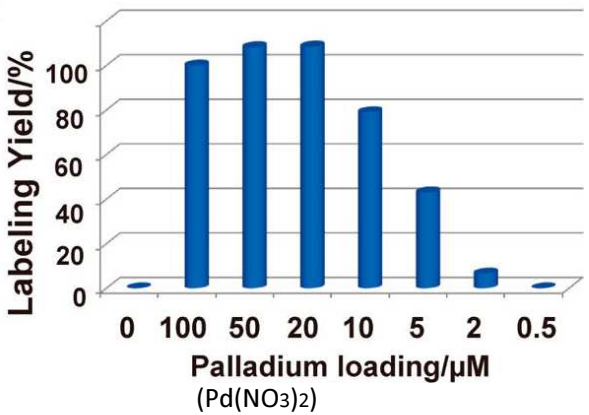

Entry	Ligand	Pd source	Yield(%)[b]
1	L1[a]	$Pd(OAc)_2$	< 5
2	L2[a]	$Pd(OAc)_2$	53
3	L3[a]	$Pd(OAc)_2$	< 5
4	—	$Pd(OAc)_2$	11
5	—	**Na_2PdCl_4**	**90**
6	—	$PdCl_2$	25
7	—	**$Pd(NO_3)_2$**	**95**
8	L4	Na_2PdCl_4	82
9	L4	$Pd(OAc)_2$	64
10	—	$Pd_2(dba)_3$	57
11	L5	$Pd(OAc)_2$	< 5
12	L6	$Pd(OAc)_2$	< 5

[b]calculated from sample florescence on SDS-PAGE

P. R. Chen *et al. J. Am. Chem. Soc.* **2013**, *135*, 7330−7338

3-2. Sonogashira coupling (3)-2

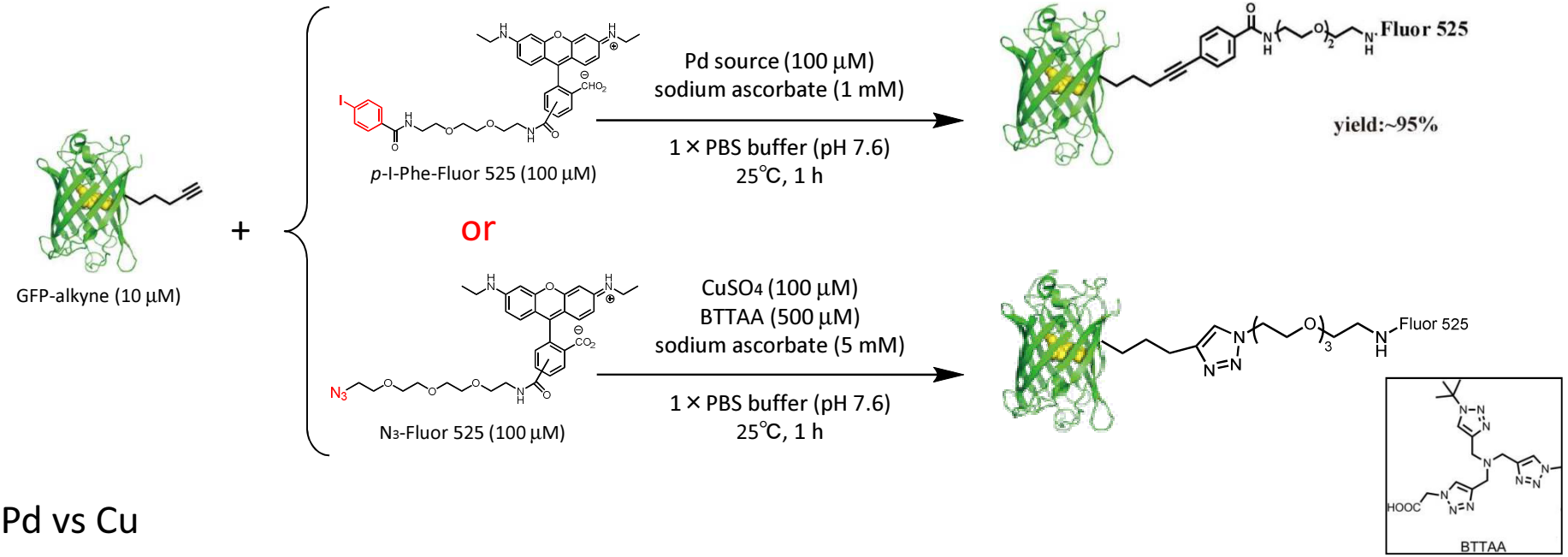

Pd vs Cu

Reaction dynamics

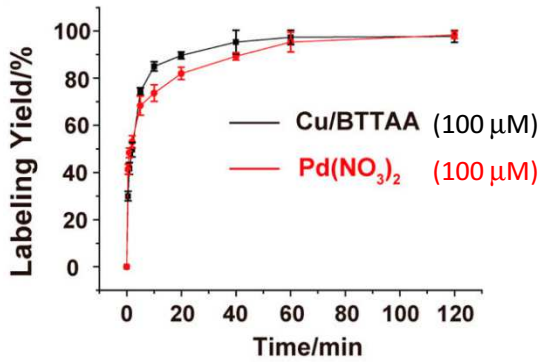

*Same reaction condition as above

Protein deactivation

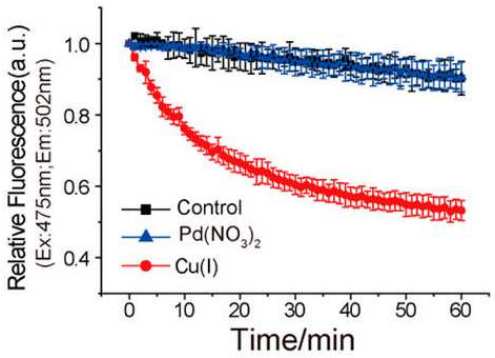

*GFP (10 μM) +
Pd(NO3)2 (100 μM) or Cu(I) (100 μM)

Acute toxicity

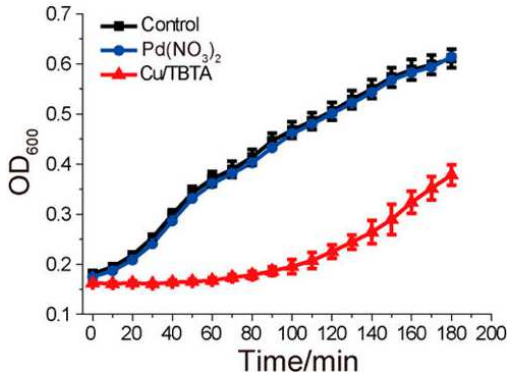

*Pd(NO3)2 (200 μM) or Cu(I) (200 μM)
incubate 25℃, 1 h

P. R. Chen *et al. J. Am. Chem. Soc.* **2013**, *135*, 7330−7338

3-3. Suzuki coupling (1)

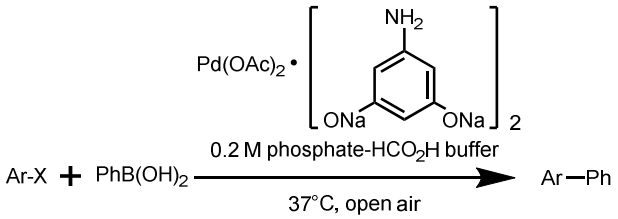

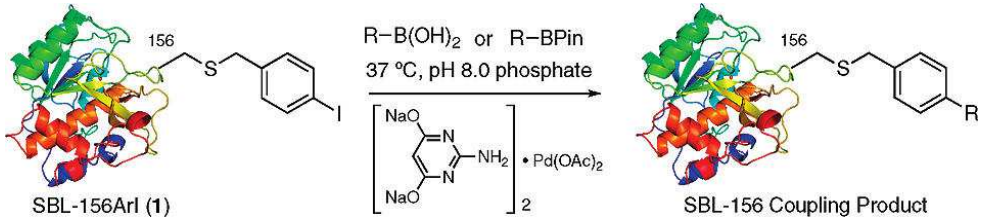

Entry	ArX	Pd Loading	Conditions	Coupling Product	Yield (%)
1	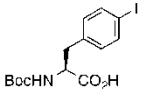	1%	37 °C, 4 h	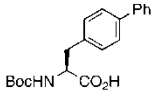	95
2	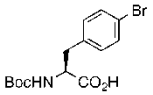	1%	37 °C, 4 h	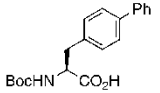	98
3	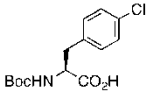	1%	37 °C, 4 h	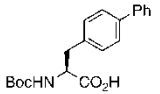	0
4	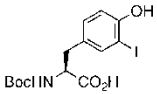	1%	37 °C, 4 h	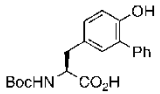	94
5	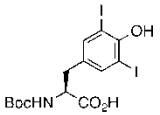	2%	37 °C, 4 h	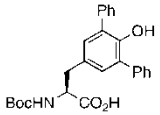	95
6	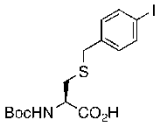	1%–10%	37 °C, 6 h	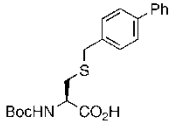	0
7	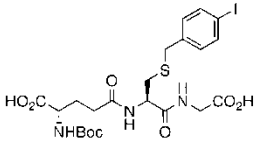	4%	37 °C, 6 h	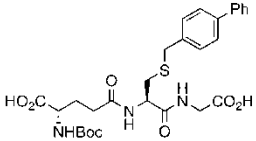	92

?

Entry	R-B(OH)$_2$ / R-BPin	Time	Conversion
1	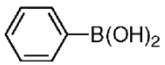	30 min	> 95%
2	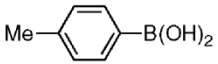	30 min	> 95%
3	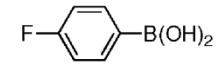	30 min	> 95%
4	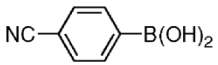	30 min	> 95%
5	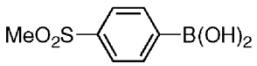	30 min	> 95%
6	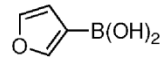	30 min	> 95%
7	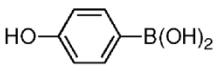	30 min	> 95%
8	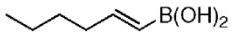	30 min	> 95%
9	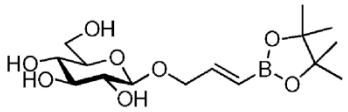	60 min	> 95%

B. G. Davis *et al. J. Am. Chem. Soc*. **2009**, *131*, 16346-16347

3-3. Suzuki coupling (2)

Cell-surface labeling (*E. coli*)

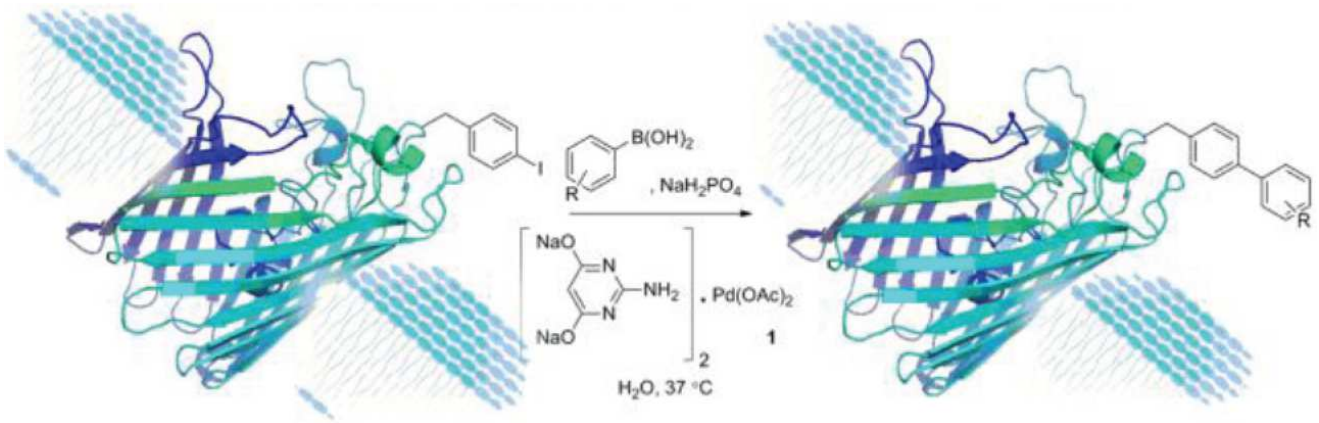

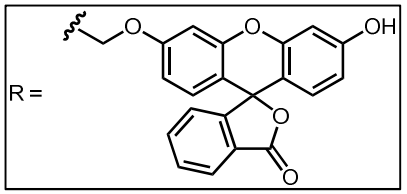

control

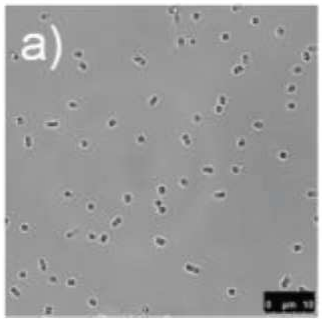

p-I-Phe mutant

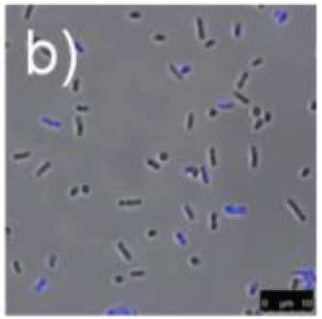

Fluorescence observed

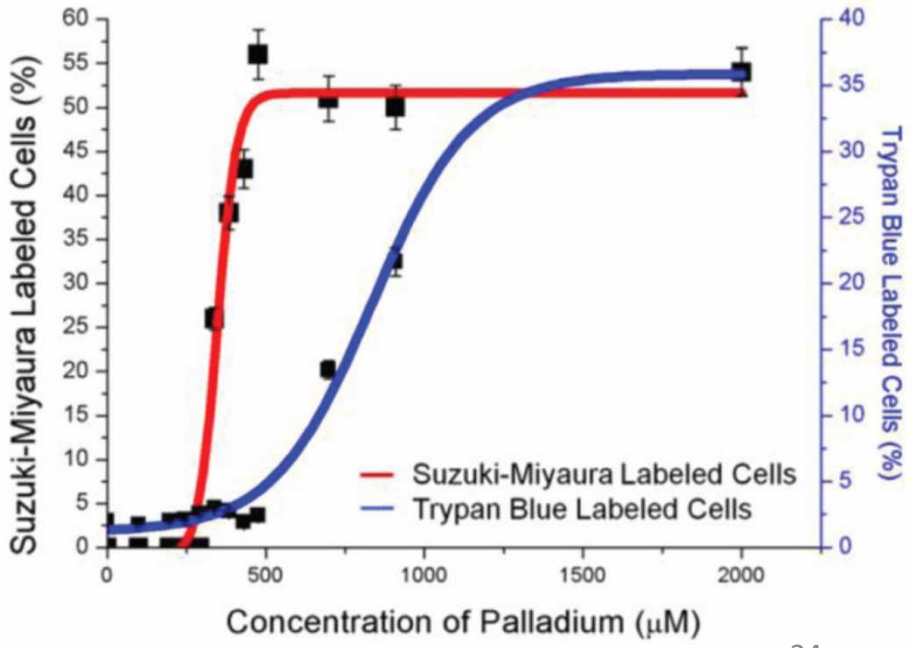

B. G. Davis *et al. J. Am. Chem. Soc.* **2012**, *134*, 800-803

3-3. Suzuki coupling (3)-1

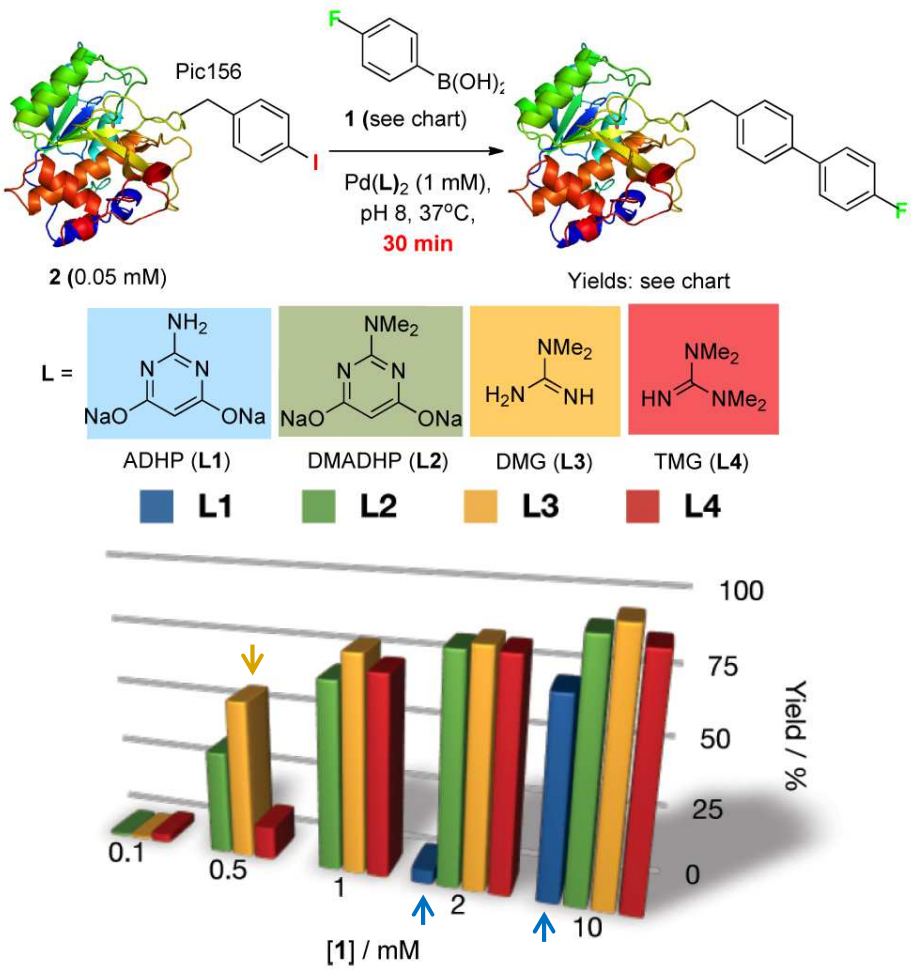

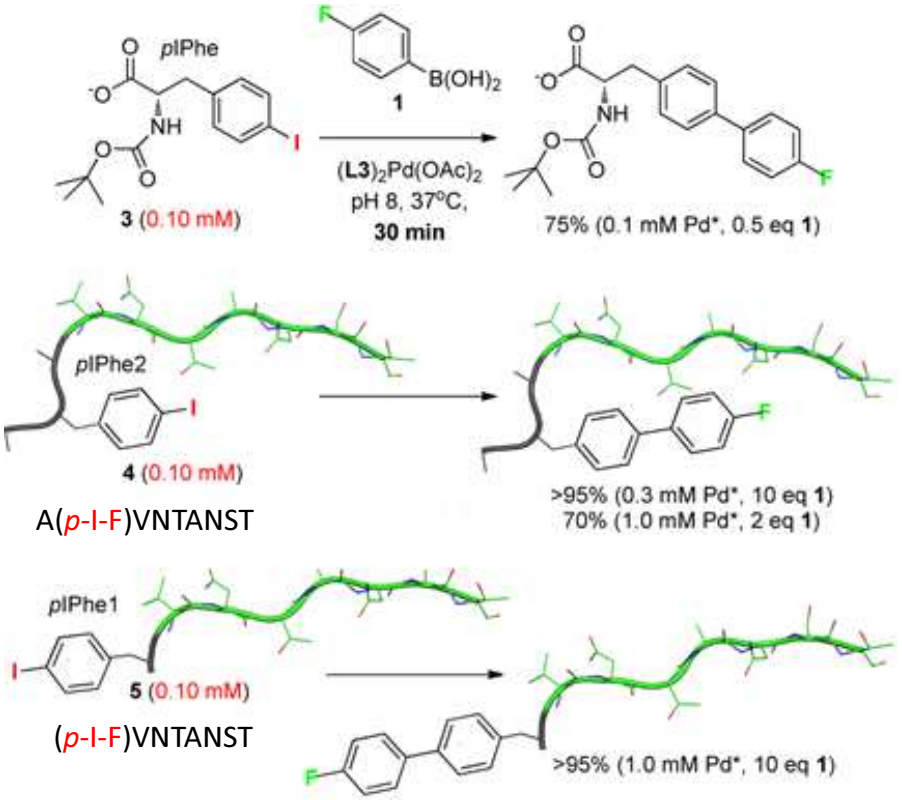

VNTANST sequence :
Comprehensive carcinoma homing peptide

B. G. Davis *et al. J. Am. Chem. Soc*. **2013**, *135*, 13612-13615

3-3. Suzuki coupling (3)-2

^{18}F・・・PET tracer, $t_{1/2}$=109 min

<1 h total reaction time is desired for PET

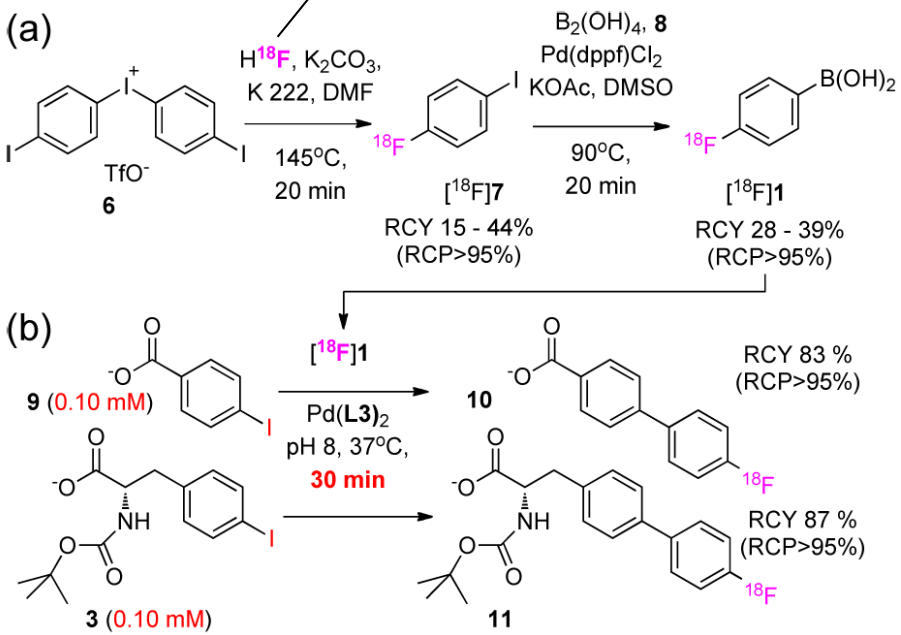

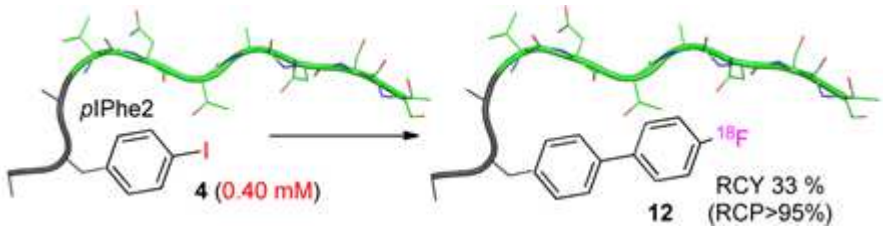

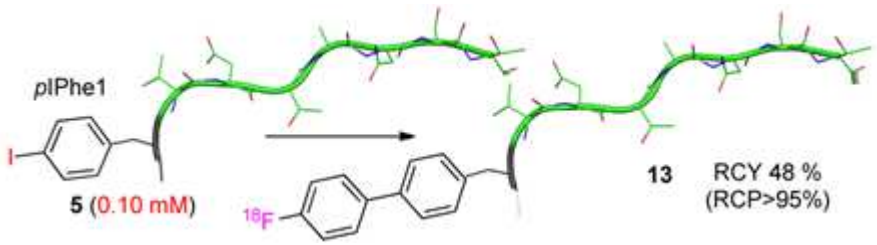

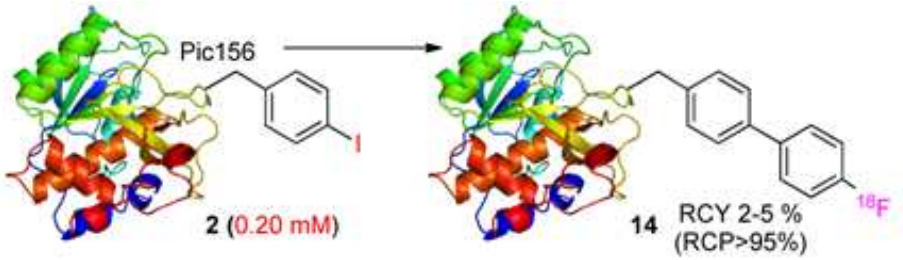

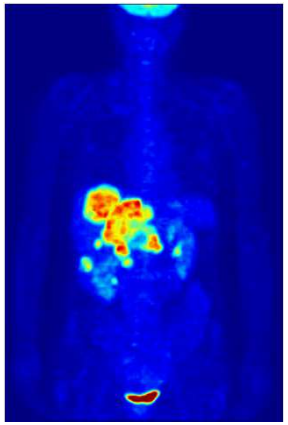

^{18}F-DG whole body PET imaging

Source:wikipedia, ポジトロン断層法

B. G. Davis *et al. J. Am. Chem. Soc*. **2013**, *135*, 13612-13615

3-3. Suzuki coupling (4)-1

Pd^0 microsphere synthesis

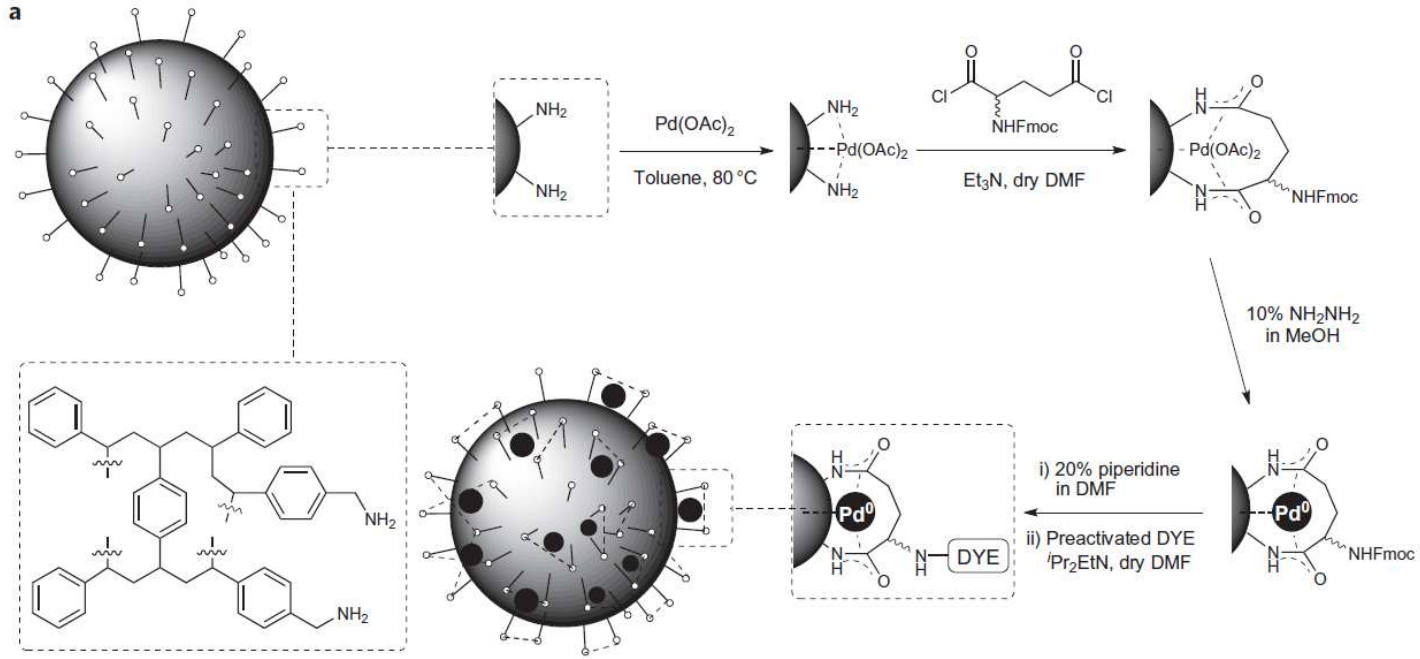

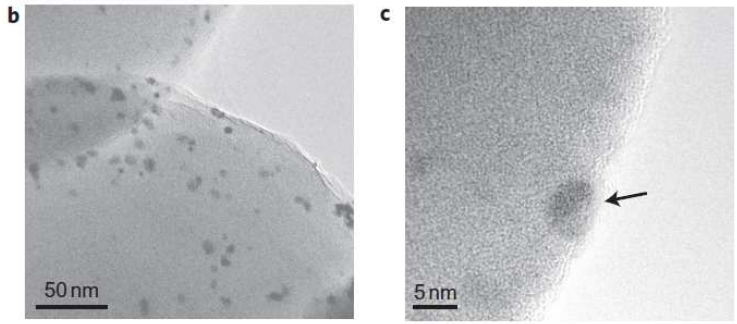

TEM of Pd^0 nanoparticle

Powder XRD patterns

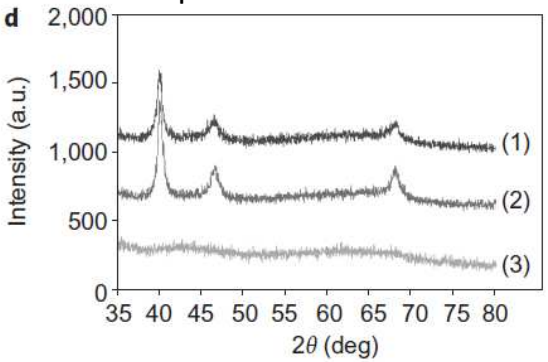

Pd^0 microsphere

Pd^0 powder

Naked microsphere

M. Bradley *et al. Nat. Chem.* **2011**, 3, 241-243

3-3. Suzuki coupling (4)-2

Pd microspheres are taken into cells (24 h, 75%~)

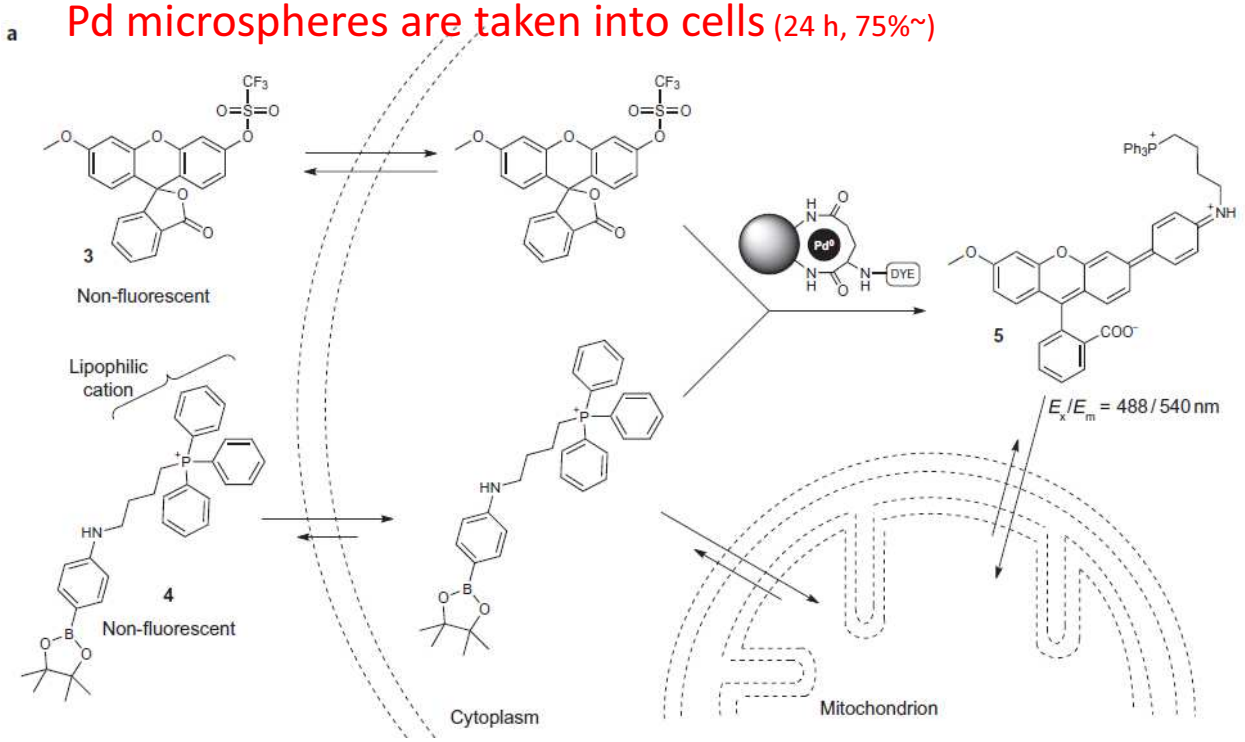

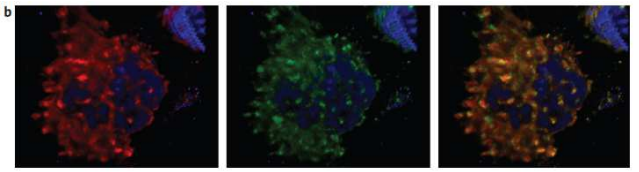

Mitochondria(red)
Synthesized compound **5**(green)
merged

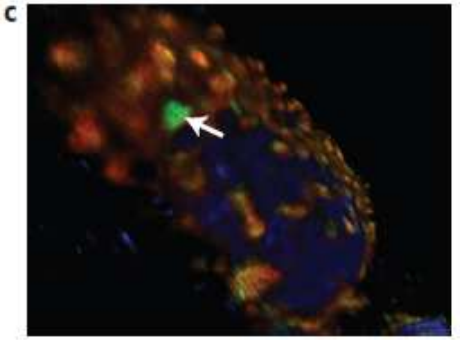

Allow: Pd microsphere
(not localized within mitochondria)

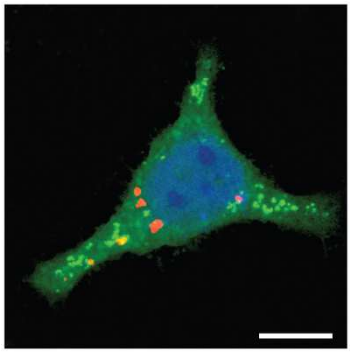

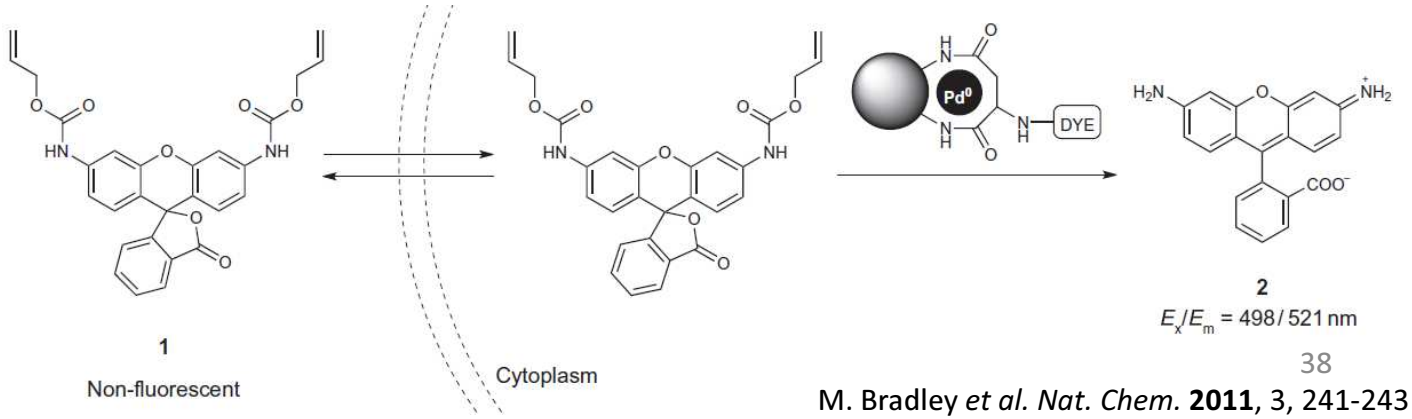

M. Bradley *et al. Nat. Chem.* **2011**, 3, 241-243

3-4. Tsuji-Trost Reaction

3. Pd

Also see Mr Suzuki's Literature Seminar (2013)

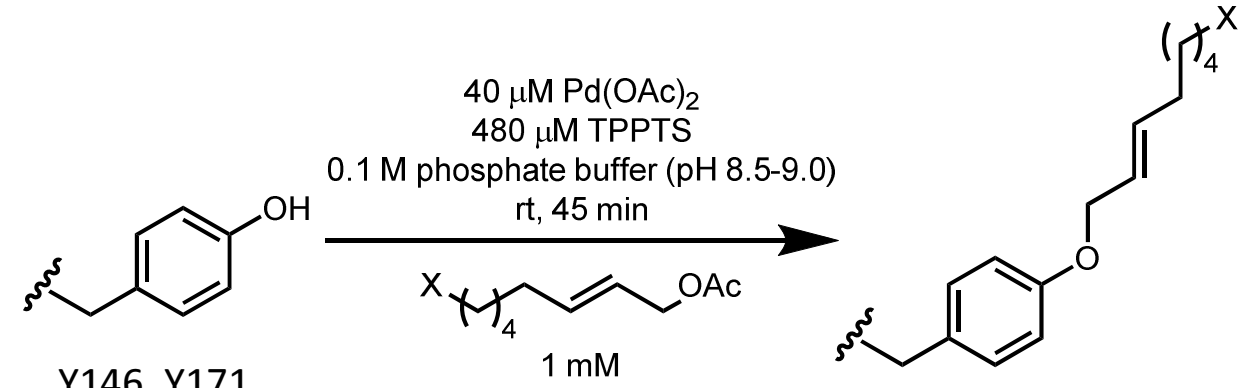

Y146, Y171
in chymotrypsinogen A

50-65% (by HPLC)
Mainly **Y171**-alkylated product

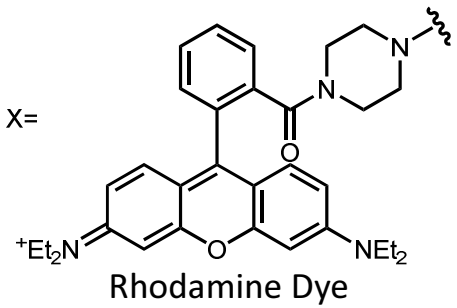

Rhodamine Dye

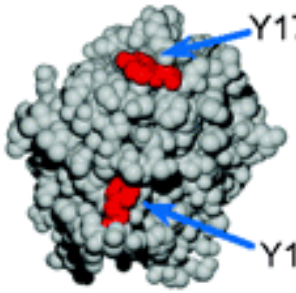

Y171 (most accessible)

Y146 (secondaly accessible)

Chymotrypsinogen A

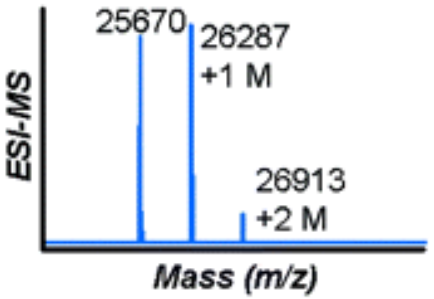

Lys-NH_2, Cys-SH and other residue were intact

M. B. Francis *et al. J. Am. Chem. Soc.* **2006**, *128*, 1080-1081

Contents

4-1. Photo Cross Linking-1

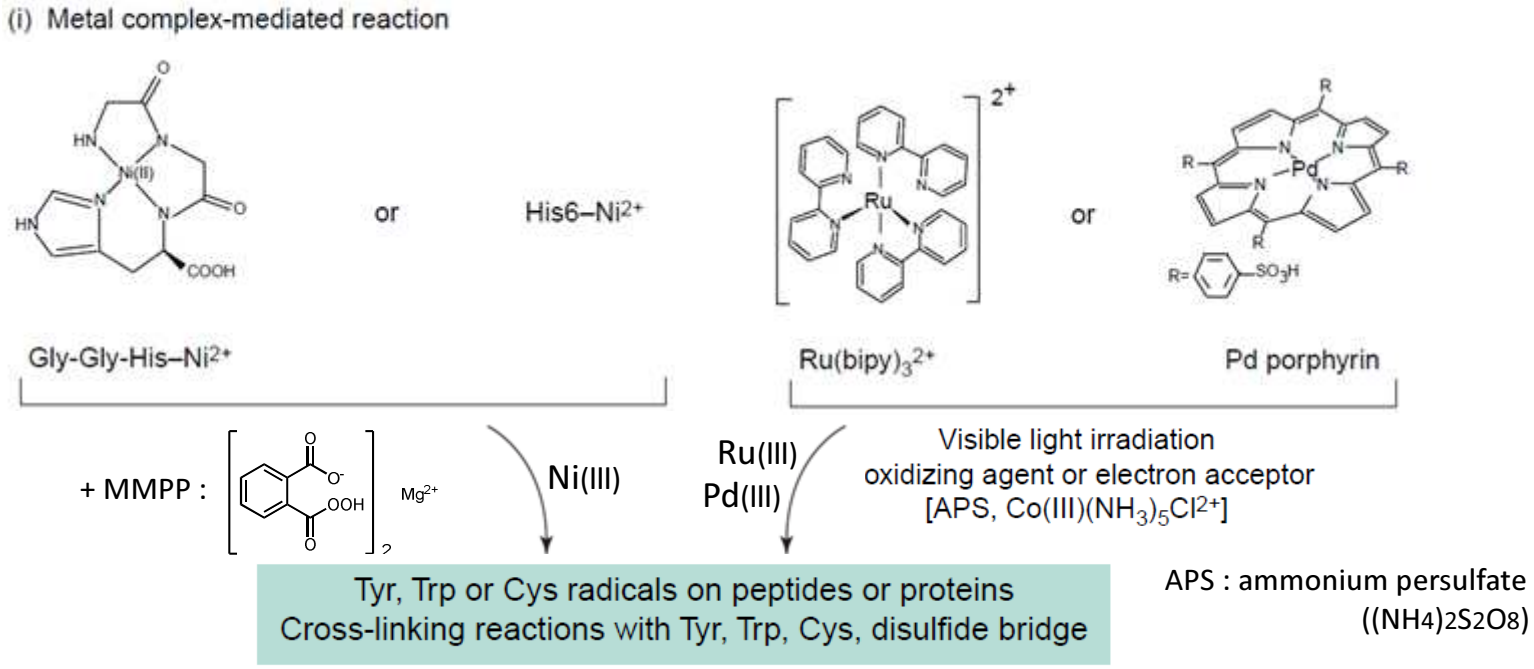

J. -C. Bonnafous *et al. Trends Pharmacol. Sci.* **26**, 210–217

4-1. Photo Cross Linking-2

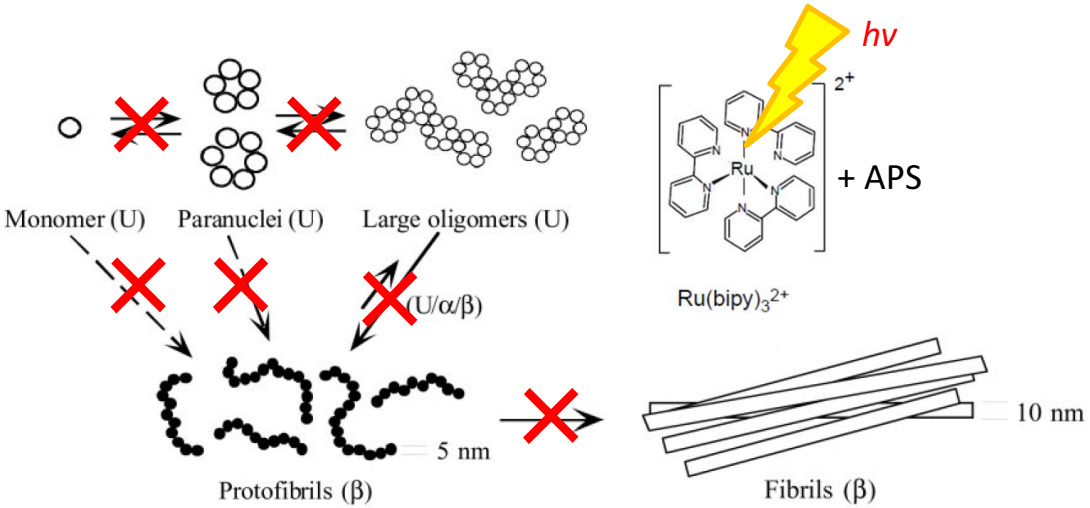

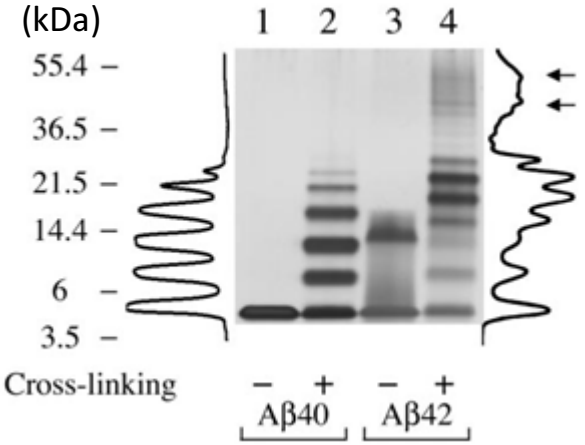

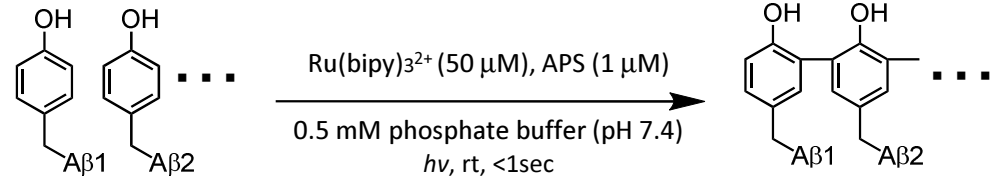

Aβ

(freshly isolated, low MW)

Cross-Linked Aβ

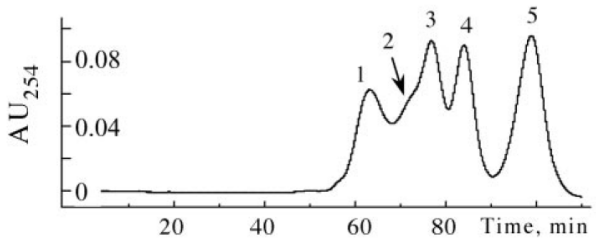

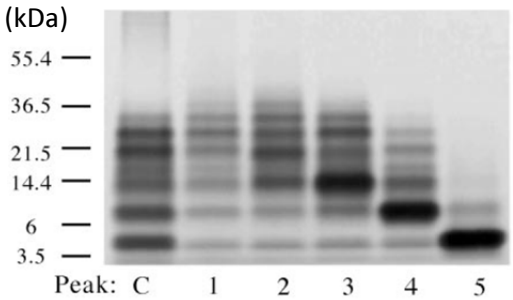

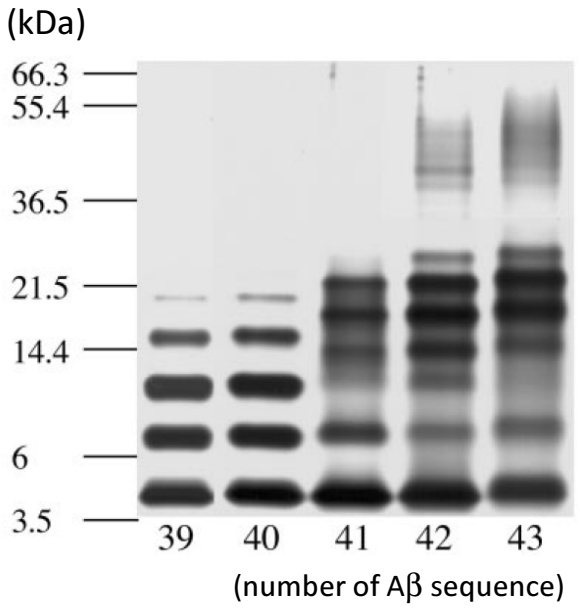

D. B. Teplow *et al. Proc. Natl. Acad. Sci. USA* **2003**, *100*, 330-335

4-2. OH· generator

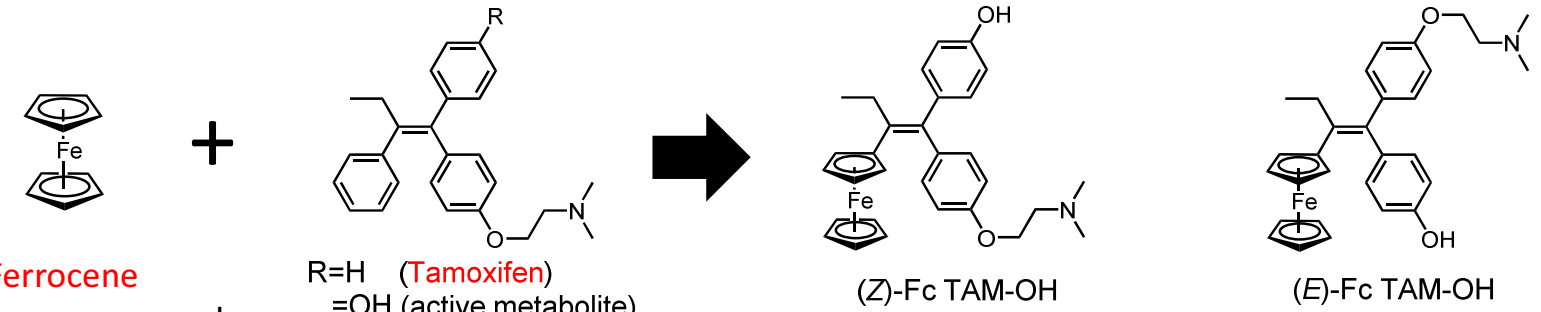

Ferrocene
antitumor compound

R=H (Tamoxifen)
=OH (active metabolite)
estrogen receptor antagonist
(anti-breast cancer)

(*Z*)-Fc TAM-OH

(*E*)-Fc TAM-OH

compound	binding affinity (%)	IC50 (μM)
oestradiol	100	-
(Z) TAM-OH	107	6.4
(Z)-Fc TAM-OH	40	3.4
(E)-Fc TAM-OH	12	4.9

G. Jaouen *et al. Chem. Commun.* **1996,** 955-956

More active derivatives are reported

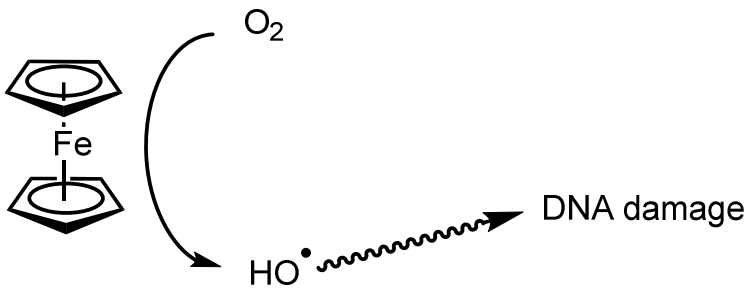

Ferrocene derivatives generate ROS and DNA damage

G. Cavigiolio *et al. Inorg. Chim. Acta.* **2000**, 42-48

in this tissue, relation of OH· and DNA damage is not associated
But there are many reports to relate them.
c.f.) D. MacNamee *et al. J. Biol. Chem. 1974,* **249**, 2447-2452

4-3. Olefin metathesis (1)-1

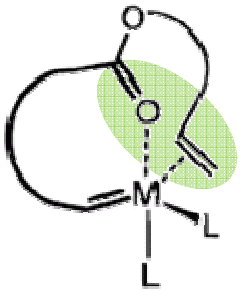

Ester chelates to [Ru] center

(M=Ru)

A. Fürstner *et al. J. Am. Chem. Soc*. **1997**, *119*, 9130-9136

Chalcogen assisted Cross-Metathesis

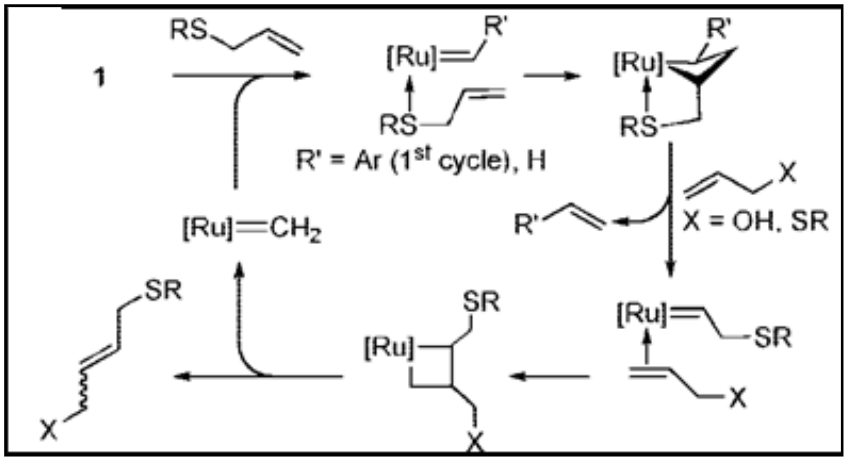

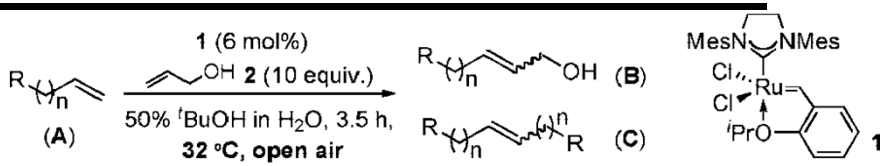

Entry	Alkene A		Cross-Metathesis B (%)[c]	Self-Metathesis C (%)[c]
1[a,b]	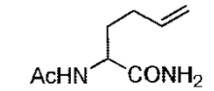	**3**	0	0
2[a]	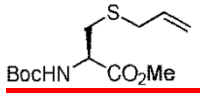	**4**	56 (74 brsm)	0
3[a]	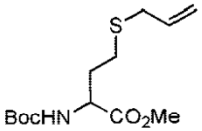	**5**	67 (99 brsm)	0
4[a]	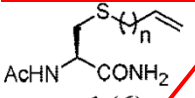 n = 1 (**6**) n = 2 (**7**) n = 3 (**8**)	**6**	68[d]	0
5[a,b]		**7**	0	0
6[a]		**8**	0	0
7	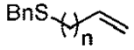	**9**	0	0
8	n = 0 (**9**) n = 1 (**10**)	**10**	52[d]	15
9	n = 2 (**11**) n = 3 (**12**)	**11**	19	0
10		**12**	8	0
11		**13**	11	0
12	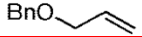	**14**	31	18
13	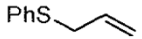	**15**	28[d]	47

B. G. Davis *et al. J. Am. Chem. Soc*. **2008**, *130*, 9642-9643

4-3. Olefin metathesis (1)-2

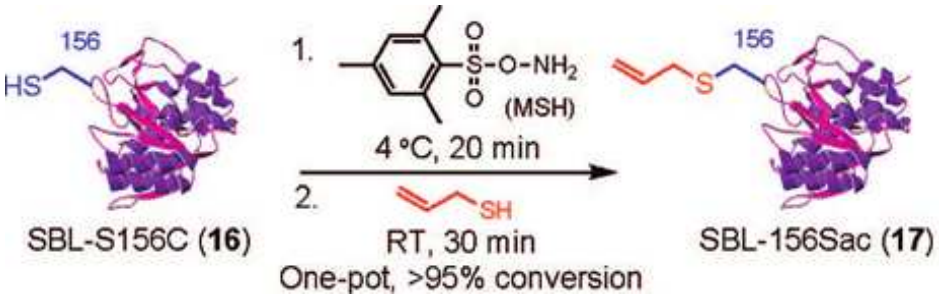

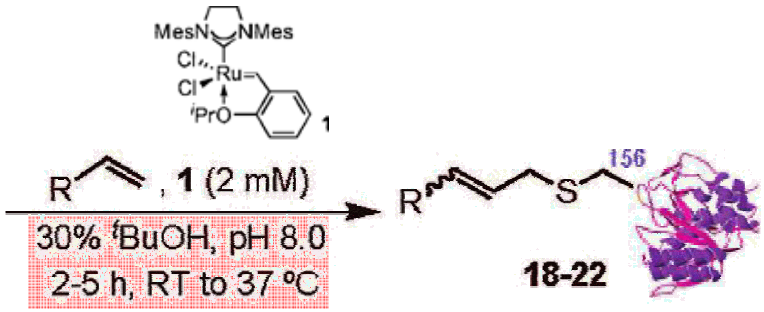

Entry	Alkene (mM)	Additives (mM)	Temp.	Prod.	Conversion (%)[a]
1	 **2** (100)	None	RT	-	0
2	**2** (100)	$MgCl_2$ (100)	RT	**18**	>90
3	**2** (100)	NaCl (100)	RT	-	0
4[b]	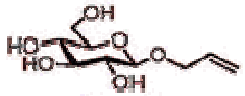 **23** (30)	$MgCl_2$ (80)	37 °C	**19**	50
5[b]	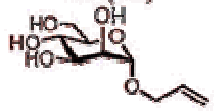 **24** (130)	$MgCl_2$ (130)	37 °C	**20**	60
6[c]	 **25** (75)	$MgCl_2$ (160)	37 °C	**21**	55
7[c]	 **26** (66)	$MgCl_2$ (130)	37 °C	**22**	60

(SBL-S156XXX have no Cys-SH)

→ Minor MS signal of **1**+**17** ···strong chelation?
by LC-MS

$MgCl_2$ disrupts nonproductive chelation of Ru + protein

B. G. Davis *et al. J. Am. Chem. Soc*. **2008**, *130*, 9642-9643

4-3. Olefin metathesis (2)-1

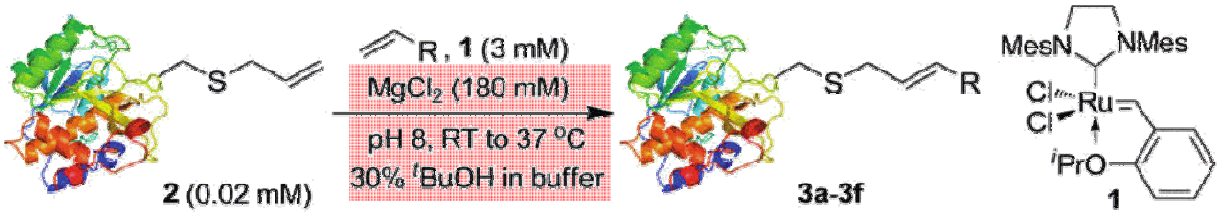

Entry	Alkene (mM)	Conditions	Prod.	Conv. (%)[a]
1	**4** (180)	RT, 2 h	**3a**	>95
2	**5** (180)	RT, 2 h then 37 °C, 30 mins	**3a**	28 >95
3	**6** (92)	37 °C, 1 h	**3b**	30
4	**7** (89)	37 °C, 1 h	**3c**	30
5	**8** (92)	37 °C, 1 h	**3d**	30
6[b]	**9** (92)	37 °C, 30 mins	**3e**	65
7	**10** (92)	RT, 1 h	**3f**	>95
8	**11** (92)	37 °C, 1 h	-	0
9	**12a** (85)	37 °C, 2 h	-	0
10	**13a** (85)	37 °C, 1 h	-	0
11	**13b** (85)	37 °C, 1 h	-	0
12	**14** (85)	37 °C, 1 h	-	0
13	**15** (180)	37 °C, 1 h	-	0
14	**16** (170)	37 °C, 1 h	-	0

Allyl alcohol, glycosides and OEG

GlcNAc derived allyl sulfide

Allyl ether of ammonium salt and GlcNAc

Hexenyl glucoside

C-glucoside

Allyl amine derivatives

Less reactive partner
→cross-metathesis
(entry 1~7)

More reactive partner
→self-metathesis
(entry 10)

Much less reactive partner
→no reaction
(entry 8,9,11~14)

(Only self-metathesis)

B. G. Davis *et al. J. Am. Chem. Soc*. **2010**, *132*, 16805-16811

4-3. Olefin metathesis (2)-2

Less hindered olefin

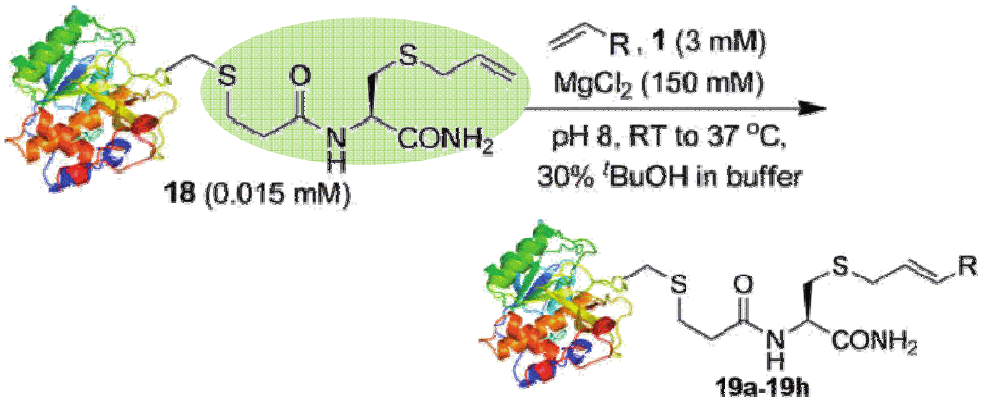

Entry	Alkene (mM)	Conditions	Prod.	Conv. (%)[a]	Conv. (hindered)
1	**4** (76)	RT, 30 mins	**19a**	>95	>95 (RT, 2 h)
2	**6** (77)	37 °C, 1 h	**19b**	>95	30
3	**7** (72)	37 °C, 1 h	**19c**	>95	30
4	**8** (77)	37 °C, 1 h	**19d**	>95	30
5	**9** (77)	RT, 2 h	**19e**	>95	65
6	**10** (80)	RT, 30 mins	**19f**	>95	>95
7	**11** (77)	37 °C, 30 mins	**19g**	29	0
8	**12a** (72)	37 °C, 2 h	**19h**	53	0
9	**13a** (77)	37 °C, 1 h	-	0 (Only self-metathesis)	0
10	**14** (72)	37 °C, 1 h	-	0	0
11	**15** (77)	37 °C, 30 mins	-	0	0
12	**16** (74)	37 °C, 1 h	-	0	0

B. G. Davis *et al. J. Am. Chem. Soc.* **2010**, *132*, 16805-16811

4-3. Olefin metathesis (2)-3

4. Others

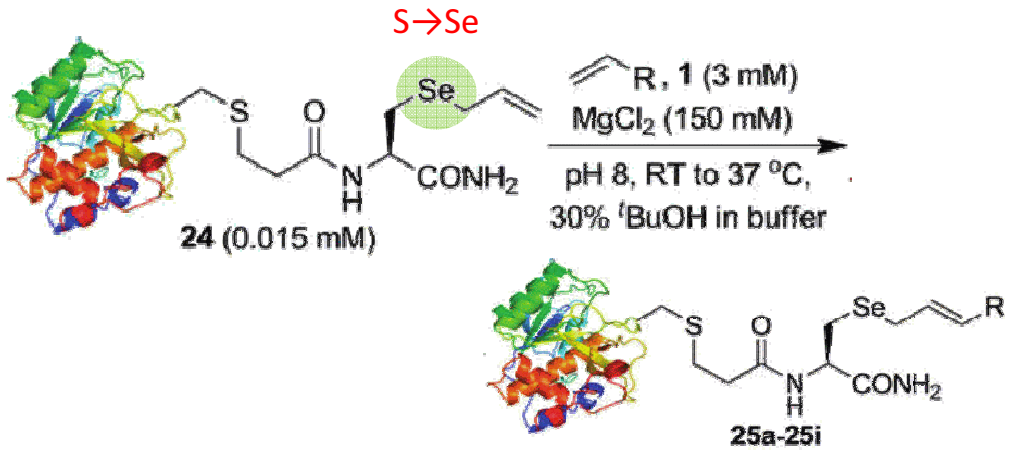

S vs Se

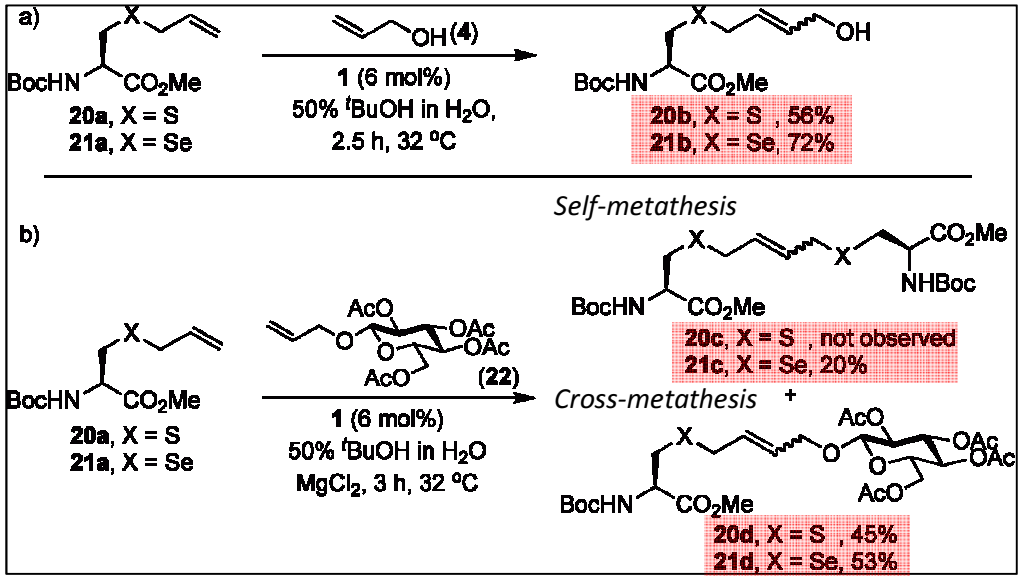

Entry	Alkene (mM)	Conditions	Prod.	Conv. (%)[a]	Conv. (S)
1	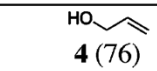 **4** (76)	RT, 15 mins	**25a**	>95	>95 (RT, 30 min)
2	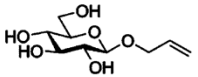 **6** (77)	37 °C, 1 h	**25b**	>95	>95
3	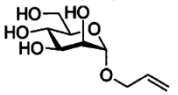 **7** (74)	37 °C, 1 h	**25c**	>95	>95
4	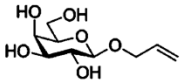 **8** (77)	37 °C, 1 h	**25d**	>95	>95
5	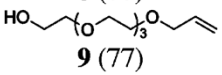 **9** (77)	RT, 1 h	**25e**	>95	>95
6	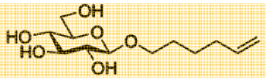 **10** (85)	RT, 30 mins	**25f**	>95	>95
7	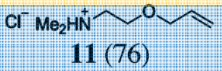 **11** (76)	37 °C, 30 mins	**25g**	>95	29
8	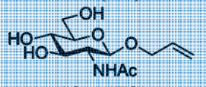 **12a** (73)	37 °C, 1 h	**25h**	>95	53
9	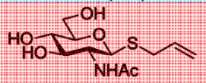 **13a** (77)	RT, 1 h (Only self-metathesis)	-	0	0
10	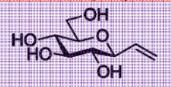 **14** (82)	37 °C, 1 h	-	0	0
11	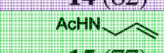 **15** (77)	37 °C, 30 mins	**25i**	90	0
12	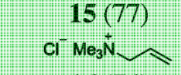 **16** (74)	37 °C, 1 h	-	0	0

B. G. Davis *et al. J. Am. Chem. Soc.* **2010**, *132*, 16805-16811

4-3. Olefin metathesis (2)-4

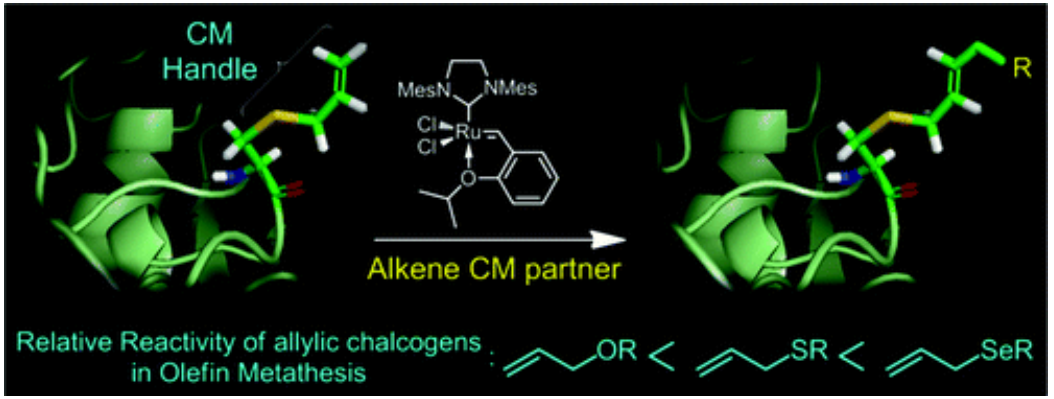

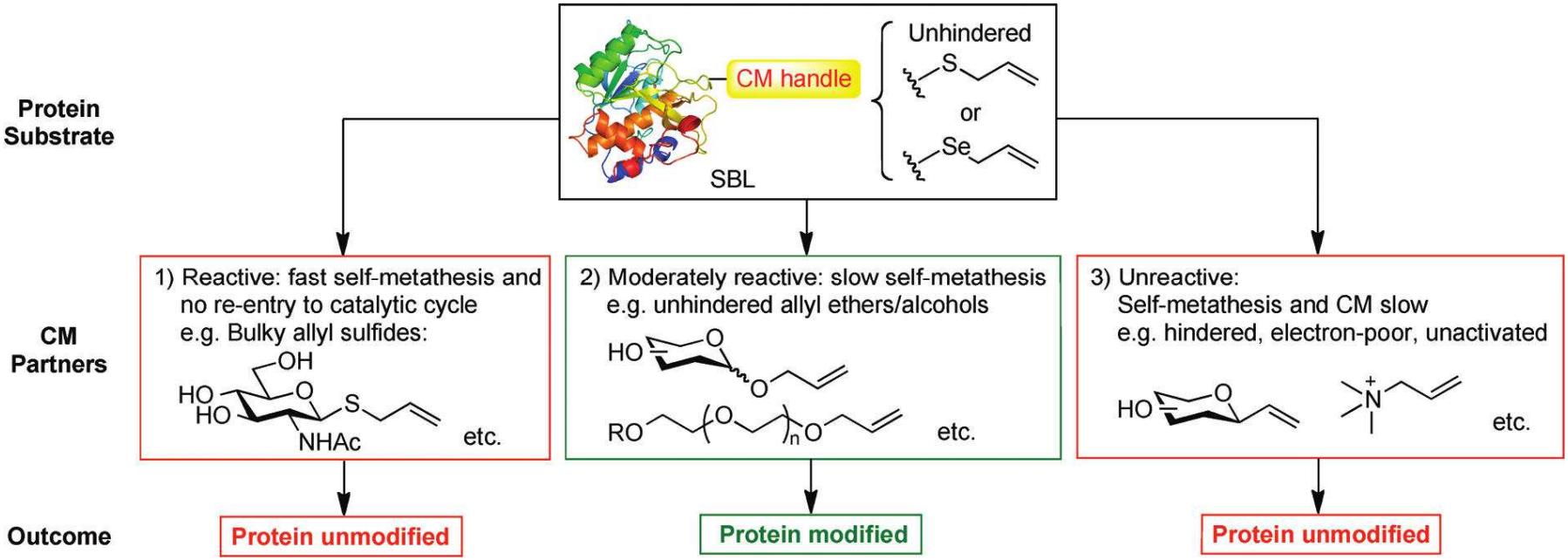

B. G. Davis *et al. J. Am. Chem. Soc*. **2010**, *132*, 16805-16811

4-3. Olefin metathesis (3)

Water soluble Metathesis catalysts

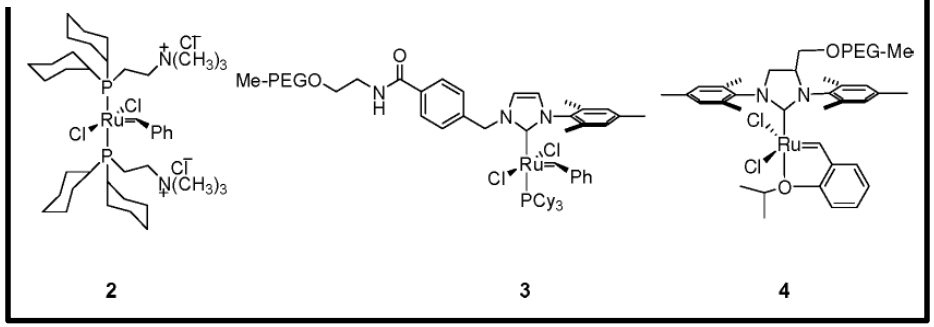

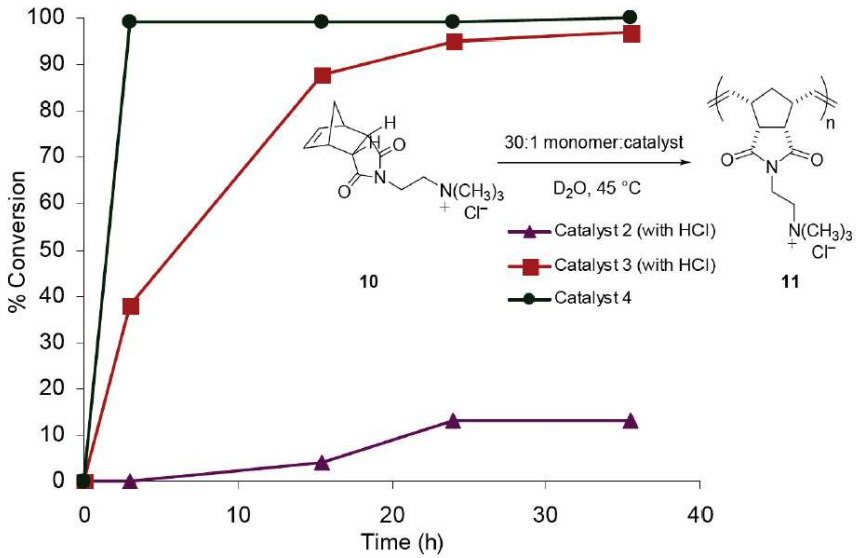

Figure 1. A comparison of the ability of water-soluble catalysts to polymerize *endo*-monomer **10** (data for catalyst **2** and **3** are obtained from ref 4).

Table 1. Ring-Closing Metathesis Reactions in Aqueous Media[a]

Entry	Substrate	Time	Product	Conversion
1	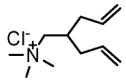 **12**	12 h	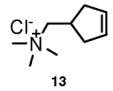 **13**	>95%
2	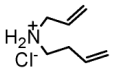 **14**	24 h	 **15**	>95%
3	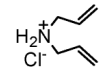 **16**	36 h	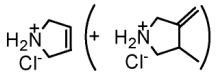 **17** **18**	67% (+28%)
4	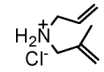 **19**	24 h	 **20**	42%
5	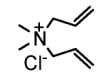 **21**	24 h	 **22**	<5%

[a] Reactions were carried out at room temperature with 5 mol % of catalyst **4** and an initial substrate concentration of 0.2 M in D_2O or H_2O. Conversions were determined by ^1H NMR spectroscopy.

Table 2. Cross-Metathesis Reactions in Aqueous Media[a]

Substrate	Time	Product	Conversion
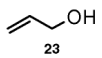 **23**	12 h	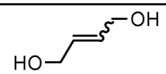	>95%[b]
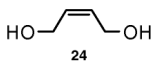 **24**	12 h	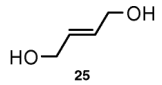 **25**	94%[c]

[a] Reactions were carried out at 45 °C with 5 mol % of catalyst **4** and an initial substrate concentration of 0.2 M in D_2O or H_2O. Conversions were determined by ^1H NMR spectroscopy. [b] $E/Z \sim 15:1$. [c] 6% of **24** remains due to thermodynamic equilibrium.

PEG : Poly Ethylene Glycol, MW≒2000

R. H. Grubbs *et al., J. Am. Chem. Soc.* ~~**2010**, *132*, 16805-16811~~ **2006**, *128*, 3508-3509

4-4. Rh carbenoid

Also see Mr Suzuki's Literature Seminar (2013)

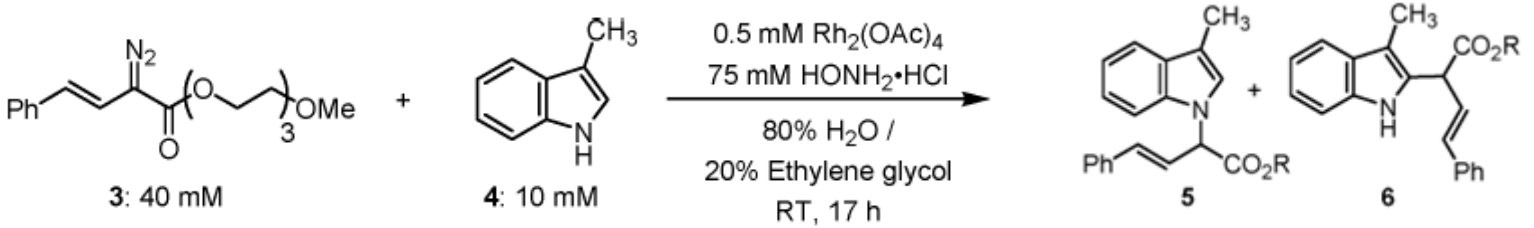

51% (**5**:**6** = 1:1.4)

R = $(CH_2CH_2O)_3CH_3$

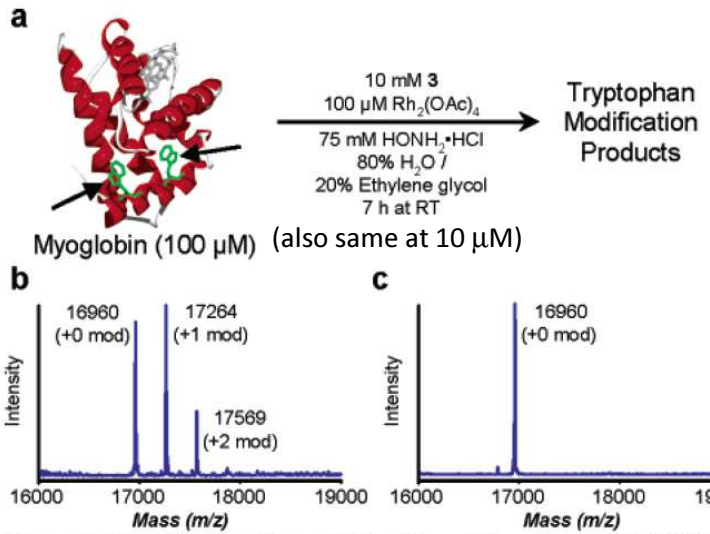

(also same at 10 μM)

Figure 1. Modification of myoglobin with metallocarbenes. (a) A 100 μM solution of horse heart myoglobin was exposed to **3** and $Rh_2(OAc)_4$ for 7 h. The two tryptophan residues are shown in green. (b) Following removal of the small molecules via gel filtration, the sample was analyzed by ESI-MS. Both singly and doubly modified protein products were identified in the mass reconstruction. (c) In the absence of $Rh_2(OAc)_4$, no products were obtained under otherwise identical conditions. (d) After digestion with trypsin, MS/MS analysis of the doubly modified peptide fragment confirmed modification of only the tryptophan residues. All assigned species agree to within 0.1% of the expected mass values.

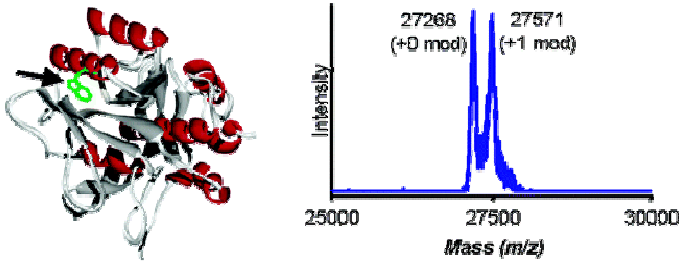

Subtilisin Carlsberg (100 μM)

Figure 2. Modification of subtilisin Carlsberg with rhodium carbenoids. Conditions: 100 μM protein, 10 mM **3**, 100 μM $Rh_2(OAc)_4$ and 75 mM $HONH_2$•HCl (pH 1.5) in 80% water/20% ethylene glycol, rt, 7 h. Following removal of the small molecules via gel filtration, the sample was analyzed using MALDI-TOF MS. Only the singly modified protein was observed, as would be expected by the single tryptophan residue (shown in green). In the absence of $Rh_2(OAc)_4$, no reaction occurred under otherwise identical conditions.

These have no Cys・・・Selective?

M. B. Francis *et al.*, *J. Am. Chem. Soc*. **2004**, *126*, 10256-10257

Contents

5. Summary

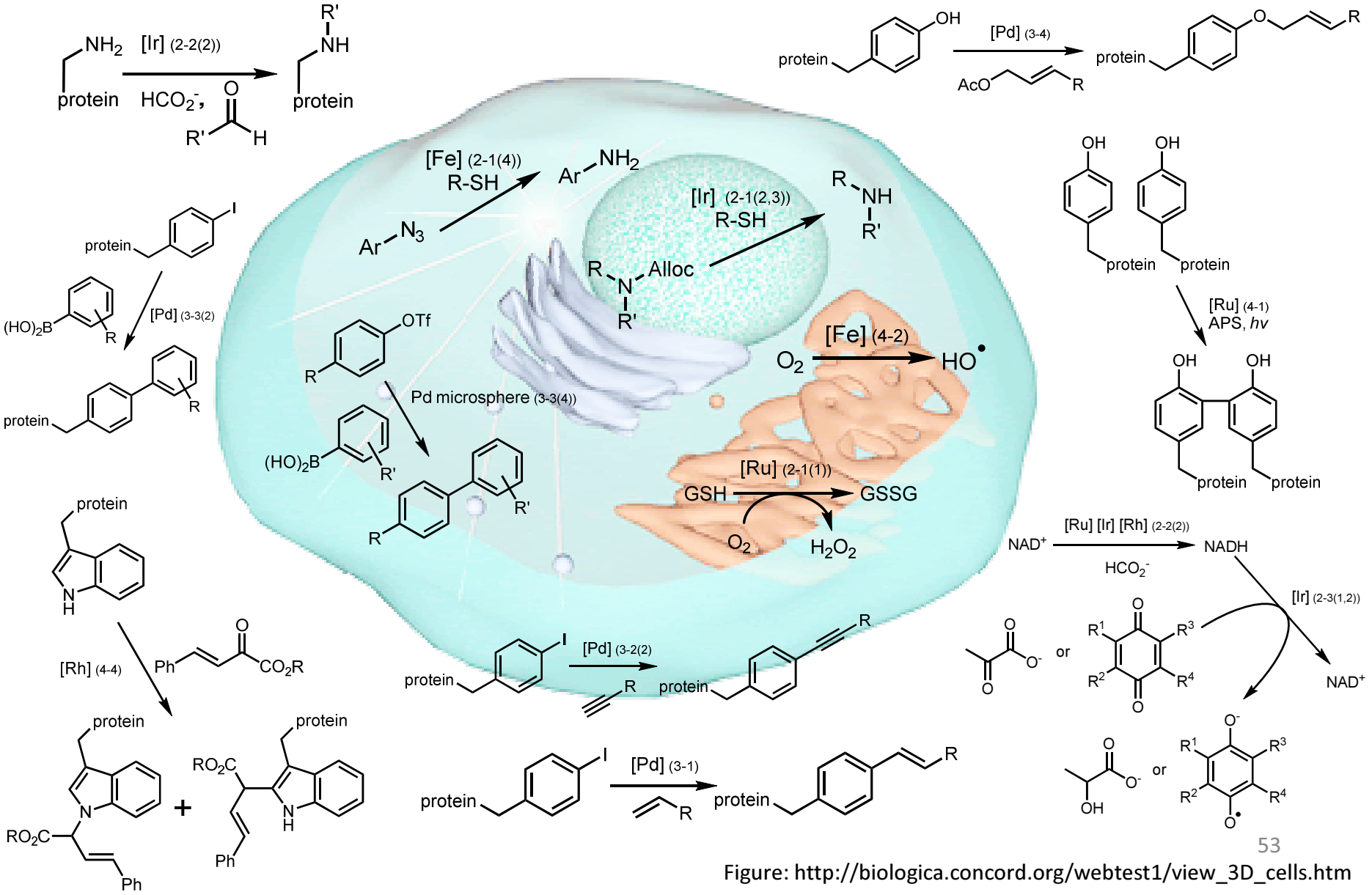

Figure: http://biologica.concord.org/webtest1/view_3D_cells.htm

Appendix

2-1. R-SH oxidation (4)

Appendix

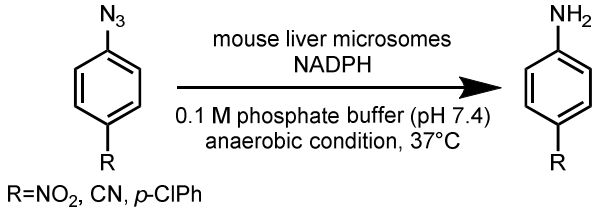

Effect of microsomal incubation conditions on the rate of formation of *p*-nitroaniline from *p*-nitrophenyl azide.

Incubation conditions	Rate (percentage of control)[a]
Complete system[b]	100
Omit glucose 6-phosphate dehydrogenase[c]	4 ± 1
Heat-denatured microsomes	0 ± 1
Plus NADPH (2 mM)	95 ± 3
Plus NADH (2 mM)	28 ± 1
Plus CO[d]	84 ± 3
Aerobic[e]	0 ± 1

[a] Rate determined as nmol of *p*-nitroaniline/30 min per mg of protein.
[b] Complete NADPH-generating system under N_2.
[c] Glucose 6-phosphate dehydrogenase omitted from the NADPH-generating system.
[d] Vials gassed with CO in the same manner as with N_2.
[e] Vials sealed with an air atmosphere.

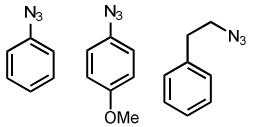

: no reduction occured

R. J. Griffin *et al. Xenobiotica* **1991**, *21*, 935-943

Ar-N3 is reduced in Liver, microsome

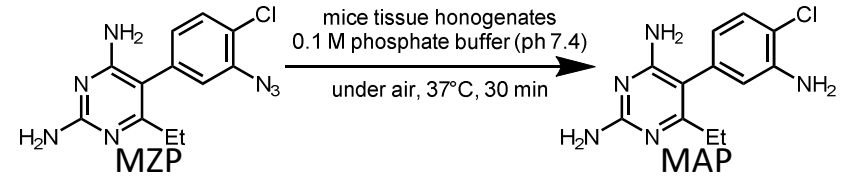

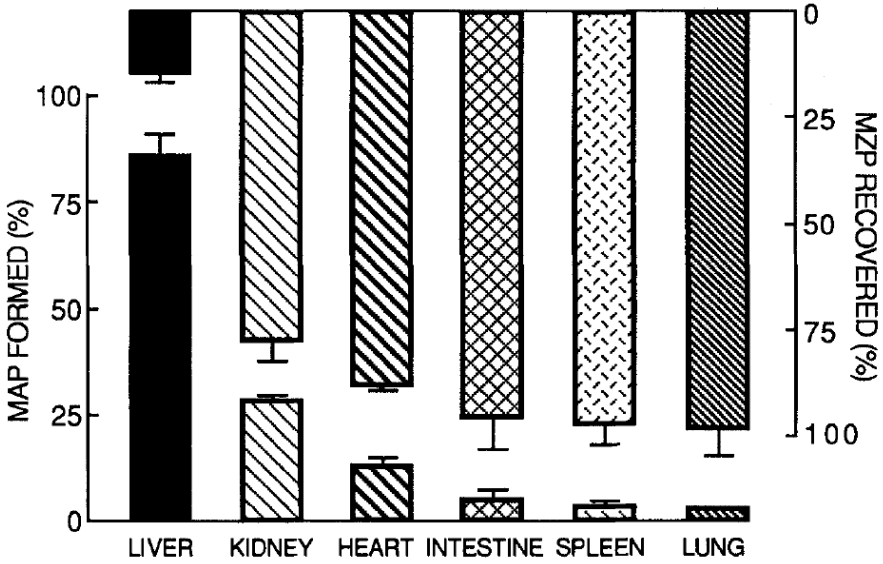

J. A. Slack *et al. Xenobiotica* **1988**, *18*, 1157-1164

Fluorescence observed *in vivo*, due to reductive metabolism of Ar-N3

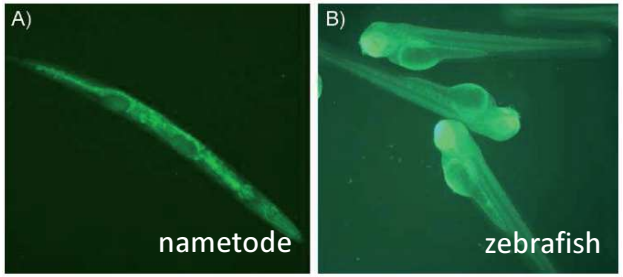

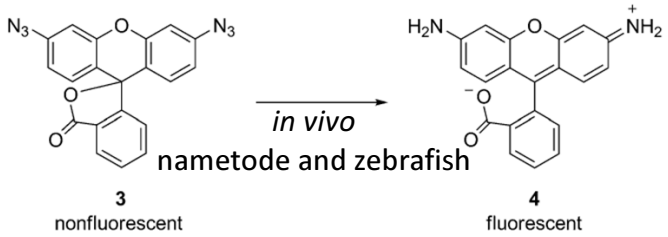

E. Meggers *et al. ChemBioChem* **2012**, *13*, 1116-1120

2-3. Reduction by NADH (1)

Appendix

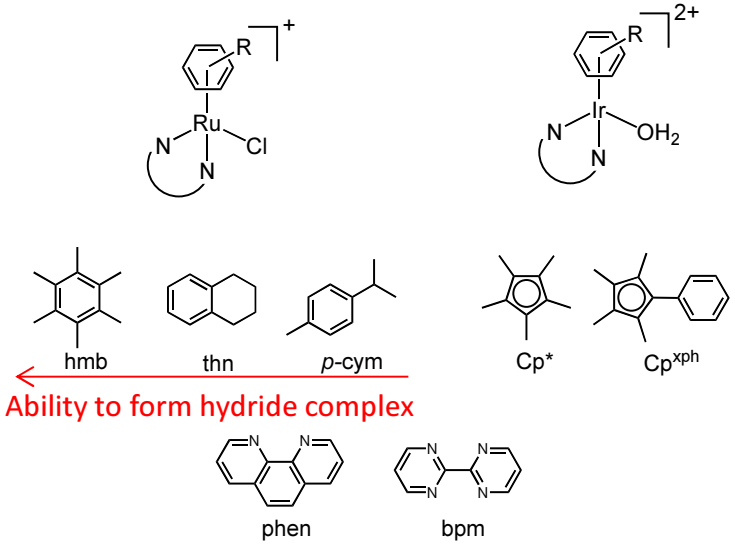

[Ru-H] (also [Ir-H]) complex reduce pyrvate

Time course

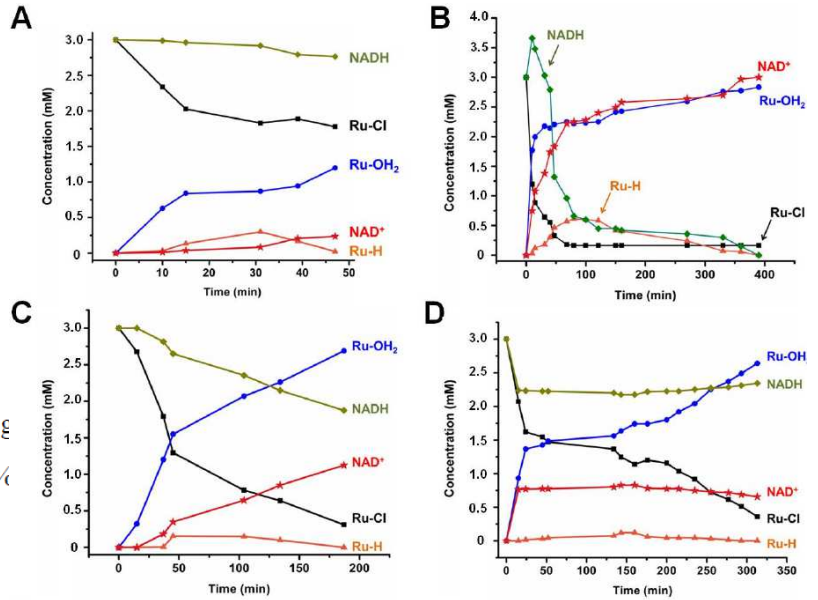

Figure S2. Time dependence of the concentrations of various species observed during the reaction of NADH with ruthenium arene complexes (as determined by integration of ^{1}H NMR peaks). The solutions contained equimolar amounts of 3 mM 1,4-NADH and (***A***) [(η^6-*p*-cym)Ru(bpm)Cl]$^+$ (**1**); (***B***) [(η^6-hmb)Ru(bpm)Cl]$^+$ (**2**); (***C***) [(η^6-thn)Ru(bpm)Cl]$^+$ (**4**); (***D***) [(η^6-*p*-cym)Ru(phen)Cl]$^+$ (**5**), in 90% H_2O/10% D_2O at 310 K.

Ability to form [Ru-H]

Table S1. ^{1}H NMR chemical shifts (ppm) of Ru–H species detected at various times during the reactions of 1,4-NADH with [(η^6-arene)Ru(N,N')Cl]$^+$ complexes **1**, **2**, **4**, and **5** in 90% H_2O/10% D_2O at 310 K.

Complex	Time (min)	Ru-H Chemical shift (ppm)
(**1**) [(η^6-*p*-cym)Ru(bpm)Cl]$^+$	31	–6.13
(**2**) [(η^6-hmb)Ru(bpm)Cl]$^+$	15	–7.44
(**4**) [(η^6-thn)Ru(bpm)Cl]$^+$	22	–6.61
(**5**) [(η^6-*p*-cym)Ru(phen)Cl]$^+$	34	–6.21

P. J. Sadler *et al.*, *Angew. Chem. Int. Ed*. **2012**, *51*, 3897 –3900

2-3. Reduction by NADH (1)

Appendix

[Ir-H] complex formed by NADH

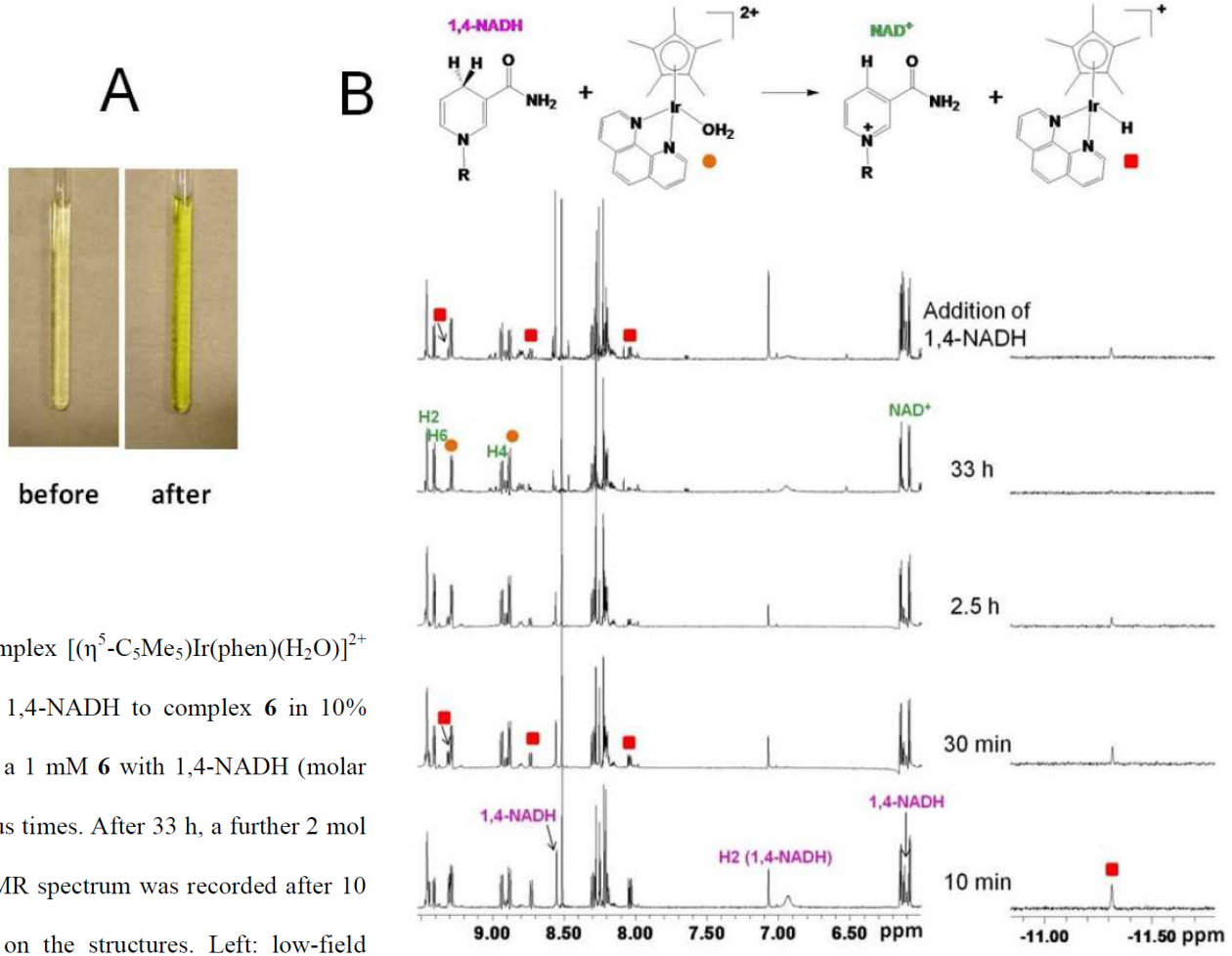

Figure S3. Conversion of 1,4-NADH to NAD^+ by complex $[(\eta^5\text{-}C_5Me_5)Ir(phen)(H_2O)]^{2+}$ (**6**). (***A***) Colour change immediately after addition of 1,4-NADH to complex **6** in 10% MeOD-d_4/90% H_2O at 298 K**.** (***B***) ^1H NMR spectra of a 1 mM **6** with 1,4-NADH (molar ratio 1:2) in 10% MeOD-d_4/90% H_2O at 298 K at various times. After 33 h, a further 2 mol equiv of 1,4-NADH was added and the resulting ^1H NMR spectrum was recorded after 10 min (top spectrum). Peak assignments are indicated on the structures. Left: low-field region; right: Ir-H hydride region (×2).

P. J. Sadler *et al.*, *Angew. Chem. Int. Ed*. **2012**, *51*, 3897 –3900

2-3. Reduction by NADH (1)

Appendix

[Ir-H] complex reduces pyrvate

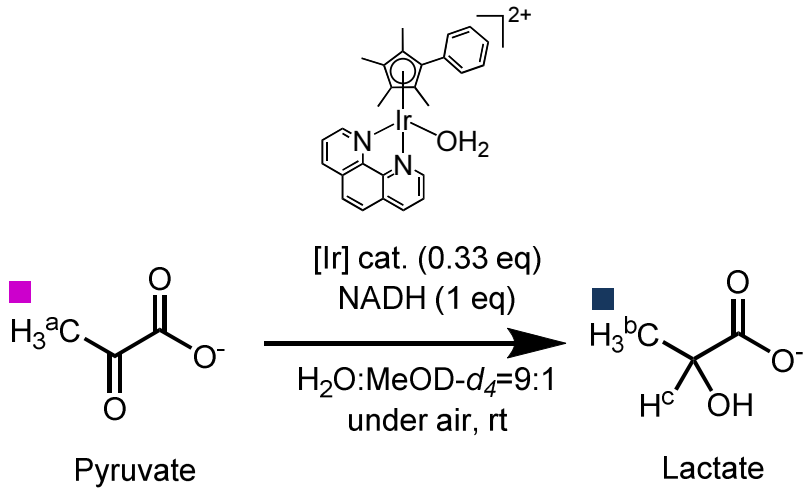

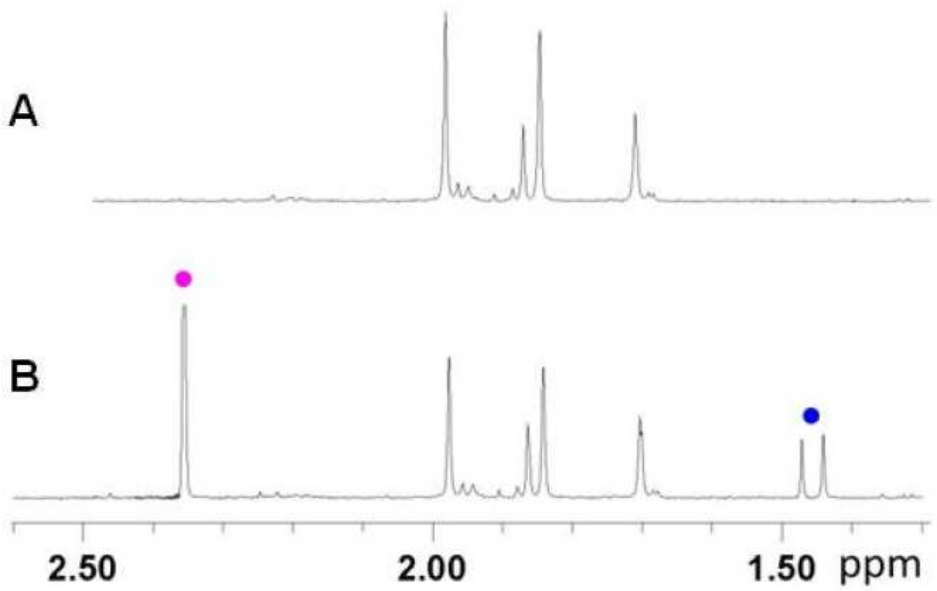

Figure S5. ^{1}H NMR spectra showing conversion of pyruvate to lactate in the presence of $[(\eta^5\text{-}C_5Me_4C_6H_5)Ir(phen)(H_2O)]^{2+}$ (**7**). (***A***) ^{1}H NMR spectrum recorded 10 min after addition of 3 mol equiv of 1,4-NADH to a 1 mM solution of **7** in 10% MeOD-d_4/90% H_2O (v/v) at 298 K. (***B***) ^{1}H NMR spectrum recorded 10 min after addition of 3 mol equiv of sodium pyruvate to the solution in (***A***). Peak assignments are indicated on the structures.

P. J. Sadler *et al.*, *Angew. Chem. Int. Ed*. **2012**, *51*, 3897 –3900

2-3. Reduction by NADH (2)

Appendix

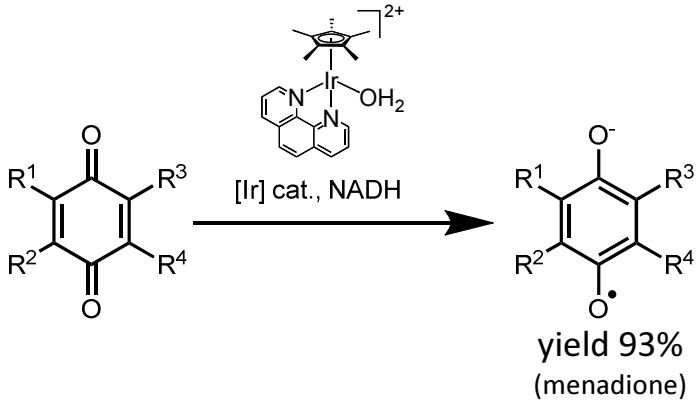

Figure 2. X-band EPR spectra at around 290 K. a) Menadione radical anion ($M^{\bullet -}$) generated by the reduction of menadione (1 mM) by NADH (0.5 mM) catalyzed by complex **1** or **3** (160 μM) in phosphate buffer (pH 7.2, 9 h). b) Simulated $M^{\bullet -}$ EPR spectrum with hyperfine coupling constants. c) Durosemiquinone radical anion ($D^{\bullet -}$) generated by reduction of duroquinone (2 mM) by NADH (1 mM) catalyzed by complex **1** or **3** (330 μM) in phosphate buffer (pH 7.2, 10 h). d) Simulated $D^{\bullet -}$ EPR spectrum with hyperfine coupling constants.

Few semiquinone radical anions ($M^{\bullet -}$) forms [Ir] adducts

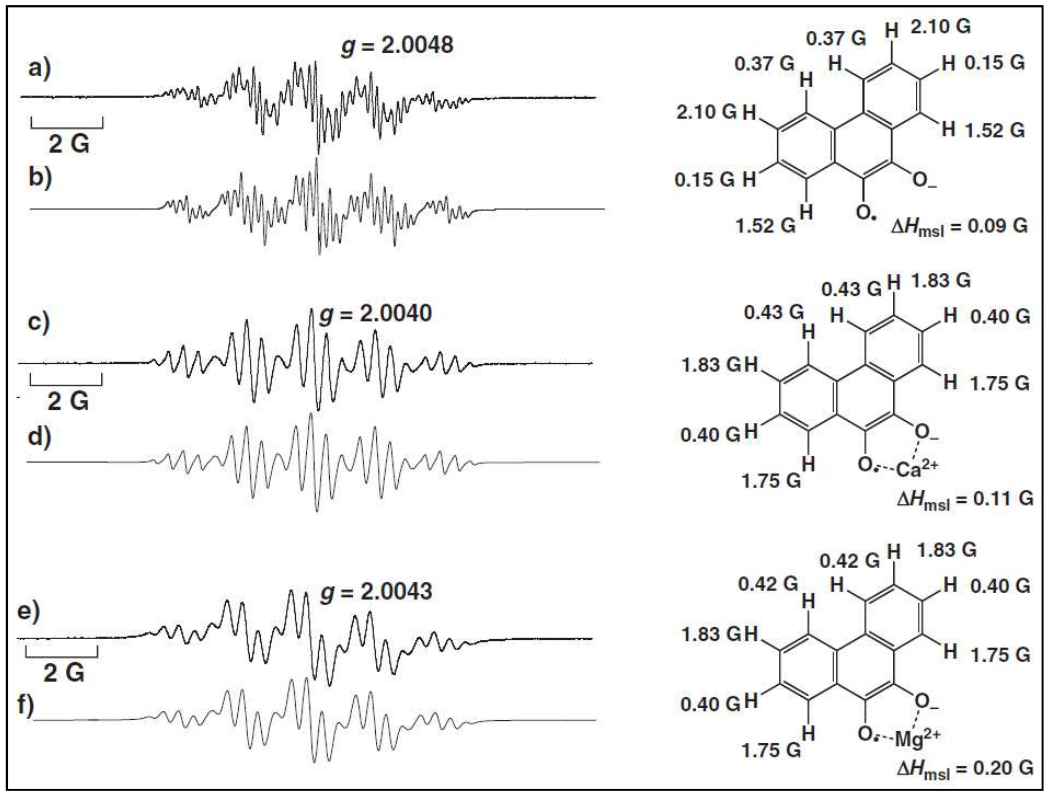

S. Fukuzumi *et al. ChemPhysChem* **2006**, *7*, 942-954

P. J. Sadler *et al.*, *Angew. Chem. Int. Ed*. **2013**, *52*, 4194-4197

3-2. Sonogashira coupling (1)

Appendix

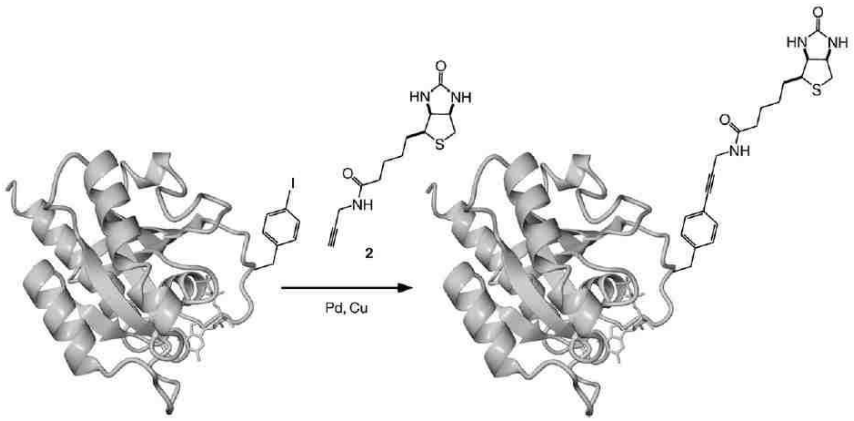

Yield 25%
(13%:dehalogenated)

Condition
- in TAPS buffer (0.09 M, pH 8.3)
- 2.3 M DMSO (18% v/v)
- iF32-Ras-His (13 μM)
- propagylated biotin (15 mM)
- $Pd(OAc)_2$ (1.7 mM)
- TPPTS (8.3 mM)
- CuOTf (0.7 mM)
- 6℃, 80min, w/o O_2

Detection by SDS-PAGE

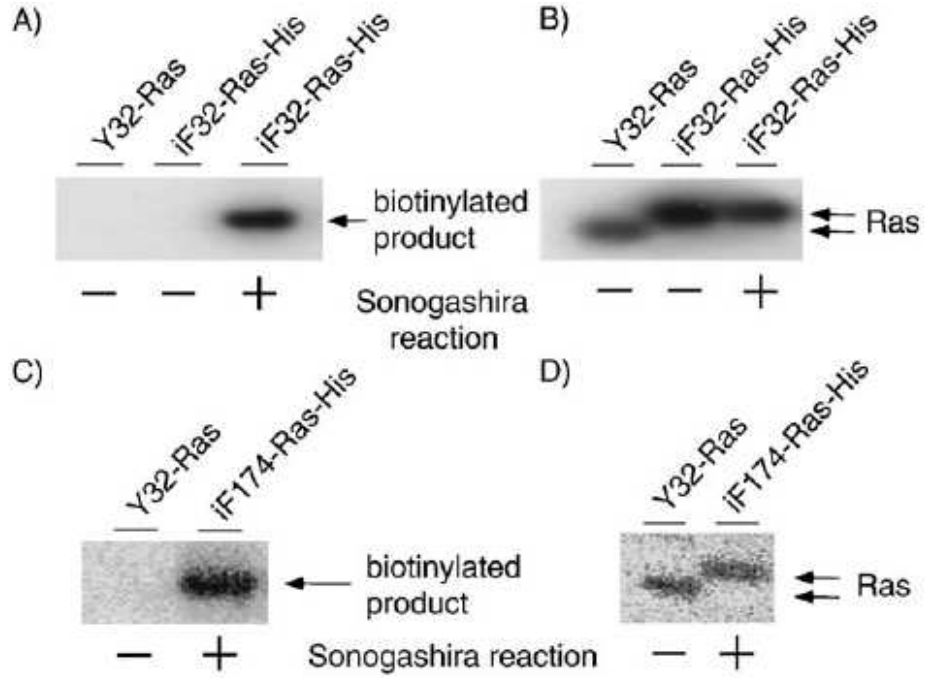

Figure 3. Detection of the biotinylated Ras protein with Streptavidin-HRP (left) or an anti-Ras antibody (right). The A), B) iF32–Ras–His, and C), D) iF174–Ras–His proteins were subjected to the Sonogashira reaction and then were directly analyzed without further purification. The wild-type Ras protein without hexahistidine residues (Y32–Ras) was used as a control.

3-2. Sonogashira coupling (2)

Appendix

E. coli cytotoxicity of Pd complex

Each treatment
→incubate 4 h
→dilute 10^6
→overnight incubation 37℃
→measurement

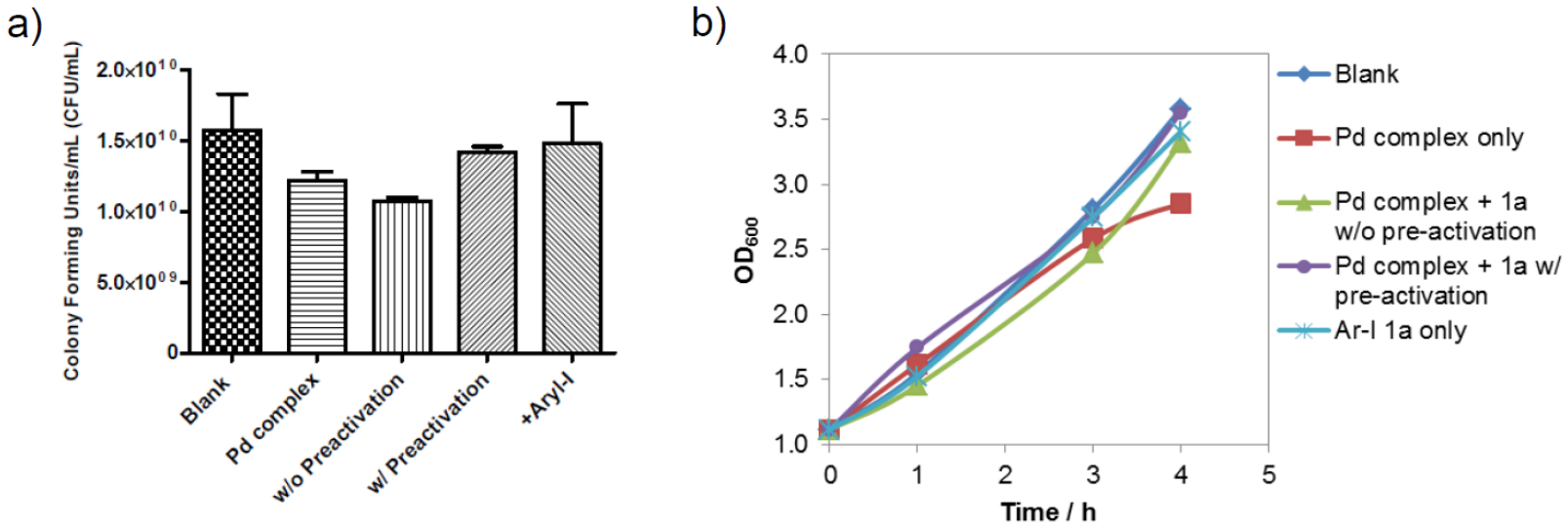

Brank : DMSO 1 %
Pd complex : DMSO 1 %, Pd complex 1 mM
w/o Preactivation : DMSO 1 %, Pd complex 1 mM, **1a** 1 mM, sodium ascorbate 8 mM
w Preactivation : DMSO 1 %, preactivated [Pd complex 1 mM, **1a** 1 mM, sodium ascorbate 8 mM] (stirred 37℃, 1 h before addition)
Ar-I : DMSO 1%, **1a** 1 mM

Q. Lin *et al. J. Am. Chem. Soc*. **2011**, *133*, 15316-15319

3-2. Sonogashira coupling (2)

Appendix

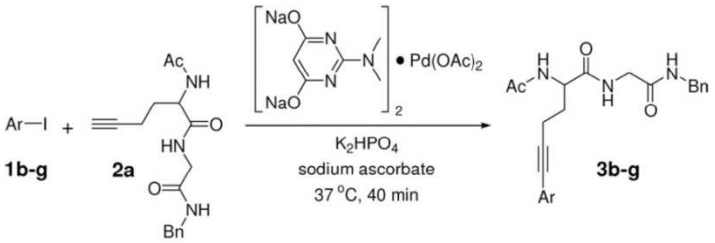

Entry	Ar-I	Pd • L2	Conversion (%)[b]
1	1b	30%	84
2	1c	30%	95
3	1d	30%	77
4	1e	30%	88
5	1f	30%	70
6	1g	30%	72

Reagents (except alkene) are mixed then stirred 37℃ 1 h, separate each half and added twice in all reaction.

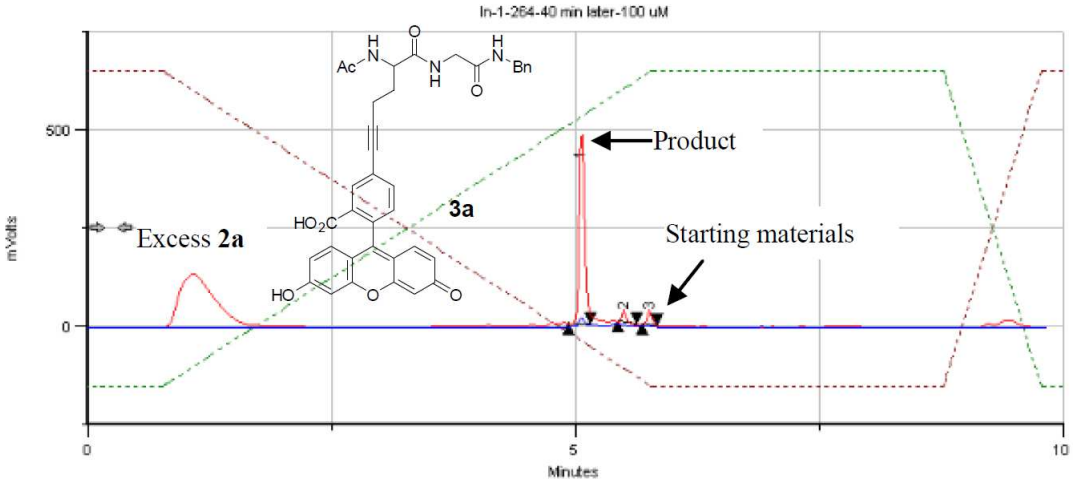

The conversions were calculated based on the disappearance of aryl iodides, whose amounts were quantified by their absorption at 254 nm (red line).

Many doubtful points…?

Q. Lin *et al. J. Am. Chem. Soc*. **2011**, *133*, 15316-15319

3-2. Sonogashira coupling (3)

Appendix

$Pd(NO_3)_2$ has no acute toxicity to *E. coli*

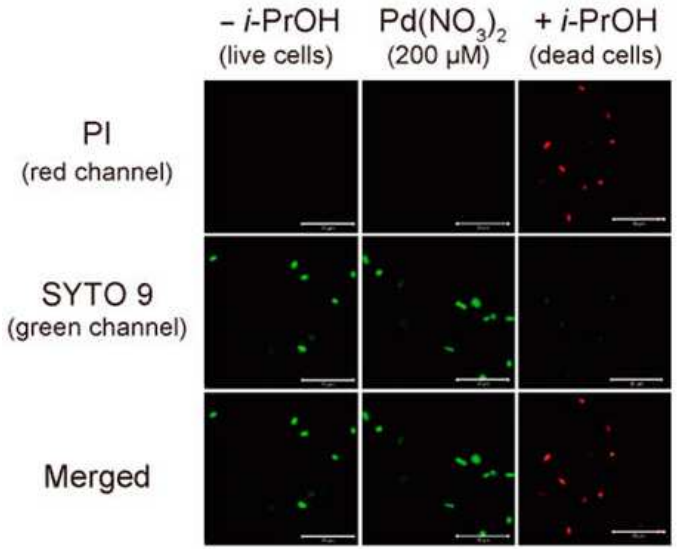

cf) SDS-PAGE fluorescence yield

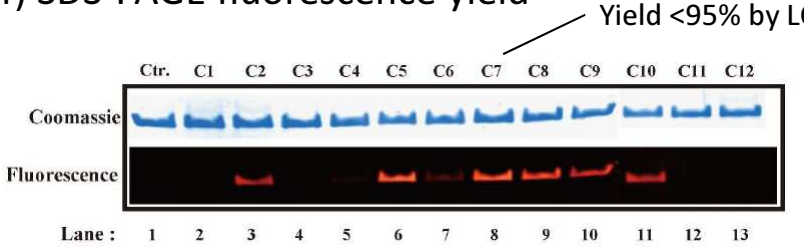

$$RF = \frac{(\text{r.f.i.} / \text{r.c.i.})_x}{(\text{r.f.i.} / \text{r.c.i.})_{max}}$$

value of C7 as $(\text{r.f.i/r.c.i})_{max}$

yield = RF × 95 (%)

r.f.i. : relative fluorescence intensity

r.c.i. : relative coomassie stain intensity

$Pd(NO_3)_2$ gives few membrane damage

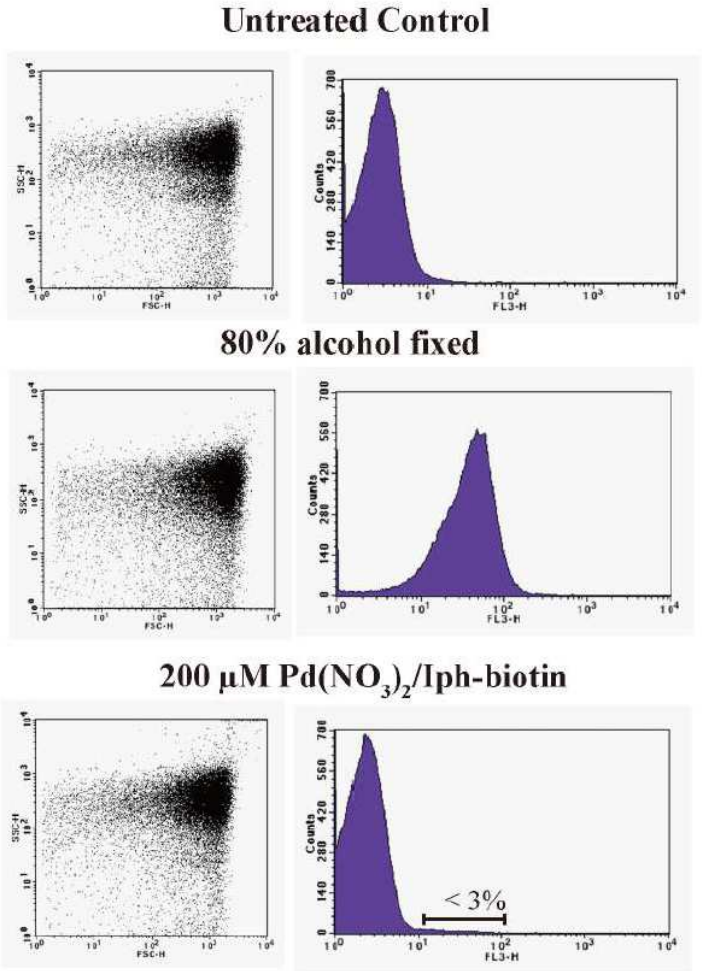

Shigella shows almost same results

P. R. Chen *et al. J. Am. Chem. Soc.* **2013**, *135*, 7330−7338

3-2. Sonogashira coupling (3)

Appendix

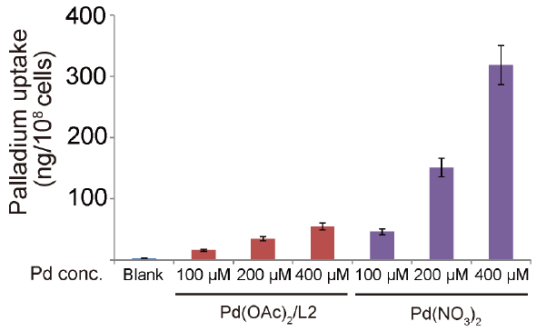

	Blank	$Pd(OAc)_2$/L2			$Pd(NO_3)_2$		
Extracellular Pd conc.	N.A.	100 μM	200 μM	400 μM	100 μM	200 μM	400 μM
Pd (ng/10^8 cells) (±10%)	3	16	35	55	46	151	318

Figure S13. **The uptake of palladium measured by ICP-MS analysis.** *E. coli* bacterial cells with and without the treatment of 200 μM $Pd(OAc)_2$/**L2** or $Pd(NO_3)_2$ for 1 h were analyzed according to a protocol described in **Supplementary Method 11**.

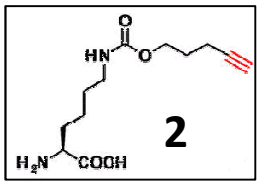

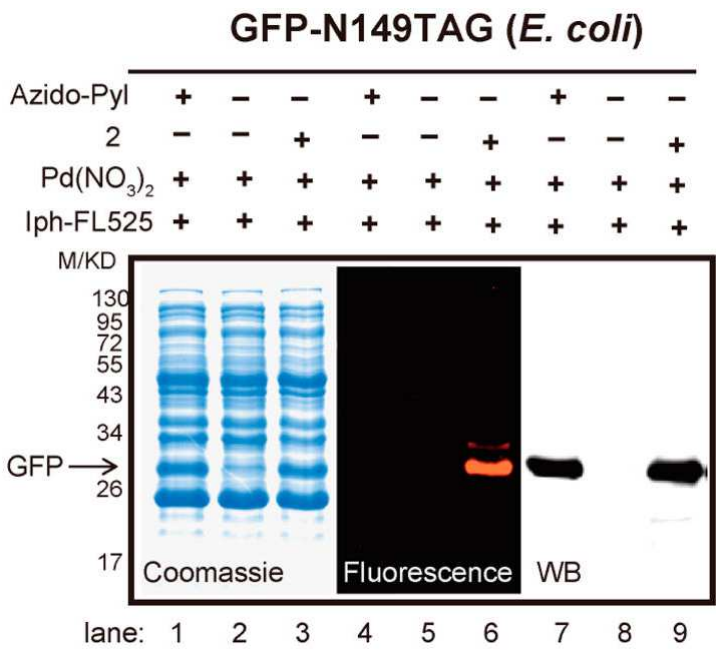

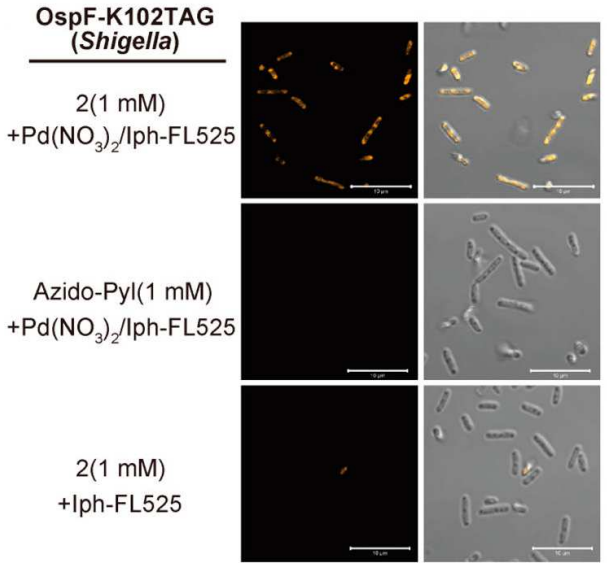

???

P. R. Chen *et al. J. Am. Chem. Soc.* **2013**, *135*, 7330−7338

3-3. Suzuki coupling (1)

Free Cys-SH inhibits coupling

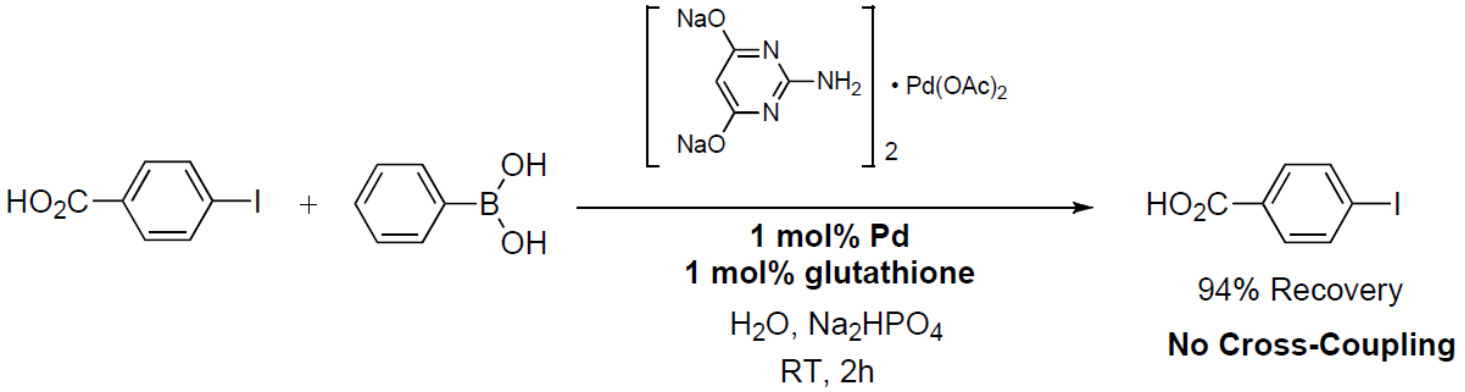

B. G. Davis *et al. J. Am. Chem. Soc*. **2009**, *131*, 16346-16347

3-3. Suzuki coupling (3)

Appendix

Toxicity of Guanidine salt

LD_{50}: 500 mg/kg (domestic rabbit)

月刊ファインケミカル 2008年6月号 72-75

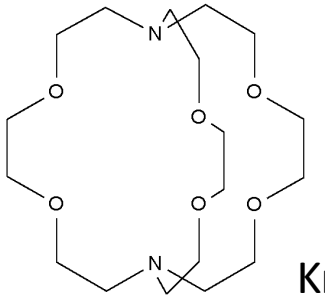

Kryptofix 2.2.2

K^+ trap

4-2. Olefin metathesis (3)

Appendix

Other water soluble Olefin metathesis catalysts

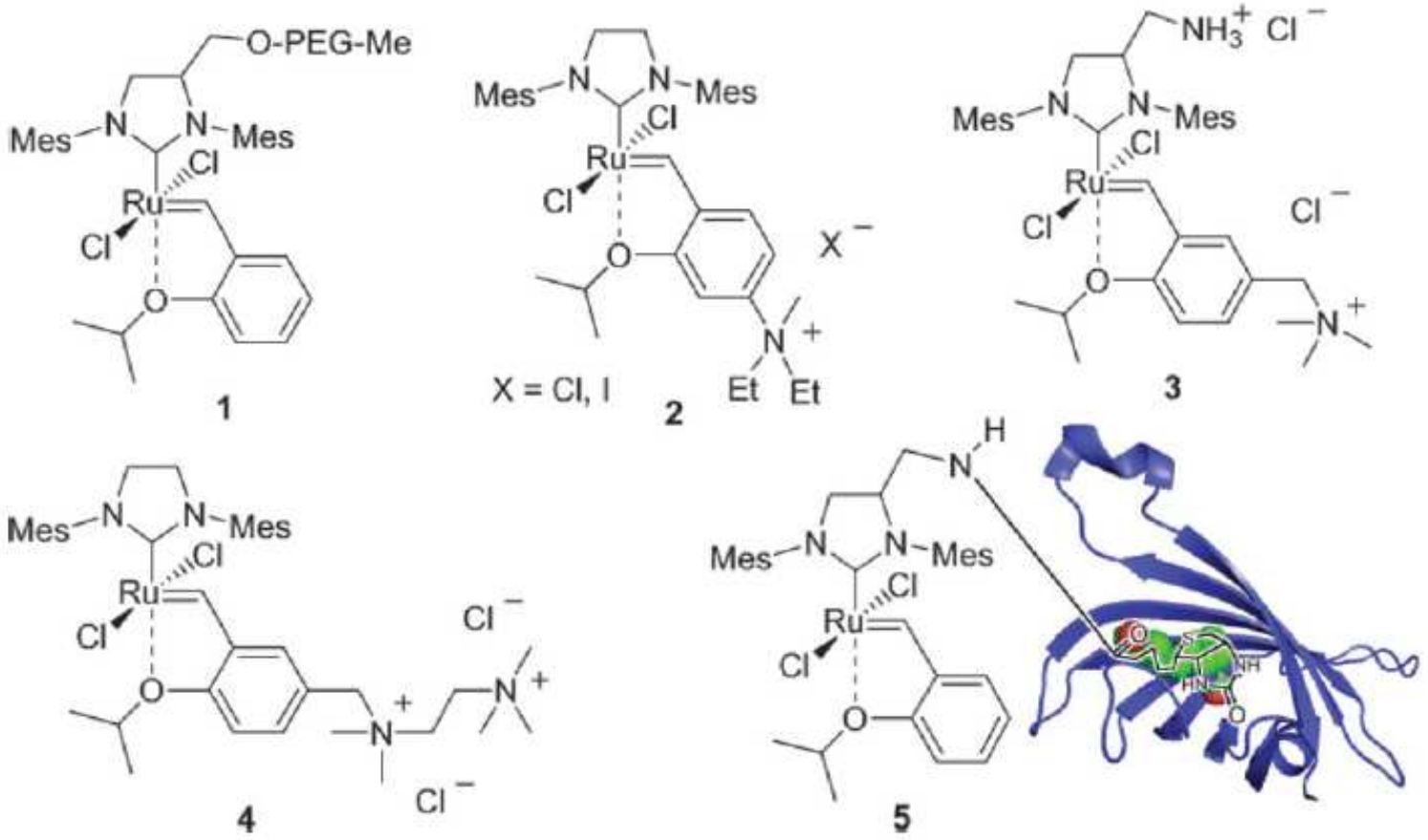

K. Grela *et al., Catal. Sci. Technol.,* **2012**, *2*, 2424-2427

4-4. Rh carbenoid

S-h insertion of Rh Carbenoid

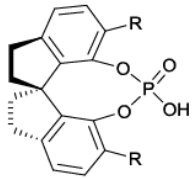

1a: R = H
1b: R = Ph
1c: R = 2-naphthyl
1d: R = 4-PhC_6H_4
1e: R = 3,5-(^{t}Bu)$_2C_6H_3$
1f: R = 2,4,6-(^{i}Pr)$_3C_6H_2$

Table 3 S–H insertions of methyl α-phenyl-α-diazo-esters with various mercaptans[a]

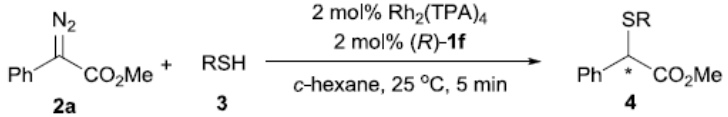

Entry	R	Product	Yield (%)	ee (%)
1	Bn (**3a**)	**4aa**	92	94 (*S*)
2	4-MeO-Bn (**3b**)	**4ab**	97	93
3	4-Cl-Bn (**3c**)	**4ac**	94	94
4	*n*-dodecyl (**3d**)	**4ad**	86	93
5	*n*-octyl (**3e**)	**4ae**	87	93
6	*n*-Pr (**3f**)	**4af**	86	93
7	*i*-Bu (**3g**)	**4ag**	89	87
8	*i*-Pr (**3h**)	**4ah**	89	78
9[b]	trityl (**3i**)	**4ai**	88	94
10	EtO_2CCH_2 (**3j**)	**4aj**	83	98
11	2-furylmethyl (**3k**)	**4ak**	85	96
12[b]	4-$MeOC_6H_4$ (**3l**)	**4al**	91	77

[a] The reaction conditions and analysis methods were the same as those described in Table 1, entry 12. [b] Using (*S*)-**1f**.

Q-. L. Zhou *et al*. *Chem. Sci*. just accepted

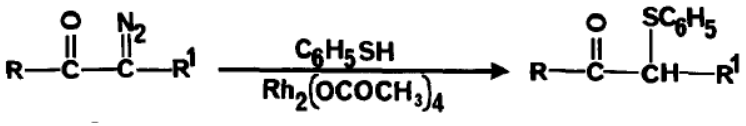

$PhCH_2CH_2CH_2COC(CH_3)N_2$(10) → $PhCH_2CH_2CH_2COCH(CH_3)SPh$ 71%

$CH_3COC(CH_3)N_2$(11) → $CH_3COCH(CH_3)SPh$ 83%

P. Ratananukul *et al. Tetrahedron Lett.* **1982**, *23*, 2509-2512

Acknowledgement
Dr. Kuninobu and Dr. Nishi
Thanks for kind lecture